



Norwegian University of  
Science and Technology

# Experimental Program for the validation of the design of a 150KWth Chemical looping Combustion reactor system with main focus on the reactor flexibility and operability

**Masoud Ghorbaniyan**

Natural Gas Technology

Submission date: July 2011

Supervisor: Olav Bolland, EPT

Co-supervisor: Aldo Bischi, EPT



**Experimental Program for the validation of the design of a  
150KWth Chemical looping Combustion reactor system with  
main focus on the reactor flexibility and operability**

Masoud Ghorbaniyan

**Master of Science in Natural Gas Technology**

**Submission date: July 2011**

**Supervisor: Olav Bolland, Energy and Process Department**

**Co-supervisor: Aldo Bischi, Energy and Process Department**

In cooperation with Valentina Bisio

Norwegian University of Science and technology-NTNU

Energy and Process Department

## **PROJECT WORK**

for

Stud.techn.

Masoud Ghorbaniyan

Feb 2011

### **Experimental program for the validation of the design of a 150kW<sub>th</sub> Chemical Looping Combustion reactor system with main focus on stable operation achievement**

#### **Background and objective**

There is an increasing interest in CO<sub>2</sub> capture and storage as a measure to reduce man-made emissions of the greenhouse gas CO<sub>2</sub>. Several CO<sub>2</sub> capture methods from power plants have been proposed and one of the best when it comes to costs and energy penalty is the Chemical Looping Combustion (CLC). The most promising way to realize this two steps combustion is the use of fluidized beds. One called Air Reactor (AR) uses air as fluidizing media. The oxygen of the air reacts exothermically with a metallic powder called Oxygen Carrier (OC) producing heat that can be used in a power cycle. While the depleted hot air is going out of the AR to a steam boiler or to a gas turbine the OC is collected and sent to another fluidized bed called Fuel Reactor (FR) and fluidized with gaseous fuel (e.g. methane). Here the fuel reacts with the oxygen carried by the metallic powder giving an endothermic or slightly exothermic reaction and the OC is ready to be collected and used again in the AR. In this way the exhaust gasses from the FR are just steam and “ready to capture” CO<sub>2</sub>.

SINTEF Energy Research and the Norwegian University of Science and Technology (NTNU) designed a 150kW<sub>th</sub> Chemical Looping Combustion (CLC) reactor system which deals with many of the industrial and scale-up issues of this technology. It consists of a Double Loop Circulating Fluidized Bed (DLCFB) reactor system where both the AR and the FR are Circulating Fluidized Beds (CFB) meant to work in the fast fluidization regime and interconnected by divided loop-seals and a bottom extraction. The purpose of the divided loop-seals is both to avoid the gas mixing between the two reactors and to lead the flux of solids entrained by one reactor into the other one or re-circulate it back to the reactor of origin. In addition the bottom extraction is bringing part of the mass from the FR to the AR in order to

maintain steady state conditions. That is because according to the design of the hot rig in the FR there will be less fluidizing gas available compared to the AR, thus fewer solids will be transported.

The air and fuel reactors have a height of 5 meters and respectively a diameter of approximately 0.25 and 0.15 meters. A one to one scale Cold Flow Model (CFM) has been built in order to test the CLC reactor system hydrodynamics and to support the design of the 150kW<sub>th</sub> unit. A first experimental campaign was performed to prove that the AR and the FR are working according to design and to find the more suitable operational window in order to couple them in the double loop configuration. These analyses were carried out making use of the following measurement devices: pressure transducers distributed all over the reactor system and disc-valves located in the down-comers after the cyclones to estimate the solid flow entrained by the reactors. A second experimental campaign needs to be performed: it will have main focus on the achievement of a stable operation of the overall DLCLCFB by means of the divided loop-seal, air staging, total solids inventory and cyclones backpressure tuning.

**The following tasks should be considered in the project work:**

Read the literature material provided in order to build up a good general understanding of the CFB reactor systems (e.g. fluidization regimes and CFB components) and the CLC technology. Where required make further investigations.

Gain a good understanding of the experimental set up together with the tools and measurement devices required to work in a powder technology laboratory (e.g. risk analysis, health and safety measures, pressure transducers, solenoid flap valve used to make solid flux measurements, etc.).

Perform an experimental program in order to gain enough information to validate the current CLC reactor system design before starting the construction of a new 150kW<sub>th</sub> test rig. Main focus on the AR and FR coupled operation as well as on the divided loop-seal and FR bottom extraction fluidization optimization.

Collect, evaluate and present the experimental results.

The project work shall comprise 50 % of a semester.

A progress plan (*Planned activities and scheduled progress*) shall be submitted to the responsible subject teacher/supervisors for comments within 14 days after the candidate has received the project description.

The work shall be edited as a scientific report, including a table of contents, a summary in Norwegian, conclusion, an index of literature etc. When writing the report, the candidate must emphasise a clearly arranged and well-written text. To facilitate the reading of the report, it is important that references for corresponding text, tables and figures are clearly stated both places.

By the evaluation of the work the following will be greatly emphasised: The results should be thoroughly treated, presented in clearly arranged tables and/or graphics and discussed in detail. The candidate is responsible for keeping contact with the subject teacher and teaching supervisors.

According to “Utfyllende regler til studieforskriften for teknologistudiet/sivilingeniørstudiet ved NTNU” § 20, the Department of Energy and Process Engineering reserves all rights to use the results in connection with lectures, research and publications.

The report must be submitted to the Department in 3 complete, bound copies. Further, a separate page must be submitted, giving a short summary of the work and stating the author’s name and title of the project work. This information will be used in case of the work being referred to in journals, and must not exceed one typed page with double spacing. Additional copies should be given directly to the supervisor(s) involved in the project according to agreement with the supervisor(s). A CD with a complete copy of the main report in Word-format or similar, shall be submitted to both the subject teacher and the Department of Energy and Process Engineering.

The main report from the project work shall be submitted to the Department of Energy and Process Engineering *within* , 2011.

---

Trygve Magne Eikevik

Deputy Head of Department

---

Olav Bolland

Subject teacher/Supervisor

Principal Supervisor: Olav Bolland

Co-Supervisor(s): Aldo Bischi

## **Preface**

My appreciation and gratitude are conveyed to the people listed below, who all contributed to the work presented in this thesis.

Professor Olav Bolland, my supervisor, for giving me the opportunity to work with things I care a great deal about, your knowledge and passionate guidance throughout the work. I am truly grateful.

Many thanks go in particular to co-supervisor Aldo Bischi. I am much indebted to Aldo for his valuable advice in science discussion, supervision in cold setup and furthermore, using his precious times to read this thesis and gave his critical comments about it.

Øyvind Langørgen, my supervisor at SINTEF research center for his great support, guidance, and for their enthusiasm.

My colleagues in the CLC group, especially Valentina Bisio, for providing such a joyful company in the lab.

All unmentioned colleagues at the Division of Energy and Process Technology for offering such a friendly and supportive working atmosphere.

My precious family and my sweet, loving, girlfriend Mona.

July 2010, Trondheim

A handwritten signature in blue ink that reads "Masoud Ghorbaniyan". The signature is written in a cursive style with a large, looping 'M' and 'G'.

## Summary

Chemical Looping Combustion (CLC) is one of the most promising way to limit the CO<sub>2</sub> release to the atmosphere among the other technologies for Carbon Capture and Storage (CCS). It constitutes an indirect fuel combustion strategy, in which metal oxide is used as oxygen carrier, to transfer oxygen from the combustion air to the fuel, avoiding direct contact between air and fuel. It is basically an unmixed combustion process (fuel and air are never mixed) whose flue gases are mainly CO<sub>2</sub> and steam. Thus, after condensation, the carbon dioxide can be easily separated from the exhaust.

SINTEF Energy Research and the Norwegian University of Science and Technology (NTNU) have designed a 150kW<sub>th</sub> second generation chemical looping combustion reactor system. It consists of a double loop circulating fluidized bed (DLCFB) reactor system where both the air reactor and the fuel reactor are Circulating Fluidized Beds (CFB) meant to work in the fast fluidization regime and interconnected by divided loop-seals and a bottom extraction to achieve high solids circulation and be flexible in operation. The chosen design solutions are aiming at high operational flexibility and fuel conversion as well as compactness for the prospective of pressurizing the reactor as a further step.

A Cold Flow Model<sup>1</sup> (CFM) has been built to verify the design of the CLC reactor system. The CFM consists of two reactors, the fuel and the air reactor, with different diameters, each one having a loop seal<sup>2</sup>. No chemical reaction happens inside the CFM. The main goal of CFM is to have the understanding of the hydrodynamics of the system.

An experimental campaign was performed in order to find the best conditions for the solid flux, reaching stability, and the proper flow regimes for the coupled reactors in the CFM. An investigation and mapping of the operating area of the coupled reactors was the target of the experiments.

As the first step and for further research, the best set of operating conditions is selected by considering the stability and solid flux in order to meet the design targets. This set of

---

<sup>1</sup> A cold flow model was used for simulating the operation of CLC in order to study the fluid dynamics of a 150-

<sup>2</sup> Loop-seal, considered heart of a CFB, returns solids captured by cyclone to the base of the riser while preventing direct flow from high pressure riser to the low-pressure cyclone.



conditions is used as the reference case. Later, all other operational modes (are explained in following paragraphs) in the cold flow model which resembles CLC are evaluated against the base data obtained.

Different operational modes of Chemical Looping Combustion were tested by means of the CFM to validate the CLC reactor system design. A significant effort was done to test the modes part-load, maximum power, maximum fuel reactor concentration and reforming. These experiments were done to define the best operational window for the CLC. In each of the mentioned modes, pressure profiles and concentration of the solids are compared to the reference case of the CFM.

The loop seal plays a key role in the operation of the CFM, for assuring the solids movement in a steady state loop. Series of experiments were performed in the CFM in order to map the operational window of the loop seals. The sensitivity of the loop seal is evaluated by measuring the pressure difference in the bottom of the fuel reactor and air reactor during the operation of the CFM to obtain an operational window for the loop seal.

For the last step, the effects of the total mass inventory circulating in the system for the five different operational modes were investigated by increasing and decreasing the inventory. For each case the pressure profiles and concentration of the solids is compared with the reference case and the results are shown in this thesis work.

It was possible to operate the reactor system in a stable way and according to design targets. At the same time the hydrodynamic viability was addressed qualitatively, of several other chemical looping modes which in principle can be managed by the double loop circulating fluidized bed architecture: part-load, maximum power, maximum fuel reactor concentration and reforming. It was possible to find one or more configurations resembling each of them.

## Nomenclature

### Abbreviations

|        |   |
|--------|---|
| AR     | Air reactor   |
| AR LS  | Air reactor loop seal                                 |
| ASTM   | American society for testing and materials            |
| CCS    | Carbon capture and storage                            |
| CFB    | Circulating fluidized bed                             |
| CFM    | Cold flow model                                       |
| CLC    | Chemical looping combustion                           |
| CLR    | Chemical looping reforming                            |
| COP    | Conference of the parties                             |
| DLCFB  | Double loop circulating fluidized bed                 |
| FR     | Fuel reactor  |
| FRLS   | Fuel reactor loop seal                                |
| GDP    | Gross domestic product                                |
| GHG    | Greenhouse gas  |
| HSE    | Health, safety and environment                        |
| IPCC   | Intergovernmental panel on climate change             |
| LS     | Loop-seal   |
| LHV    | Lower heating value                                   |
| NTNU   | Norwegian university of science and technology        |
| OC     | Oxygen carrier  |
| PCC    | Post combustion capture                               |
| PSD    | Particle size distribution                            |
| PT     | Pressure transducer                                   |
| SD     | Standard deviation                                    |
| TSI    | Total solids inventory                                |
| UNEP   | United nations environment program                    |
| UNFCCC | United nations framework convention on climate change |
| WMO    | World meteorological organization                     |

## Symbols

|                 |   |   |
|-----------------|---|---|
| $d_{50}$        | Mass median particle diameter           | [ $\mu\text{m}$ ]                                   |
| D               | Reactor diameter                        | [m]   |
| G <sub>s</sub>  | Solids flux                             | [ $\text{kg}\cdot\text{m}^{-2}\cdot\text{s}^{-1}$ ] |
| g               | Gravitational acceleration              | [ $\text{m}\cdot\text{s}^{-2}$ ]                    |
| L, h            | Reactor height                          | [m]   |
| M               | Molecular mass                          |   |
| Me              | Metal                                   |   |
| MeO $\alpha$    | Oxidized metal oxide                    |   |
| MeO $\alpha$ -1 | Reduced metal oxide                     |   |
| P               | Pressure                                | [Pa]  |
| R               | Ratio                                   |   |
| U               | Gas velocity                            |   |
| $u_0$           | Superficial gas velocity                | [ $\text{m}\cdot\text{s}^{-1}$ ]                    |
| $u_{mf}$        | Particles minimum fluidization velocity | [ $\text{m}\cdot\text{s}^{-1}$ ]                    |
| V               | Volume                                  | [ $\text{m}^3$ ]                                    |
| T               | Temperature                             | [ $^{\circ}\text{C}$ ]                              |
| t               | Time                                    | [sec]   |
| x               | Degree of oxidation                     |   |

## Greek letters

|               |                      |                                   |
|---------------|----------------------|-----------------------------------|
| $\mu$         | Dynamic viscosity    | [Pa·s]                            |
| $\rho$        | Density              | [ $\text{kg}\cdot\text{m}^{-3}$ ] |
| $\phi$        | Particles sphericity |                                   |
| $\varepsilon$ | Voidage              |                                   |
| $\lambda$     | Excess air ratio     |                                   |

### Dimensionless numbers

|                 |                           |  |
|-----------------|---------------------------|--|
| Ar              | Archimedes number         | $d_{50}^3 \cdot \rho_p \cdot (\rho_p - \rho_g) \cdot g \cdot \mu^{-2}$ |
| Fr              | Froud number              | $u_0^2 \cdot g^{-1} \cdot D^{-1}$                                      |
| Re <sub>p</sub> | Particles Reynolds number | $\rho_g \cdot u_0 \cdot d_{50} \cdot \mu^{-1}$                         |

### Subscripts

|     |                      |
|-----|----------------------|
| g   | Gas                  |
| mf  | Minimum fluidization |
| o   | Oxygen               |
| oc  | Oxygen carrier       |
| p   | Particles            |
| red | Reduced              |
| sph | Sphericity           |

# Table of Contents

|  |    |
|--|----|
| Summary .....  | V  |
| 1. Introduction .....  | 1  |
| 2. Background.....   | 4  |
| 2.1. Carbon Capture and Storage (CCS)-----                             | 4  |
| 2.2. Methods of CO <sub>2</sub> Capturing -----                        | 6  |
| 2.2.1. Post-Combustion Capture (PCC).....                              | 6  |
| 2.2.2. Pre-Combustion Capture.....                                     | 8  |
| 2.2.3. Oxy-fuel combustion for CO <sub>2</sub> capture .....           | 9  |
| 3. Theory.....   | 13 |
| 3.1. Chemical Looping Combustion (CLC)-----                            | 13 |
| 3.2. Hydrodynamics -----   | 18 |
| 3.2.1. Regimes of Fluidization.....                                    | 18 |
| 3.2.2. Circulating Fluidized Beds .....                                | 20 |
| 3.3. Particles characterization -----                                  | 21 |
| 3.4. 150 kW <sub>th</sub> DCFB CLC reactor – Hot rig -----             | 25 |
| 3.4.1. Oxygen Carrier.....   | 27 |
| 3.4.2. Components .....  | 31 |
| 3.4.3. Design Parameters and Main Dimensions .....                     | 37 |
| 3.5. 150 kW <sub>th</sub> DCFB CLC reactor – Cold Flow Model -----     | 38 |
| 3.5.1. Scaling strategy.....   | 38 |
| 4. Experimental Part .....   | 42 |
| 4.1. Overall view of the CFM -----                                     | 42 |
| 4.2. Measurement equipment-----  | 47 |
| 4.2.1. Mass flow controllers (Brooks® Mass Flow Meter Model 5863)..... | 47 |
| 4.2.2. Pressure Transducers .....                                      | 47 |
| 4.2.3. Scales .....  | 49 |
| 4.3. Software (LabVIEW) -----  | 50 |
| 4.4. Mass flux Measurement -----                                       | 51 |
| 4.5. Health and safety-----  | 53 |
| 4.6. Accuracy and Errors-----  | 54 |

|  |     |
|--|-----|
| 5. Experiments and Results .....                   | 56  |
| 5.1. Procedure for Starting the Experiments -----  | 56  |
| 5.2. Overview of experiments -----                 | 58  |
| 5.3. Validating the data and design condition----- | 59  |
| 5.4. Operational Modes -----                       | 68  |
| 5.4.1. Part Load.....                              | 68  |
| 5.4.2. Maximum Power.....                          | 72  |
| 5.4.3. Maximum Fuel Reactor Concentration.....     | 75  |
| 5.4.4. Chemical Looping Reforming .....            | 78  |
| 5.5. Inventory -----                               | 83  |
| 5.6. Loop seal sensitivity-----                    | 86  |
| 6. Conclusion.....                                 | 88  |
| 7. Reference .....                                 | 91  |
| 8. Appendix .....                                  | 94  |
| 8.1. Appendix I-----                               | 94  |
| 8.2. Appendix II-----                              | 99  |
| 8.3. Appendix III-----                             | 103 |

## Table of Figures

|   |    |
|---|----|
| Figure 1-1: green house gas emission by country.....  | 2  |
| Figure 1-2: Growth of global trade in goods, gross domestic product (GDP), energy use, CO2 emissions, and global population, 1975–2007.....   | 3  |
| Figure 2-1: CO <sub>2</sub> capture and storage from power plant .....  | 5  |
| Figure 2-2: Three CO <sub>2</sub> capture processes .....   | 6  |
| Figure 2-3: The basic principle of post-combustion .....  | 7  |
| Figure 2-4: The basic principle of pre-combustion .....   | 9  |
| Figure 2-5: The basic principle of oxy-combustion.....  | 10 |
| Figure 2-6: Classification of oxy-combustion methods for CO <sub>2</sub> captures .....   | 12 |
| Figure 3-1: Rotating bed reactor with radial gas flow.....  | 14 |
| Figure 3-2: Basic scheme of chemical looping combustion .....   | 16 |
| Figure 3-3: Hydrodynamics regimes of fluidization.....  | 18 |
| Figure 3-4: Basic scheme of a circulating fluidized bed system .....  | 21 |
| Figure 3-5: Geldart’s particle classification for fluidization.....   | 24 |
| Figure 3-6: Process diagram of the CLC rig.....   | 25 |
| Figure 3-7: Fluidization regime of the AR and FR.....   | 26 |
| Figure 3-8: Schematic drawing of the loop seals used in the CLC Model .....   | 31 |
| Figure 3-9: On site picture of loop seal which is used in Cold Flow Model rig.....  | 32 |
| Figure 3-10: Picture of the Cyclones which are used in the Cold Flow Model rig .....  | 33 |
| Figure 3-11: Typical cyclone configuration .....  | 34 |
| Figure 3-12: Place of different nozzles in the riser.....   | 35 |
| Figure 3-13: Simple sketch of Downcomer.....  | 36 |
| Figure 3-14: On site picture of Lifter, Figure 3-15: Schematic of Lifter.....   | 37 |
| Figure 3-16: Triangular scaling strategy .....  | 39 |
| Figure 4-1: 3D CAD General assembly of reactor system .....   | 42 |
| Figure 4-2: CFM scheme in which are shown all the positions for the air injections. ....  | 43 |
| Figure 4-3: On site picture of filter box.....  | 44 |
| Figure 4-4: Particle Size Distribution (PSD) of the Fe-Si Powder used in the Cold Flow Model (CFM) experiments.....   | 45 |
| Figure 4-5: CFM scheme in which the positions of the pressure transmitters are shown. ....  | 46 |
| Figure 4-6: ® Mass Flow Meter Model 5863.....   | 47 |
| Figure 4-7: Electric FCX-AII V5 Differential Pressure Transmitters .....  | 48 |
| Figure 4-8: Picture of the pressure transmitter which are in used in the Clod Flow Model rig.....   | 48 |
| Figure 4-9: Mettler Toledo XS 32000L.....   | 49 |
| Figure 4-10: The control system layout for the CFM.....   | 51 |
| Figure 4-11: Picture of the flap valve which is used in Cold Flow Model rig.....  | 52 |
| Figure 4-12: Picture of protective mask .....   | 54 |
| Figure 5-1: Pressure measurements in some key points along the AR (left) and FR (right) reactors ....   | 59 |
| Figure 5-2: Pressure measurements at the bottom AR (left) and FR (right) loop-seals, plotted as function of the time. Example of reactor system operation in steady state conditions. Each of them is plotted |    |

|   |    |
|---|----|
| together with the AR and FR pressures measured at the points where the two loop-seals return legs are merging .....   | 61 |
| Figure 5-3: left) Pressure profile measured across the DLCFB reactor system in stable operation, which gave high solids exchange, approaching 2kg/s. right) corresponding estimation of the particles concentration along the reactor bodies. ....                          | 62 |
| Figure 5-4: Pressure profiles of the DLCFB reactor system at the variation of the bottom extraction/lift superficial gas velocity. Pressures of AR (left) and FR (right) are presented separately for sake of simplicity .....  | 63 |
| Figure 5-5: Pressure (left) and concentration (right) profiles of the fuel reactor (FR) of the DLCFB reactor system at the variation of the FR superficial gas velocity. Pressure of AR is not presented for sake of simplicity, because it was almost not influenced ..... | 64 |
| Figure 5-6: The place of air injections (Blue Arrows), and the path of flow in coupled experiment along the body of reactors(White Arrows) in “Standard experiment” .....   | 66 |
| Figure 5-7: Velocity profile along the risers and duct of cyclones in “standard” experiment.....  | 67 |
| Figure 5-8: Pressure and solids concentration profiles of AR (a1 and b1) and FR (a2 and b2) at part load conditions of 75% and 50% fuel load.....   | 70 |
| Figure 5-9: Pressure and solids concentration profiles of AR (a1 and b1) and FR (a2 and b2) resembling a power increase and a gas turbine application.....  | 73 |
| Figure 5-10: Pressure and solids concentration profiles of AR (a1 and b1) and FR (a2 and b2) at FR maximum solids flux/concentration achieved .....   | 76 |
| Figure 5-11: basic process of CLR(a).....   | 80 |
| Figure 5-12: Pressure and solids concentration profiles of AR (a1 and b1) and FR (a2 and b2) resembling two reforming applications .....  | 82 |
| Figure 8-1: Pressure and solids concentration profiles of AR and FR in standard condition with different inventories .....  | 94 |
| Figure 8-2: Pressure and solids concentration profiles of AR and FR in part load operation with different inventories.....  | 95 |
| Figure 8-3: Pressure and solids concentration profiles of AR and FR in maximum power condition with different inventories.....  | 96 |
| Figure 8-4: Pressure and solids concentration profiles of AR and FR in maximum fuel reactor concentration condition with different inventories .....  | 97 |
| Figure 8-5: Pressure and solids concentration profiles of AR and FR in reforming condition with different inventories.....  | 98 |





## 1. Introduction

CO<sub>2</sub> can be produced through either human activities like burning fossil fuels, deforestation, refrigerating systems, agriculture activities, or the carbon cycle naturally. If we take the industrial revolution in the period from the 18<sup>th</sup> to the 19<sup>th</sup> century as a starting point, the global atmospheric concentration of CO<sub>2</sub> has increased by 35%. Human activities such as burning oil, coal, gas and deforestation are the reasons that have caused the increase of CO<sub>2</sub> in the atmosphere. In the other hand, a natural source of CO<sub>2</sub> occurs in the carbon cycle where billions of tons of atmospheric CO<sub>2</sub> is removed from the atmosphere by ocean and plants, and released back into the atmosphere annually through natural processes e.g. in an ideal situation, carbon dioxide emissions and removals from the carbon cycle are almost equal, thus the whole system is in balance [1].

As said, CO<sub>2</sub> is emitted principally from the burning of fossil fuels, both in large combustion units such as those used for electric power generation and in smaller, distributed sources such as automobile engines and furnaces used in residential and commercial buildings. CO<sub>2</sub> emissions also result from some industrial and resource extraction processes, as well as from the burning of forests during land clearance.

It is also universally known that fossil energy conversion process create harmful emissions that have a huge impact on the greenhouse effect. It was scientifically demonstrated that the increase in anthropogenic greenhouse gases, due to the industrialization, was the cause for the temperature rise. In these last year's many laws have been enact in order to protect the environment by an effective control of hazardous pollutants emission. Therefore, knowing that carbon dioxide accounts for 64% of the enhanced greenhouse effect, interest in topics like CO<sub>2</sub> capture and storage has grown more and more.

Energy consumption is always increasing and for sure it cannot be reduced or stopped; that is the reason why a long-term energy strategy for low or zero carbon-emission technology is needed.

This plan also includes the utilization of renewable and nuclear energy. The latter plays now a remarkable role in electricity production, but it has always had social and political problems; there are safety issues yet to be solved and the debate on what to do with the radioactive waste

is still open. Most of the people, on the contrary, vote for renewable energies, because of their regenerative and environment-friendly nature. However, they still have complex constraints and they probably will never be dominant in world's energy supply. For this reasons in the future fossil fuels will still be fundamental.

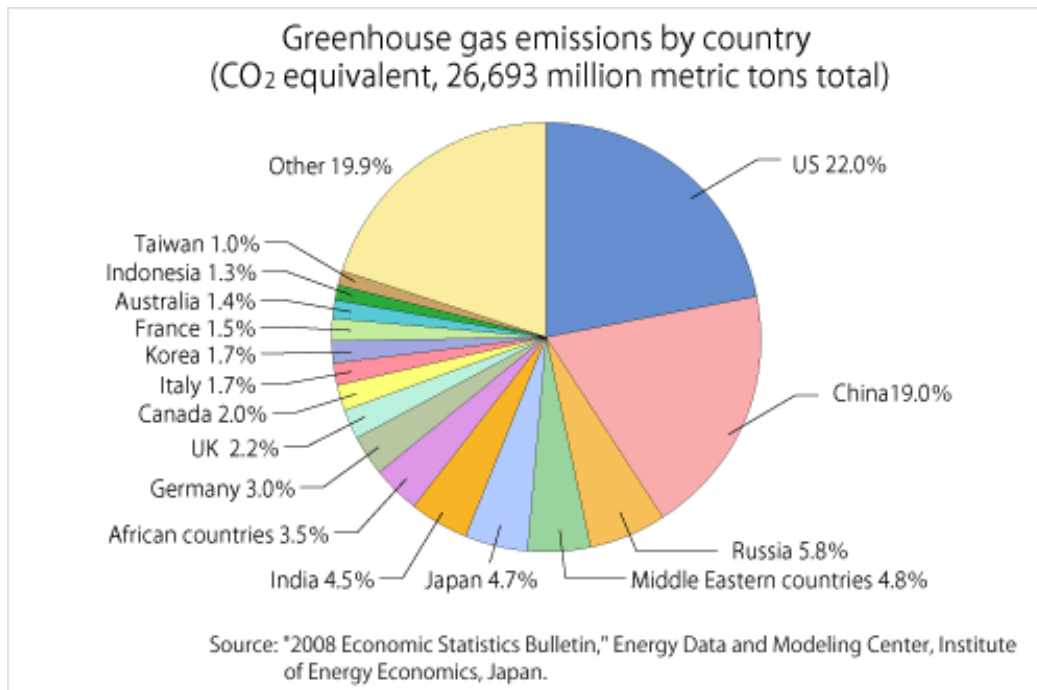


Figure 1-1: green house gas emission by country

As mentioned there is a big effort all over the World to reduce the human made emissions of greenhouse gasses, e.g. increasing investment in renewable energies and biomasses. Nevertheless greenhouse gases, emissions are still increasing because of the economical growth of the world requiring always more energy which is mainly produced utilizing fossil fuels because renewable energies are still not economically convenient.

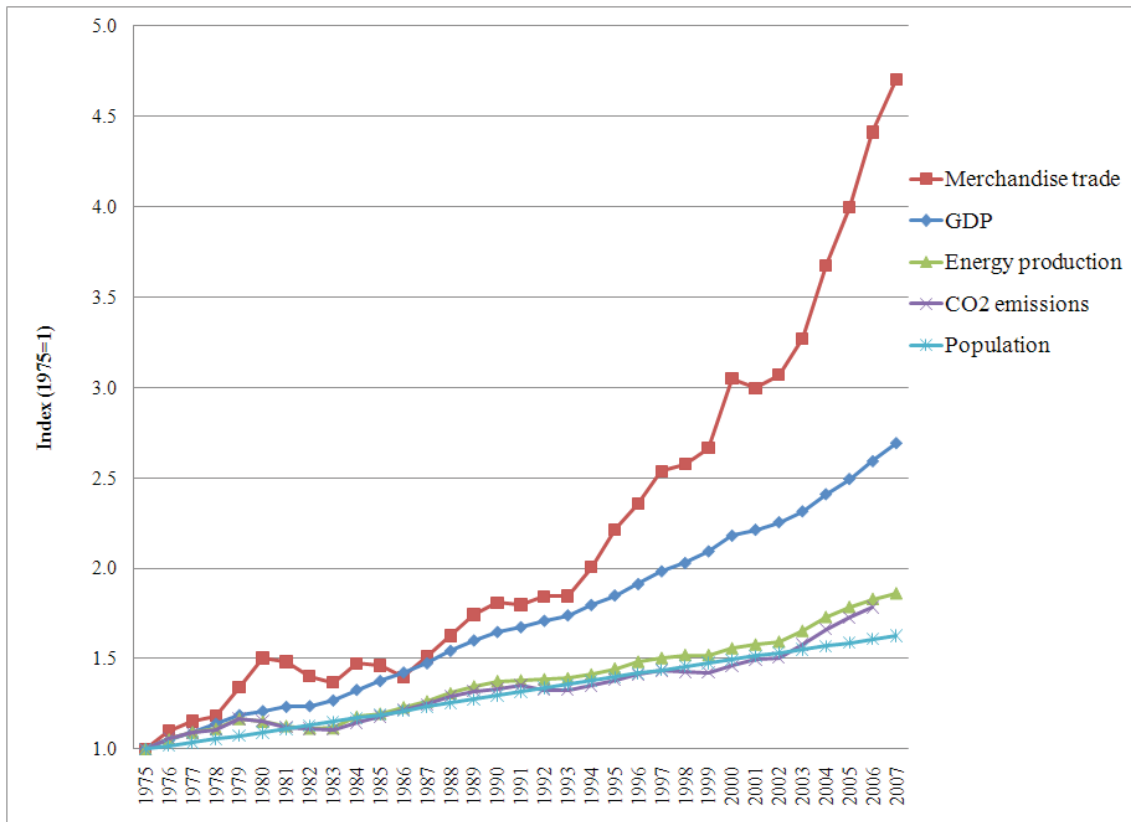


Figure 1-2: Growth of global trade in goods, gross domestic product (GDP), energy use, CO2 emissions, and global population, 1975–2007. Data obtained from World Bank Development Indicators (2010)

A lot of research is therefore done to find concepts with low energy demand and hence low operating cost. Chemical Looping Combustion (CLC) is one of the most promising technologies when it comes to capture costs [2].

The idea standing behind CLC was first introduced by Lewis and Gilliland (1946) in a patent to produce a gas mixture of hydrogen and carbon monoxide. Later Richter and Knoche (1983) and Ishida et al. (1987) proposed the CLC principle to reduce the exergy loss of a conventional combustion process [3].

SINTEF Energy Research and the Norwegian University of Science and Technology (NTNU) have designed a 150kW<sub>th</sub> atmospheric CLC reactor system. The chosen design solutions are aiming at high operational flexibility and fuel conversion as well as compactness for the prospective of pressurizing the reactor as a further step [2].

## 2. Background

### 2.1. Carbon Capture and Storage (CCS)

The proposed European strategy to meet the challenge of future energy supply is based, among others like e.g. renewable, on fossil fuel conversion and subsequent capture and sequestration<sup>3</sup> of the greenhouse gas CO<sub>2</sub>. The idea is to deposit concentrated CO<sub>2</sub> in safe geological storages like gas fields instead of uncontrolled emission in the atmosphere [4].

This method has been selected as one of the most effective option for mitigating the global warming by the Intergovernmental Panel on Climate Change (IPCC). This organization was established in 1988 by the United Nations Environment Program (UNEP) and the World Meteorological Organization (WMO). Its tasks are to assess information on climate change and its effects on the environment; to discuss options for mitigating it and provide solutions for adapting to it. The IPCC is also responsible for communications, related to scientific/technical/socio-economic advices, with other organizations, such as the Conference of the Parties (COP) and the United Nations Framework Convention on Climate Change (UNFCCC). In the past years many Reports and Technical Papers were produced; among them, the Special Report on CO<sub>2</sub> Capture and Storage can be found. [5]

This Report provides an exhaustive description about CCS. It is a process based on three steps:

- Separation of carbon dioxide from fossil fuels combustion power plants and, in general, from industrial and energy-related sources;
- Transport to a pre-established storage location;
- Long-term isolation from the atmosphere.

The first phase, or rather the CO<sub>2</sub> capture, is the most energy-consuming between the three, so that it has to be deeply studied. It can be divided into separation and compression. At the beginning, the carbon dioxide has to be captured; this operation can be applied to large point sources, such as fossil fuel power plants, biomass energy facilities, natural gas production plants, synthetic fuel plants, fossil fuel-based hydrogen production plants and others.

---

<sup>3</sup> Carbon sequestration is the process of removing carbon from the atmosphere and depositing it in a reservoir.

Capturing CO<sub>2</sub> requires considerable energy. In a ‘generic’ power generation plant such as that shown in Figure 2-1, there is a significant loss of conversion efficiency, and indeed a significant portion of the CO<sub>2</sub> produced comes from the CCS operation. To calculate the real (or net) reduction of emissions to the atmosphere, different quantities have to be analyzed: the fraction of CO<sub>2</sub> captured and the increased CO<sub>2</sub> production caused by the decrease of the plant efficiency. The increased CO<sub>2</sub> production resulting from the loss in overall efficiency of power plants due to the additional energy required for capture, transport and storage and any leakage from transport result in a larger amount of CO<sub>2</sub> produced per unit of product (lower bar) relative to the reference plant (upper bar) without capture. [6]

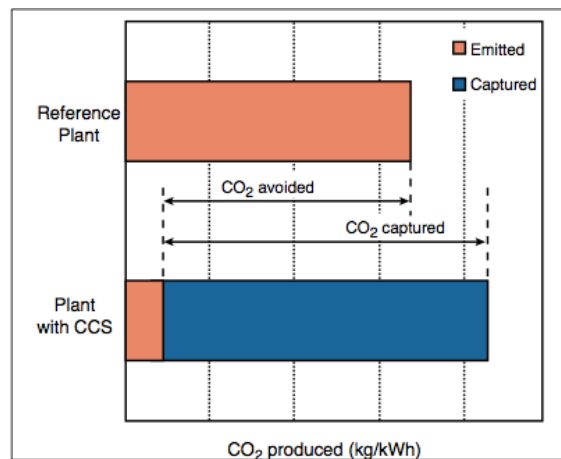


Figure 2-1: CO<sub>2</sub> capture and storage from power plant [6]

The additional energy required by a plant equipped with a CCS system can be considered, in average, equal to 10-40% of the energy needed by a plant of equivalent output, without CCS. The existing techniques usually can capture about 85-95% of the carbon dioxide that passes through the capture plant. Hence the net reduction in CO<sub>2</sub> emissions to the atmosphere, using CCS, will be around 80-90%.

So, accurate calculations are necessary to assess the real advantages of the application of this method.

## 2.2. Methods of CO<sub>2</sub> Capturing

There are three primary methods of capturing CO<sub>2</sub>: Pre-combustion, or separating CO<sub>2</sub> from gasified fossil fuel prior to combustion; post-combustion, which captures CO<sub>2</sub> from the flue gas stream after the fossil fuel is burned; and oxy fuel combustion, where the combustion of fuel takes place in an oxygen-rich environment, resulting in flue gas more ready for sequestration.

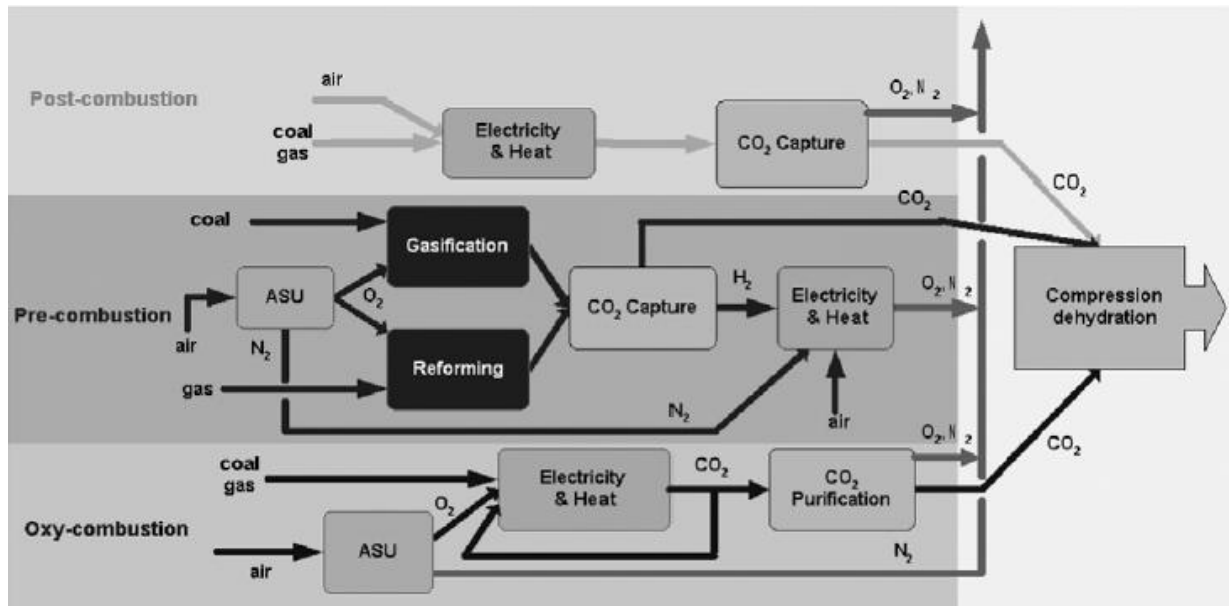


Figure 2-2: Three CO<sub>2</sub> capture processes [7]

### 2.2.1. Post-Combustion Capture (PCC)

This process, as the name can suggest, is used to rinse existing emissions. A significant issue in this area is the real composition of the flue gases from power stations, and in particular the presence of impurities has to be considered. In fact, not only O<sub>2</sub>, N<sub>2</sub>, CO<sub>2</sub> and H<sub>2</sub>O will be found, but also unwanted pollutants like particulates, NO<sub>x</sub>, SO<sub>x</sub>, heavy metals and others. The percentages of these elements depend on the type of fuel used, but in any case impurities have to be removed before proceeding with capture, leading to an increase in costs.

Therefore, many problems have yet to be solved; this is the reason why this process is not considered the best. However, several different techniques have been studied and implemented,

most of them commercially available. Among them, the one based on the absorption process carried out by chemical solvents is seen as the preferred choice, because of its high capture efficiency and selectivity, as well as lower costs and energy use in comparison with other post-combustion methods. This technique works as it follows.

At first the flue gases are subjected to cooling, in order to reach temperature levels compared to those required for efficient carbon dioxide absorption; after that they are inserted into a CO<sub>2</sub> absorber. Here they have to pass through an absorbing solution, containing a chemical solvent which reacts with the CO<sub>2</sub> and manages to absorb up to 85% of the gas. After that, this quantity is removed from the solution by heating, so that the process can restart; in fact, at higher temperatures the capacity of the absorbent to maintain the gas attached decreases. In the meantime, the clean flue gases are released into the atmosphere. The carbon dioxide is then compressed and cooled; the result of this operation is that it is transformed into liquid, easier to handle for transport and storage [9].

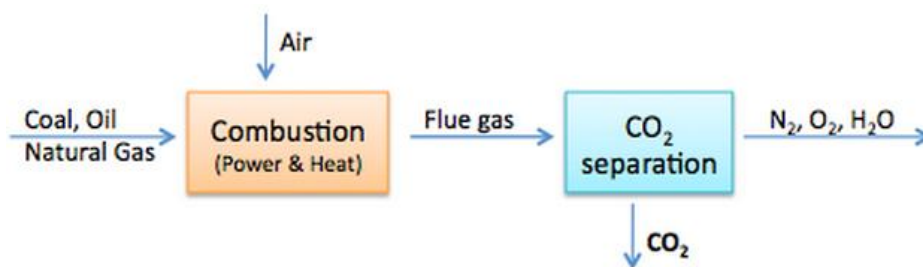


Figure 2-3: The basic principle of post-combustion [8]

One of the clearest benefits of this method is the fact that it can be used for retrofitting, i.e. it can be added to an already existing plant: it is not necessary to anticipate its presence in the first design phases, and usually there is no need to modify the original structure. [10]

Many things though are fundamental for the efficiency of the process, for example the correct choice of the solvent, related to the fuel used; the addition of equipment for eliminating impurities and for maintaining the solution quality, avoiding, as much as possible, corrosion or degradation of materials; an evaluation of the energy required for the entire system, also taking into account the one necessary for CO<sub>2</sub> compression. The amount of energy is thus very high and this causes a significant decrease of the power plant efficiency. For this reason, several studies are still ongoing; for instance, different types of solvent are being analyzed so that to



achieve a reduction in energy consumption. Innovative process designs are also being introduced. However, it is yet to be proved that these methods will bring to real advantages. [11]

### 2.2.2. Pre-Combustion Capture

In this case, the goal is to remove CO<sub>2</sub> from the fossil fuel prior to the combustion phase. The process usually is constituted by this sequence of operations.

At first, it is necessary to convert the fuel into a mixture of hydrogen, H<sub>2</sub>, and carbon monoxide, CO. This can be obtained following two different paths:

Steam reforming, based on the addition of steam to the primary fuel. The basic reaction (endothermic) in this instance is:



Partial oxidation (alias gasification if solid fuels are used), based on the addition of oxygen to the primary fuel. Basic reaction (exothermic):



The following reaction is required to transform CO in CO<sub>2</sub>, and it is generally called “shift” reaction. It is basically an addition of steam:



Then the separation of CO<sub>2</sub> is made, following a similar process as the one in the post-combustion capture. In this case, however, the fuel used has a reduced content of carbon, leading to a smaller amount of gas that has to be separated and processed. [11]

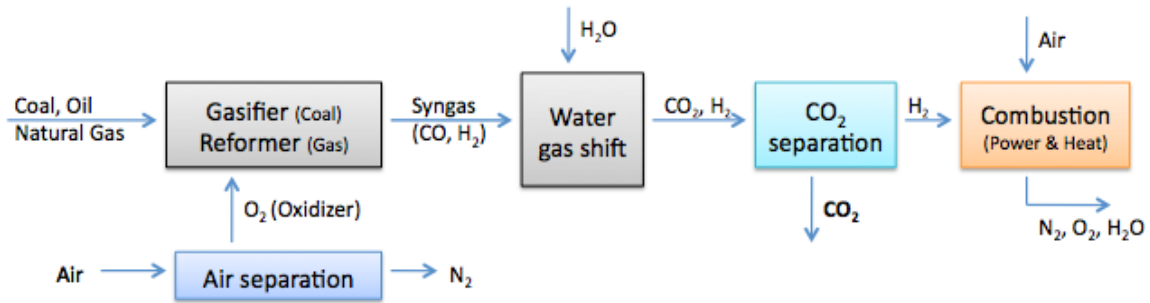


Figure 2-4: The basic principle of pre-combustion [8]

So, it can be noticed that pre-combustion process may be used for two distinct aims:

- H<sub>2</sub> production, as this is nowadays studied as a possible fuel above all for vehicles, but also for power plants. Unfortunately the element will not be perfectly pure, but it will contain a certain percentage of impurities like methane, CO and CO<sub>2</sub>, even if in small quantities.
- Carbon reduction in fuels, by the capture and storage of carbon dioxide.

Unlike the previous method, this cannot be added at an already existing plant, because substantial changes have to be made on the original structure. Thus, pre-combustion regards only new plants, and it has to be designed at the same time as the entire system.

On the other hand, it has been demonstrated that by the application of this method up to 90% of the carbon dioxide can be captured.

However, using pre-combustion capture leads to a significant increase of the costs (about twice as high as the ones resulting from using post-combustion); so, even in this case, further analysis are required to find a way to reduce investments, ensuring in the meantime a good efficiency of the process. [10]

### 2.2.3. Oxy-fuel combustion for CO<sub>2</sub> capture

The process of fuel which is burned with pure oxygen instead of air as the primary oxidant is called oxy-fuel combustion. Since the nitrogen part of air is not heated, the fuel consumption

is reduced, and it is possible to obtain higher flame temperature. The idea behind the oxy-combustion is to let the combustion occur with pure oxygen, because it prevents the combustion products to be diluted by nitrogen (and the presence of other pollutants such as  $\text{NO}_x$ ). Further, having zero oxygen excess avoids the combustion products of being diluted with oxygen [8].

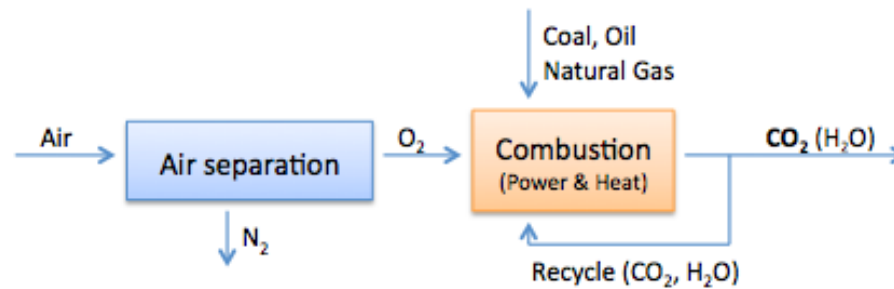


Figure 2-5: The basic principle of oxy-combustion [8]

In this way, the quantity of nitrogen will be significantly reduced (there will always be a small percentage, depending on the type of fuel used) and the products will be, mainly, just water vapor and carbon dioxide, which can be easily separated through a cooling process. After the condensation of the vapor, a  $\text{CO}_2$  rich gas-stream is created, containing around 80-98% of the dioxide, also depending on the fuel used. These gases are then compressed and dried; they can also be further purified before being sent to storage.

The efficiency of the capture system in this case can be considered equal to 100%; this means that almost 100% of the carbon dioxide can be captured [10].

The challenges for these processes which should be pointed out are with substituting the combustive agent, the combustion temperature will change; in particular, the temperature in a reaction using oxygen can reach up to  $3500\text{ }^\circ\text{C}$ . This temperature is unsustainable by materials that are generally used in power plants, and it brings to high stresses in these materials. So, the heating must be controlled, usually by a strict evaluation of the proportion of flue gas and water recycled back in the combustion chamber. Moreover, new materials, with higher resistance, are being studied.

The production of pure oxygen also constitutes a problem. Different techniques can be utilized; among them, the most used is distillation at cryogenic temperatures. This option consists in the compression of the air followed by its purification: adsorbers remove hydrocarbons, water, CO<sub>2</sub> and N<sub>2</sub>O. After that, air passes through heat exchangers for cooling and finally it is separated into O<sub>2</sub> and N<sub>2</sub> with a distillation process. These operations, unfortunately, lead to major energy costs, so this technique is very expensive. This is the reason why a lot of efforts are concentrated on research about a different solution: polymeric membranes, or oxygen transport membranes. These components are made by ceramic and metal oxides, and they have certain oxygen permeability, depending on the oxygen ion vacancies in the metal oxide lattice. This technique may be really efficient, but it still is at an early stage of development; it will require more years of researches. [11]

In general, oxy-fuel combustion is still not ready to be used, but several studies are being conducted in order to find solutions for the problems previously discussed. Between the emerging technologies, the chemical looping combustion process is gaining more and more importance.

Figure 2-6 shows classification of Oxy-combustion power cycles based on integration of the air separation process and the power cycle.

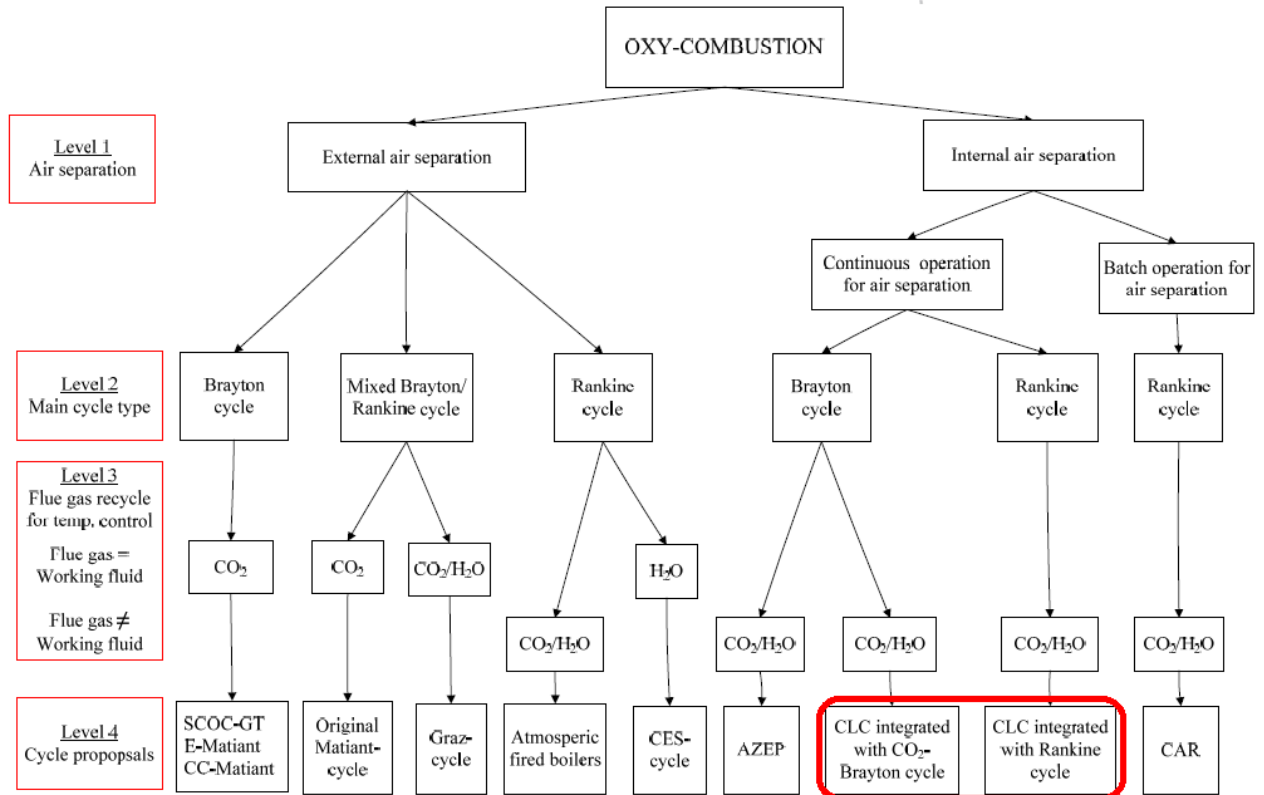


Figure 2-6: Classification of oxy-combustion methods for CO<sub>2</sub> captures [8]

As shown in the figure 2-6, Chemical looping combustion (CLC) is closely related to oxy-fuel combustion as the chemically bound oxygen reacts in a stoichiometric ratio with the fuel. In the CLC process the overall combustion reaction takes place in two reaction steps in two separate reactors. In the reduction reactor, the fuel is oxidized by the oxygen carrier, i.e., the metal oxide MeO. The metal oxide is reduced to a metal oxide with a lower oxidation number, Me, in the reaction with the fuel. In this manner, pure oxygen is supplied to the reaction with the fuel without using a traditional air separation plant, like cryogenic distillation of air [12].

### 3. Theory

#### 3.1. Chemical Looping Combustion (CLC)

Combustion is defined as a rapid chemical reaction of oxidants with fuels, during which heat is produced. Chemical looping combustion constitutes an indirect fuel combustion strategy, in which metal oxide is used as oxygen carrier, to transfer oxygen from the combustion air to the fuel, avoiding direct contact between air and fuel. It is basically an unmixed combustion process (fuel and air are never mixed) whose flue gases are mainly CO<sub>2</sub> and steam. Thus, after condensation, the carbon dioxide will be easily separated from the exhaust. Moreover, during the normal combustion process, irreversibilities cause penalties in the efficiency of the conversion of fuel energy into work. With CLC these penalties are reduced precisely for the presence of multiple sub-reactions and chemical intermediates. For these reasons, this technology is seen as one of the most promising way to limit the CO<sub>2</sub> releases in the atmosphere.

In 1946 for the first time the basic principle of CLC was introduced by Lewis and Gilliland, whose aim was the production of a gas mixture of hydrogen and carbon monoxide. The idea of using this principle in order to reduce the exergy loss of a conventional combustion process was proposed by Richter and Knoche, in 1983, and Ishida et al. in 1987. Thereafter, it has been studied as a possible technique for capturing CO<sub>2</sub> [3].

Different approaches for chemical looping combustion have been investigated. Basically, there are three possible choices of reactor set-up:

##### Move feed

In this method, the oxygen carrier material is maintained static in a fixed bed and the feed is switched to the reactor between different gas compositions. For this reason, a complicated system of valves is required in order to allow variations in the feed and also in the outlets for the effluent gases. The basic process consists in four steps:

- Full oxidation of natural gas by the OC material
- Flushing (in general using steam)

- Re-oxidation of the OC with air
- Flushing

The main problems of this model are mostly related to the valves; the system needed is very sophisticated and for a full scale power plant there can be troubles in the calculation of valve size. In addition, changes in particle volume during operation are not well tolerated. This can lead to formation of fines due to particle crushing. A solution can be found in adding post reactor cyclones to remove the fines.

### Move reactor

In this approach is considered the idea of moving a fixed reactor between different gas streams. One of the most interesting examples is the study of a rotating bed reactor where the oxygen carrier material is rotated between the natural gas stream and the air stream, by means of a doughnut shaped fixed bed. To avoid the mixing of the two reacting gases is important to provide streams of an inert gas (for example steam) between them. The fact that the reaction is exothermic causes an increase in moles of gas and in gas temperature, which leads to volume expansion. For this reason a radially directed gas flow is adopted, so that the expansion can be compensated by the radial reactor volume increase.

The goals that the rotating bed reactor should reach are compactness and easiness to operate, especially in comparison with the move feed concept [13].

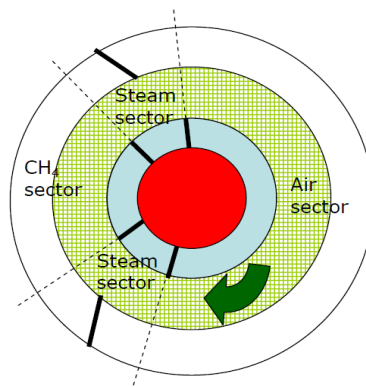
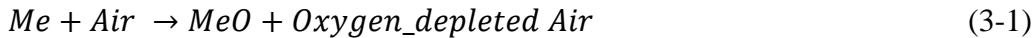


Figure 3-1: Rotating bed reactor with radial gas flow. In this drawing, the thick black lines represent separation walls, while the light blue parts are the sectors where the gases are fed, and the green area is the rotating oxygen carrier bed [13]

### Move material

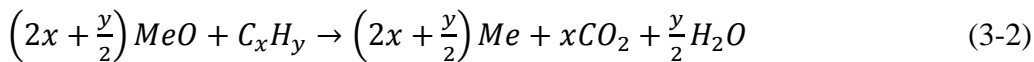
The third alternative consists in moving the oxygen carrier material.

One of the most promising and followed scheme is made of two different fluidized beds reactors where a metallic powder circulates, playing the role of oxygen carrier. This gets oxidized and then reduced cyclically: in the oxidizer (air reactor) combustion takes place, while the oxygen present in the air reacts with the oxygen carrier. This reaction is strongly exothermic, and can be schematized as it follows:



The air heated up and depleted of the oxygen can be utilized for two main purposes: steam production or expansion in a turbine, if the reaction occurs in a pressurized environment.

After that, the metal oxide generated during the oxidation is moved to the reducer (fuel reactor), where the particles are reduced by the introduction of fuel. This reaction can be endothermic or slightly exothermic, depending on the type of particles and fuel; the products are mainly CO<sub>2</sub> and H<sub>2</sub>O, as can be seen in the following:



The separation of the carbon dioxide will be complete after the condensation of the steam. It has been proved that the overall reaction (oxidation + reduction) is equivalent to the conventional combustion of the fuels, releasing the same amount of energy. Moreover, the fact that the process consists in an indirect fuel conversion in two different reactors leads to a reduction in the exergy loss. The exergy is defined as the maximum amount of available work that can be extracted from a system during a transformation from a reference state to the equilibrium. Every non-ideal process causes an exergy loss, but this can be minimized by analyzing and finding the most effective energy management. A way to increase the overall energy conversion efficiency of the process is the integration of energy with a low exergy rate into energy with higher exergy rates, where the exergy rate is the ratio between the usable work



and the total amount of energy. During the chemical looping combustion, low grade heat is recuperated while producing a larger amount of high grade heat.

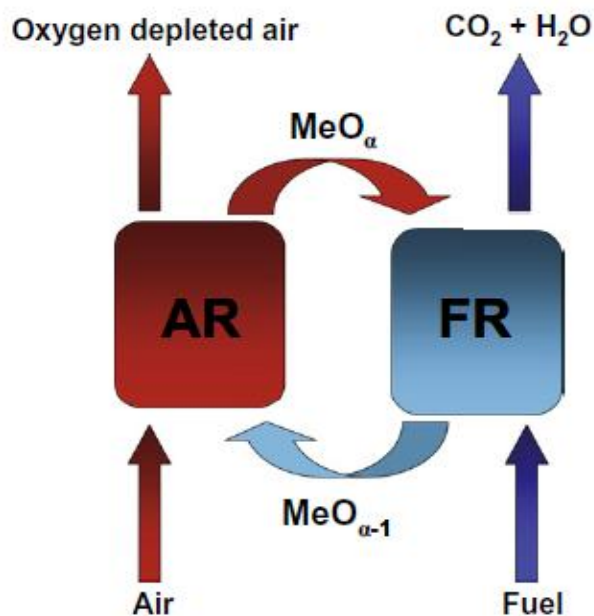


Figure 3-2: Basic scheme of chemical looping combustion [3]

Most of the chemical looping combustion cycles are designed to operate with a solid oxygen carrier. It was proved, however, that by using liquid and particularly gas phase carriers the thermodynamic advantages of CLC can be maximized. Richter and Knoche suggested as a possible carrier Cadmium; this should have been in vapor or liquid phase for at least part of the cycle. After that, another suggestion came from McGlashan et al.: using Zn as a carrier the cycle could have reached high theoretical efficiency and for this reason there could have been the possibility of generating both hydrogen and power. Recently, another model was proposed, using Na instead of Zn. This choice was made because  $\text{Na}_2\text{O}$ , the principal Na oxide stable at high temperature, is in the liquid state while produced in the oxidizer (that means less difficulties in transfer it to the reducer and less fouling in the reactors). This method has advantages as well as disadvantages; many issues have still to be solved, from corrosion problems due to the high reactivity of Na, to errors caused by the assumption of considering ideal liquid mixtures [14].

In general, further improvements are strongly requested for gaseous fuels: they require an increase in fuel and metal oxide conversion efficiencies in the reducer, or anyway a minimum carbon deposition, higher solids circulation rates and reactor dimensions. Thus, solid fuels are gaining importance, especially because of their potential economic impact. However, even in this case there are still a lot of unresolved questions, mostly concerning ash removal, solids feeding and mixing, solid fuel conversion, OC interaction with pollutants like sulfur or mercury [4]. Moreover, the oxygen carrier should respond to precise criteria, which will be soon presented.

Before introducing in details the model developed by SINTEF Energy Research and Norwegian University of Science and Technology (NTNU), some issues about particles and hydrodynamics have to be discussed.

## 3.2. Hydrodynamics

### 3.2.1. Regimes of Fluidization

“Fluidization is defined as the operation through which fine solids are transformed into a fluid-like state through contact with a gas or a liquid” [15].

Different hydrodynamic regimes of fluidization can be obtained, as the gas velocity increases. Considering a bed of granular solids on the bottom of the column, the injection of gas through it will cause the changing of the regimes, as shown in the picture below [16].

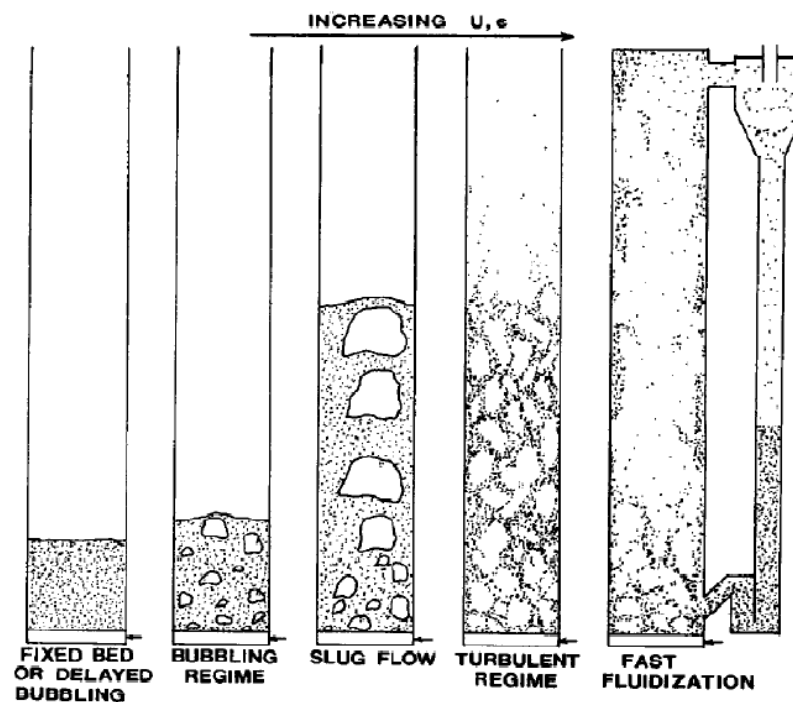


Figure 3-3: Hydrodynamics regimes of fluidization. The transitions between one and the other are due to variations in the gas velocity ( $U$ ) and in the voidage ( $\epsilon$ ) [16]

When the velocity of the gas injected is very low, the particles lay stationary on the bottom part of the column, creating a fixed or packed bed, where the gas flows through interstices in the solids. In this type of bed, solids are not able to move respect to each other, even if it is possible to have moving packed bed where the particles are in motion respect to the walls of the column.

Increasing the velocity of the gas, the first change occurs, the result being the presence of bubbles and thus the starting of the bubbling phase. The bubbles, which can be considered gas voids where the presence of solids is little or even null, are surrounded by the so called emulsion phase, i.e. the gas-solid suspension. The bubbles will rise in the bed, thanks to the buoyancy force, transporting the gas from the bottom to the top of the column [15]. Transition from fixed bed to fluidization is reached when the velocity equals the value for the minimum fluidization velocity, i.e. the lowest gas velocity that allows the suspension by the gas for all the particles contained in the bed [17]. The bubbles form as soon as the superficial gas velocity equals the value for the minimum bubbling velocity. All these values for the velocities have been estimated by scientists and can be calculated by means of dimensional correlations.

Increasing further the superficial gas velocity, the dimensions of the bubbles increase. When it is reached a size comparable to the width of the bed (or the column diameter), the transition to the slug flow occurs. In this regime, bubbles flows through the bed as a slug. Even in this case is possible to estimate a minimum slugging velocity thanks to previous studies. However, the slugging phase does not occur always: it is impossible when having shallow beds, columns with very large diameter or very fine particles ( $d_p < 60 \mu\text{m}$ ), because it would be impossible for the bubbles to reach dimensions that can be compared to the column diameter.

Going even higher with the velocity leads to turbulent beds, in which rapid coalescence and breakup of bubbles can be observed. For this reason, it cannot be identified a proper bubble phase, but there will be a high expansion characterized by violent activities and particles thrown away from the bed surface. Visually, in the flow will still be found voids, like in the previous ones, but here they will be considerably smaller and more regular [16]. This regime has a lot of advantages while doing the comparison with the lower velocity regimes. First, the heat transfer is increased, due to a much higher value for the heat transfer coefficient, caused also by the fact that it is obtained a better gas – solids contact. Moreover, the temperature will be more uniform than in the other cases.

Heat transfer coefficients are further increased with the transition from turbulent regime to fast fluidization that occurs, as in the previous cases, when the superficial gas velocity is increased. Here the interface between the dense bed and a more dilute freeboard region becomes less and less distinct. Visually, the main features of this regime are the presence of clusters,

continuously forming and disintegrating, moving up and down in a flowing gas – solid continuum, high slip velocity between the solids and the gas, and the best mixing achievable. Having an excellent contact between solids and gas deals also to an even more uniform temperature in the system and to the fact that the residence time distribution for the particles can be considered almost equal to the one related to the condition of perfect mixing.

The effects of the different variables on fluidized bed are shortened in the following table.

Table 3-1: Features of fluidized beds in different flow regimes [18]

| Flow regime       | Superficial gas velocity | Residence time of gas and solids | Contact between solids and gas | Height of reactor | Reactor diameter | Solids inventory | Solid conveying |
|-------------------|--------------------------|----------------------------------|--------------------------------|-------------------|------------------|------------------|-----------------|
| Bubbling bed      | Low                      | Long                             | -                              | Low               | Bigger           | More             | -               |
| Turbulent bed     | Medium                   | Short                            | +                              | Medium            | Big              | More             | -               |
| Fast fluidization | High                     | Shorter                          | +                              | High              | Small            | Less             | +               |

### 3.2.2. Circulating Fluidized Beds

A consequence of the existence of several regimes of fluidization is the presence of different configurations to choose to reach the established contact between solids and gas in order to have the desired reactions.

Fixed beds were already mentioned. Those, as well as fluidized beds, characterized by the fact that a distributor situated in the bottom of the column is used to introduce gas or liquid that support the particles, have been widely utilized in combustion processes.

In the past two decades another kind of beds has gained more and more importance, especially when dealing with major applications. It is the case of circulating fluidized beds (CFB); a

general understanding of how they work can be found just analyzing the name. ‘Circulating’ is referred to the fact that the solids, usually introduced near the bottom of the column, should be entrained to the top by a sufficient upwards flow of fluid (in the riser), but then the majority of them should be captured and returned continuously to the bottom (through the downcomer). ‘Fluidized bed’ underlines the need for the particles to be supported by a fluid [17].

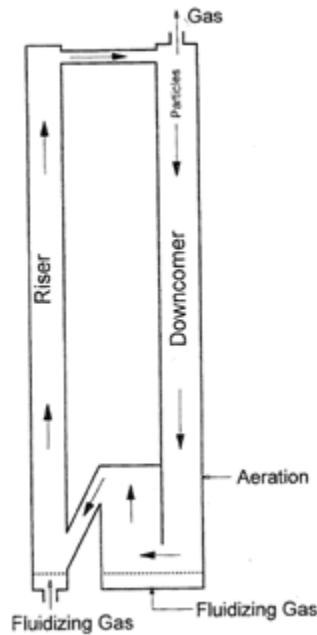


Figure 3-4: Basic scheme of a circulating fluidized bed system [17]

The CLC reactor system designed by SINTEF and NTNU take advantage of this technology.

### 3.3. Particles characterization

In order to analyze the behavior of the system is important to pay attention to the particles and their characteristics.

Two parameters are used to characterize the particles in a circulating fluidized bed. These are sphericity  $\Phi_s$  and equivalent spherical diameter  $d_{sph}$ , and they are defined as it follows:

$$\Phi_s = \left( \frac{\text{surface of a sphere}}{\text{surface of a particle}} \right)_{\text{same volume}} \quad (3-3)$$

$$d_{sph} = \left( \frac{6 \cdot V_{particle}}{\pi} \right)^{\frac{1}{3}} \quad (3-4)$$

Multiplying the two parameters, the particle size  $d_p$  can be found. All the particle properties depend from this value. For example, reducing it the particle strength is increasing, and phenomenon like agglomeration become more important, because of a greater surface/volume ratio for the particles. Other than that, more difficulties will be found in particle separation, while there will be higher reactivity and solubility due to the increase of the specific area (defined as surface area of the particle divided by its volume).

Moreover, attention should be paid to the type of particles involved. In fluidizing solids with gases four different behaviors can clearly be recognized; following the Geldart classification, these are the groups:

### **Group A**

This group includes particles that have a small mean size and/or a low density, lower than 1.4 g/cm<sup>3</sup>. These characteristics lead to bed that can expand significantly before the start of the bubbling phase, and that usually collapses slowly cutting off the gas supply.

The mixing is very quick because of the high circulation of the powder obtained even when there are few bubbles.

### **Group B**

Here we have materials with mean size between 40 μm and 500 μm and density between 1.4 g/cm<sup>3</sup> and 4 g/cm<sup>3</sup>. Bubbles start to appear at the minimum fluidization velocity of just above it. The bed does not expand considerably and collapses very quickly when cutting off the gas supply. While not in the bubbling phase, the circulation of the powder is very little or absent.

### **Group C**

In this group we find all the particles that are in any way cohesive. The inter-particle forces are higher than the ones that can be exerted on the material by the gas, and this makes the fluidization of the particles extremely difficult. It is not impossible though, in fact it can be reached with the help of vibrators or mechanical devices.

Anyway, for particles belonging to this group the mixing is very low and thus the heat transfer between the bed and a surface decreases, compared to what happens for materials belonging to the other groups.

### **Group D**

This last category comprises large and/or very dense particles.

Even in this case the solids mixing are very poor, and the flow regime can be turbulent leading to problems due to particle attrition.

However, the fluidization can be obtained in the case of relatively sticky materials, because of the risk of agglomeration is avoided by large particle momentum and low particle-particle contacts.

A certain type of bed, defined as spouted bed, can be formed with these materials, if the gas is injected only through a hole located in a centered position. [19]



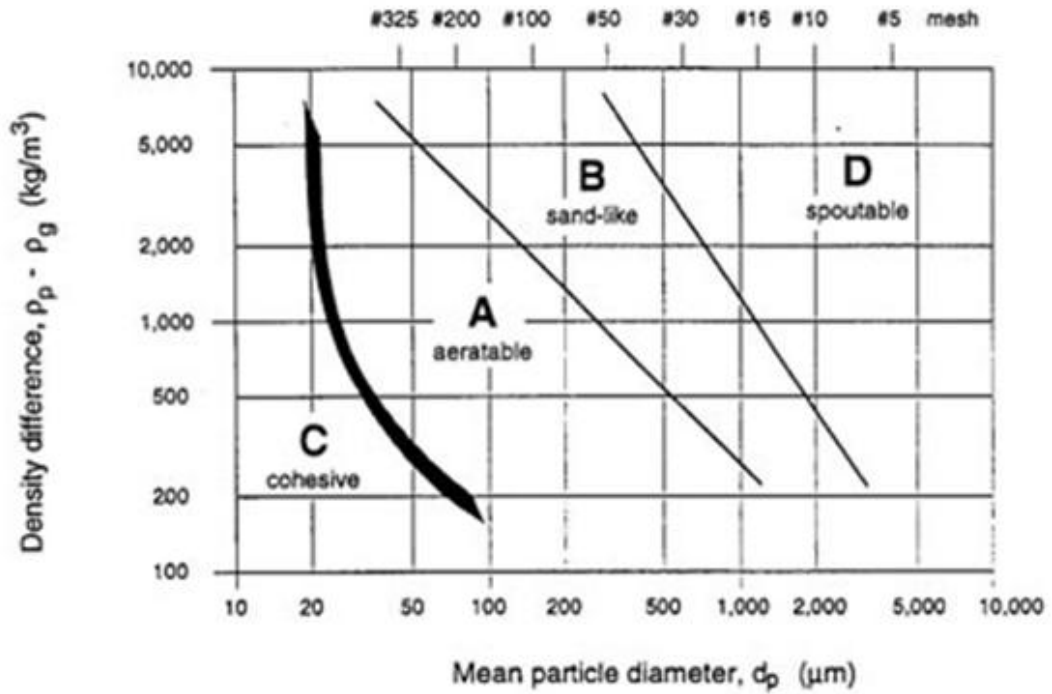


Figure 3-5: Geldart's particle classification for fluidization [19]

The particles used in the reactor built by SINTEF and NTNU should belong to the group A in order to reach the established fluidization regime and adequate mixing and heat transfer<sup>4</sup>.

<sup>4</sup> More info at section 3.5.1

### 3.4. 150 kW<sub>th</sub> DCFB CLC reactor – Hot rig

Following the described principles of the third alternative for chemical looping combustion, SINTEF Energy Research and Norwegian University of Science and Technology – NTNU have designed a 150 kW<sub>th</sub> double loop circulating fluidized bed reactor system (DLCFB), aimed to work as a steam boiler. Other than for chemical looping combustion, this system is meant to be able to operate also as a chemical looping reformer (section 5.4.4) The main purpose of this project is to be strongly industrial oriented in order to make the step from lab-scale to industrial application easier. Before being able to build the hot rig, however, it was necessary to design a cold flow model (CFM), in which there are no chemical reactions, to verify the hydrodynamic viability of the system and to predict the gas and the solids behavior [20]. In the CFM, air will be used as a fluidizing medium, while the hot rig is designed to operate with steam.

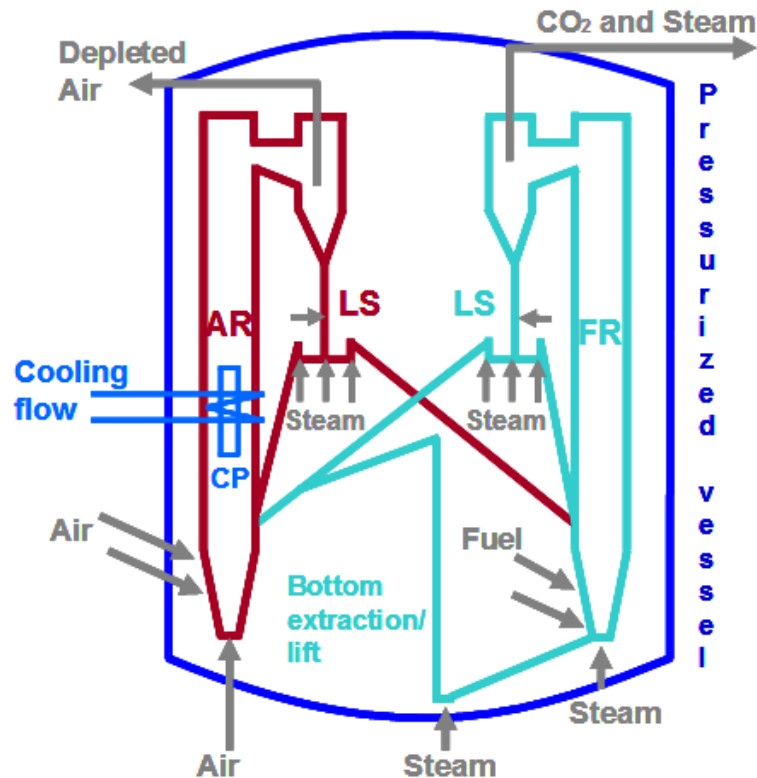


Figure 3-6: Process diagram of the CLC rig [3]

In order to develop the project in an industrial context, the system has to be very compact. Other advantages derive from this quality: the costs will be reduced because of the smaller

amount of the material required and of the easier handling; the quantity of the material not taking part of the reactions (“parasitic” oxygen carrier) will be reduced [3].

Regarding the hydrodynamics, in this system both the AR and the FR are circulating fluidized beds. For this reason, the rig can be called double loop circulating fluidized bed reactor system (DLCFB): two loops are present, and the coupling of the two reactors is possible thanks to the presence of two essential components, the loop seals. These are the elements that allow the circulation of the solids between the reactors.

Moreover, the FR is designed to operate in a fast fluidization regime in order to have all the advantages previously discussed: a better gas – solids contact with a higher fuel conversion, maximizing the solids concentration in the upper part (exit) of the reactor while minimizing it in the bottom part, having in this way a more homogeneous particle distribution and a steep concentration profile in the FR (but not vertical) [3]. The AR can operate in turbulent or fast fluidization. To decide which one is the best, the oxygen conversion X (which will be presented in section 3.1.1) should be calculated; then should be chosen the option that allows the higher X.

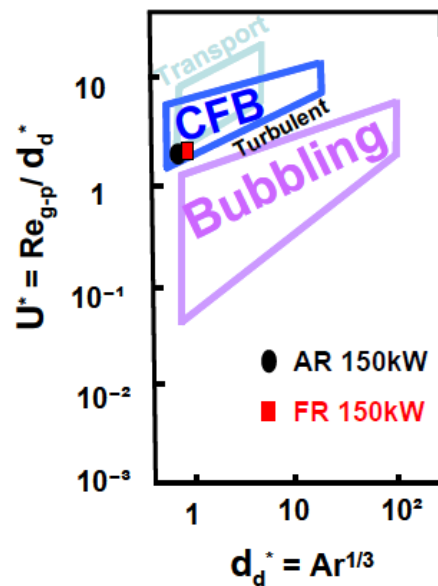


Figure 3-7: Fluidization regime of the AR and FR according to the classification of Lim et al., 1995[3]

The injection of steam, air and fuel is one of the key factors that help making it possible to control the hydrodynamic behavior of the system, and it is accomplished using injection nozzles, located in strategic places in such a way to obtain the required fluidization regime. Each reactor is equipped with three injection nozzles: the primary one, located at the bottom of the reactor, and two levels of secondary ones, placed above, but still along the bottom part of the reactor. This part should not be perfectly cylindrical; instead, the section should be tapered, in order to avoid the presence of particles agglomerates increasing the gas velocity in that area. Other than that, a uniform superficial gas velocity profile across the secondary air injections would be achieved, dealing to a more even acceleration of the solids, closer to the conditions of fully developed flow. Both the reactors are then also equipped with a heavy load cyclone, integrated into the external solids recycle loop, to perform the particle separation from the exit air and fuel streams. To avoid particle losses, their role is essential, especially when dealing with gas turbine application, where the fluid circulating in the system must have precise characteristics, not to create problems or malfunctions. More about the cyclones will be discussed in the following section. Moreover, the rig needs a cooling system. The cooling panels selected are integrated into the reactor body and they are a type of industrial protruding panels. Their position should be established after some considerations. In fact, not only they cannot be placed too close to the exit of the reactors because they will cause problems in the solids flow, but also not too close to the bottom part because they could disturb the achievement of a fully developed solid flux [3]. Besides, to further increase the circulation between the reactors, and especially the solids entrainment from the fuel to the air reactor, a lift was added to the design.

To better understand the behavior of the rig and the process, insights about some important issues are needed, other than more details about the components of the system.

### **3.4.1. Oxygen Carrier**

Choosing the best oxygen carrier is crucial in the development of the CLC reactors, because it affects the oxygen transport, therefore the reaction and the behavior of the whole system.

It will depend on the type of fuel used, but it should have:

- high mechanical stability, in order to sustain several oxidation-reduction cycles without showing signs of chemical or mechanical degradation and to avoid a loss of reactivity;
- high oxidation and reduction reaction rates, to limit the necessary residence time;
- high enough oxygen transportation capacity, to reduce the necessary solids circulation rate in the CLC;
- good resistance to attrition;
- high availability;
- low cost;
- environmental harmlessness, in such a way to be acceptable to health, safety and environment (HSE) standards in force [4].

Other than that, specific properties have to be analyzed to characterize the oxygen transport capability of oxygen carriers and to evaluate the necessary solid circulation rate in a chemical looping system.

- Oxygen Ratio

$$R_0 = \frac{M_{OC,ox} - M_{OC,red}}{M_{OC,ox}} \quad (3-5)$$

Where:

$M_{OC,ox}$  = molar mass of fully oxidized OC

$M_{OC,red}$  = molar mass of fully reduced OC

This parameter can be defined as the ratio between the mass of oxygen in the fully oxidized material and its total mass, and it is an index of the maximum quantity of oxygen that can be theoretically extracted from the air. The higher  $R_0$ , the less solid circulation is required to the functioning of the rig.

- Conversion (degree of oxidation)

$$X = \frac{M_{OC,actual} - M_{OC,red}}{M_{OC,ox} - M_{OC,red}} \quad (3-6)$$

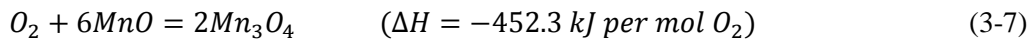
Where:

$M_{OC,actual}$  = actual molar mass of OC

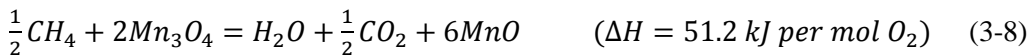
This parameter consists in the ratio between the actual mass of oxygen in the OC and the maximum quantity of oxygen in the fully oxidized state, and it is important to state the difference between the conversion at the entrance of one reactor and its exit ( $\Delta X$ ) that can be seen as an index of the exploitation of the maximum oxygen capacity. The higher the conversion difference between the two reactors, the lower is the necessary solid circulation rate, while there is an increase in the necessary solids inventory due to the smaller amount of oxidized oxygen carrier particles in the fuel reactor.

Based on the 2010 study of Fossdal et al. at SINTEF Material and Chemistry about industrial tailings and by-products, the choice of the most promising material to be used as an oxygen carrier was made, and a specific manganese ore was selected. At the design temperature of 1000°C, the oxides present in the reducer and in the oxidizer will be MnO and Mn<sub>3</sub>O<sub>4</sub>. The reactions, considering methane the reference fuel, will be:

- Oxidation in the AR

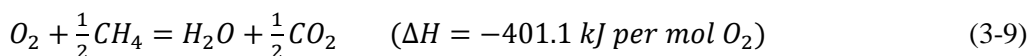


- Reduction in the FR



Where  $\Delta H$  is the variation of enthalpy that occurs during the reaction.

Thus, the overall reaction will be:



In this way the oxygen ratio  $R_0$  for the CLC cold rig proposed by SINTEF and NTNU will be equal to 0.07. However, it was established that the manganese oxide alone was not sufficient to meet the required mechanical strength. For this reason 40÷45% of manganese ore, on a weight basis, was mixed with an inert support material like alumina,  $Al_2O_3$ , decreasing the value of the oxygen ratio to 0.03. In the meantime, considering the residence time of the OC particles in the FR as being equal to 8 seconds (results evaluated from tests on the cold rig, [3]) and knowing the reversible oxygen capacity of the manganese ore (measured without inert support)  $\Delta X$  will be around 0.2. Thanks to these values is possible to calculate the required OC mass flow between AR and FR, depending on the fuel input. So, 12  $g/s$  of oxygen are needed to fully oxidize the fuel in the case of the 150  $kW_{th}$  rig. Exploiting 20% of the maximum oxygen ratio  $R_0$  of 3% the OC mass flow required will be 2  $kg/s$ .

However, it has to be pointed out that there will be a variation in density of 14.9% because of the transition between  $MnO$  and  $Mn_3O_4$ ; this can lead to stress and fragility for the material. For this reason, it was decided by Fossdal et al. (2010) to add calcium in such a way to obtain perovskite phases, gaining a better mechanical stability. In this way, the value for  $R_0$  will further decrease to 0.056, even if fundamental parameters like the kinetics and the reversible cyclic capacity will not be too different from the ones obtained in the case of pure manganese ore, there will be just a variation in the  $\Delta H$  calculated for the oxidation and reduction reactions [3].

### 3.4.2. Components

The 150 kW<sub>th</sub> DLFCFB CLC reactor (hot rig) consists of the following different components: loop seal, downcomer, lifter, air reactor riser, fuel reactor riser, cyclone and also some measurement equipment. In the following section the different parts are explained briefly.

#### 3.4.2.1. Loop seals (LSs)

The key factor for a good operation of a circulating fluidized bed is assuring the solids movement in an endless loop. To obtain that, particular devices should be used, and as long as the amount of particles to be moved is usually very large, these devices should be non-mechanical, to avoid possible wear or seizure and higher costs. Furthermore, between the possible choices the best seems to be the loop seal.

As already mentioned, it is a non-mechanical device, i.e. just aeration gas is required to govern the flow rates of solids.

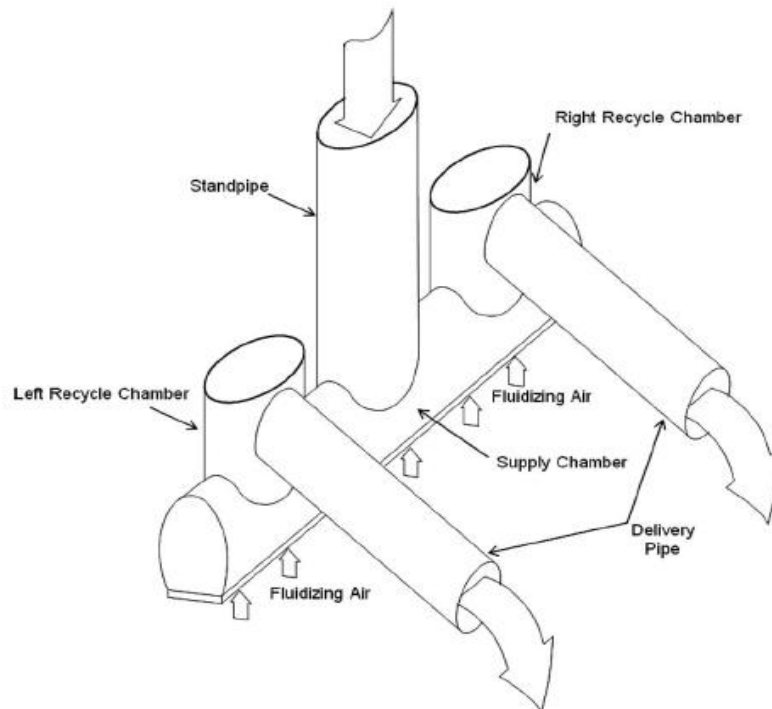


Figure 3-8: Schematic drawing of the loop seals used in the CLC Model developed by SINTEF and NTNU





Figure 3-9: On site picture of loop seal which is used in Cold Flow Model rig

A loop seal usually consists of different sections. The ones in the model designed by SINTEF and NTNU are divided into a supply chamber and two recycle chambers (because of the two coupled reactors; just one is needed when having one reactor), and their main goal is to prevent unwanted gas mixing between the two reactors. The supply chamber is situated in the bottom section of the standpipe (or downcomer) and its aim is to supply the solids to the recycle chambers, which will transfer them to air and fuel reactor respectively by means of fluidization that will allow them to behave like a liquid [15]. Three injection nozzles are in place, one at the bottom of each section. They provide air injection for the CFM; it will be steam injection for the hot rig. They can be regulated in order to reach the desired level of fluidization and to control the distribution of the solids flow between the two exits. Other than those three, there is another air injection, which is usually situated in strategic places in the loop seal, called grease air. The aim of this air is to help the movement of the solids through the system: in fact it reduces not only the friction between the wall and the particles, but also the inter-particle frictional forces, acting like a lubricant. The amount of air injected should be strictly controlled to avoid problems; it should not exceed the minimum fluidization velocity for the average particle size of the circulating solids [15].

A fundamental parameter, while analyzing this component, is the loop seal exit pressure. This value has to be higher than the pressure in the bottom of the reactors; if this condition is not accomplished, there will be no pressure seal in the loop seal.

### 3.4.2.2. Cyclones

As already mentioned, large cyclones are required in circulating fluidized bed reactors to perform an efficient separation of the solids flowing in the system.

The mixed stream enters the cyclone from the top and is exposed to a radial centrifugal force. In this way, the solid particles will strike the outside wall and exit the component from the bottom end, while the air will flow in a spiral pattern from the top to the bottom, exiting then on the top, following a straight path in the center of the cyclone.



Figure 3-10: Picture of the Cyclones which are used in the Cold Flow Model rig

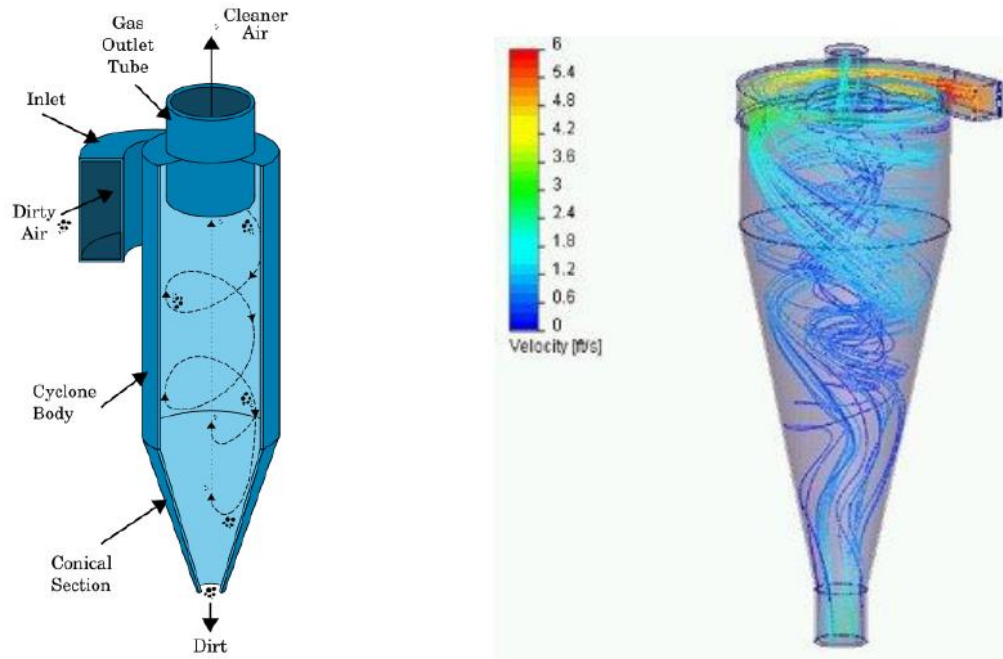


Figure 3-11: Typical cyclone configuration (Left), Flow simulation of a cyclone separator (Right) [21]

The cyclones used in the CLC rig proposed by SINTEF and NTNU are heavy load cyclones. That means that they are designed to deal with a high amount of solids in the gas stream. Their efficiency has to be as high as possible in order to satisfy particle emissions requirements, other than making possible for the system to be integrated in a gas turbine cycle, reducing the oxygen carrier refilling and thus the operational costs.

Several studies have been developed on the design of the cyclones for circulating fluidized bed reactors to find a configuration which allows the achievement of all the targets just discussed. However, the knowledge is still limited and still the proper design has not been found. It is proved, nevertheless, that the maximal achievable separation efficiency is usually higher while increasing the solids load, because of the formation of strands in the inlet area of the cyclone. To increase the separation efficiency is also essential that the gas-solids suspension entering the cyclone is continuously accelerated, to have a higher solids momentum flux in the inlet part. In addition, another factor that concurs to reach the same goal is having fine particles with

a narrow particle size distribution, as long as it also causes an increasing solids momentum flux [22].

### 3.4.2.3. Reactors risers

The risers are represents the places where the reactions take place.

In the AR riser, the oxygen carrier is oxidized by the air injections (primary, secondary one, secondary two). This reaction is strongly exothermic and, considering a reactors temperature of 1000 °C, the heat release in the AR will be 169.1 kW. To survive this high temperature, proper insulation and cooling panels are required. At the top of the reactor is situated the exit section for the depleted air.

In the FR riser the reduction reaction takes place. The oxidized oxygen carrier is introduced in the bottom part of the reactor, where it is fluidized with the injections of steam and gaseous fuel, reaching usually the fast fluidization regime. The injection of steam is essential to achieve the desired fluidization regime, securing sufficient gas velocities and good gas-solid contact. It is used steam instead of air to avoid possible reactions with the fuel.

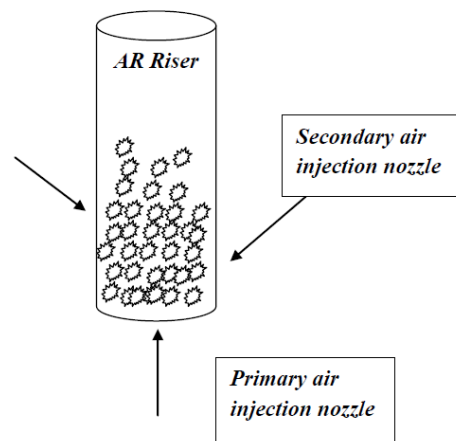


Figure 3-12: Place of different nozzles in the riser

#### 3.4.2.4. Reactors Downcomers

The downcomer is the pipe used to connect the cyclone to the loop seal; thus, it transports the particles from a low pressure area to a high pressure area, just taking advantage of the gravitational force.

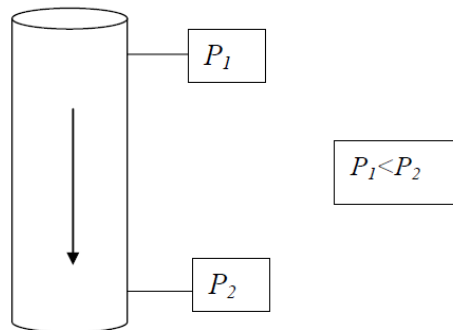


Figure 3-13: Simple sketch of Downcomer

#### 3.4.2.5. Lifter

As already mentioned, the lifter is a pipe added to design in order to further enlarge the exchange of mass between the two reactors, and especially from the fuel reactor back to the air reactor. This is obtained thanks to the presence of two steam injection nozzles, the primary one placed in the bottom part and the secondary one higher in the lifter. Other than that, the pressure difference between the reactors helps the solids flow: in fact, the pressure is usually higher in the bottom of the FR.

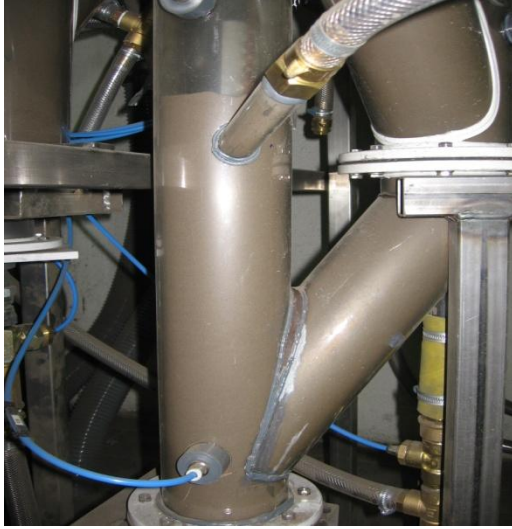


Figure 3-14: On site picture of Lifter

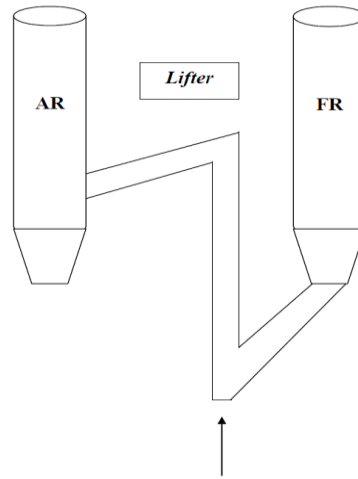


Figure 3-15: Schematic of Lifter

### 3.4.3. Design Parameters and Main Dimensions

Table 3-2 shows the main design dimensions and parameters for the Chemical Looping Combustion.

Table 3-2: Design parameters for the CLC rig

| Design parameters                         | Value       | Unit                 |
|---|-------------|----------------------|
| Fuel Thermal input                        | 150         | [kW <sub>th</sub> ]  |
| Excess air ratio ( $\lambda$ )            | 1.2         | [-]                  |
| Fuel LHV (methane)                        | 50.01       | [MJ/kg]              |
| Reactors design temperature               | 1000        | [°C]                 |
| Oxygen carrier oxygen ratio $R_0$         | 0.03        | [-]                  |
| Oxygen carrier conversion $\Delta X_{FR}$ | 0.2         | [-]                  |
| Oxygen carrier circulation rate           | 2           | [kg/s]               |
| Heat release AR                           | 169         | [kW]                 |
| Heat release FR                           | -19         | [kW]                 |
| Particle diameter $d_{50}$                | 70          | [ $\mu\text{m}$ ]    |
| Particle density                          | 2000        | [kg/m <sup>3</sup> ] |
| Particle sphericity                       | $\approx 1$ | [-]                  |
| AR diameter                               | 0.25        | [m]                  |
| FR diameter                               | 0.15        | [m]                  |
| Reactor height                            | 5           | [m]                  |

### **3.5. 150 kW<sub>th</sub> DCFB CLC reactor – Cold Flow Model**

To better investigate the hydrodynamic behavior of the double loop circulating fluidized beds system different options can be used. A Computational Fluid Dynamics analysis is often chosen to have a more detailed simulation of which conditions are going to be achieved. In the industrial field, however, is usually preferred the scaling strategy, which consists in building a smaller model operating at ambient conditions instead of high temperatures. This was the option selected by SINTEF and NTNU. A 1:1 scaled cold model of the hot rig was built, using air injection to simulate steam injection, and non-reacting metallic powder instead of the oxygen carrier.

This choice allowed the possibility of testing the components design. The goal was to find a way to operate the single components, loop seals, cyclones, risers and lifter, and the whole system, in order to reach the desired flow regime, a high gas-solids contact efficiency, and a good solids circulation rate between the reactors, as long as a good solids distribution in the riser. All these objectives can be achieved finding the optimal volume flows for each air injection nozzles, trying always to maintain a certain mass balance between air and fuel reactor. A way to analyze the hydrodynamic behavior of the rig is plotting the pressure profiles of the reactors as a function of height.

Before introducing the experimental part, the scaling strategy will be briefly explained.

#### **3.5.1. Scaling strategy**

A fundamental feature, studied in the development of the cold flow model design, is the maintenance of scaling relationships. Without paying attention to this, in fact, the simulation of the hydrodynamic behavior of the rig would not be trustworthy.

The approach used by SINTEF Energy Research/NTNU can be defined a ‘triangular correlation’, as shown in the picture below.

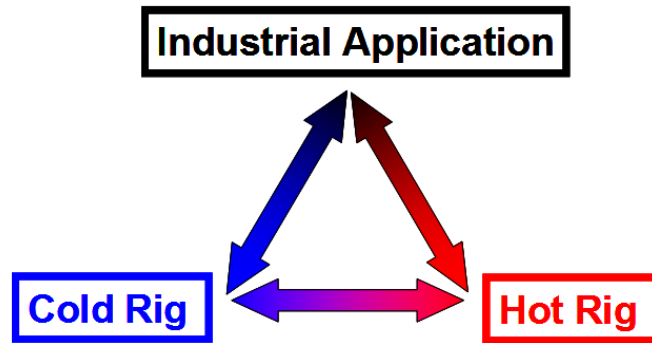


Figure 3-16: Triangular scaling strategy [20]

The first design was the one regarding the hot 150 kW<sub>th</sub> rig. After that, an estimation of the industrial prototype was made, deciding to set the thermal load around 15 MW<sub>th</sub> (that means increasing the diameter of a 10 factor). The industrial application had some certain values in common with the hot rig, namely operating temperature and pressure, particle size distribution and sphericity, gas composition. Other parameters, like the gas velocity, are established in a way so that they can assure the achievement of the desired fluidization regime. The last step was the design and building of the cold rig, following a 1:1 scale compared to the hot rig.

In this case the Glicksman scaling relationships were used. They can be obtained after non-dimensionalizing the equations for conservation of momentum and motion regarding to the fluid and the particles. These equations are considered the most precise and useful when dealing with scaling between cold and hot models. Actually two different sets of equations exist: the full and the simplified set. In the former, the non-dimensionalizing leads to several dimensionless parameters. However, it is usually complicated and impractical to match all these parameters in the design of the models, especially because they imply restrictions to the dimensions of the cold rig: it has to be ¼ of the original atmospheric one. In this case a higher freedom was required, in order to be able to choose a different scale. Thus, the simplified set was selected. This set is valid only for high or low Reynolds particles numbers: in the case of the cold CLC rig proposed by SINTEF and NTNU, Re is low, so the reduced version of the equations is applicable.

The dimensionless parameters to analyze are the following:



- Froude Number  $\frac{u_0^2}{gD}$
- Particle/gas density ratio  $\frac{\rho_p}{\rho_g}$
- Reactor height/diameter ratio  $\frac{L}{D}$
- Superficial gas velocity/minimum fluidization velocity ratio  $\frac{u_0}{u_{mf}}$
- Dimensionless flux  $\frac{G_s}{\rho_p u_0}$
- Particle sphericity  $\varphi$
- Dimensionless particle size distribution PSD

These quantities should have the same values for both the hot rig and the cold rig; thus, a lot of design parameters for the cold model were calculated as to reach this goal. However, this condition is hardly ever verified. In fact, it is very complicated to handle parameters such as particles size and density or fluidizing gas viscosity and density; moreover, it can happen that, while trying to reach the equality between the values, the changes lead to unwanted modifications in the fluidization regime and in the behavior of the system. This is the reason why several scaled cold models have mismatching for some parameters (the difference can be up to tens of percentage points).

SINTEF and NTNU decided to build a cold rig of the same dimensions of the hot one, because it was proved that the bigger the size is, the smaller is the rate of change of hydrodynamic parameters with the diameter. Regarding the particles characteristics, two different ways of calculation were investigated.

The first attempt followed the intention of verifying as much as possible the Glicksman equations (the simplified set). On top of that, in order to reach a higher precision, two dimensionless numbers were added:

- Particle Reynolds number  $Re_p$
- Archimedes number  $Ar = \rho_g (\rho_p - \rho_g) \frac{d_p^3 \cdot g}{\mu_g^2}$

This addition was made so that it would have been possible to check that the fluidization regime remained the same as the one in the hot rig. Moreover, the particles from the two rigs should have been in the same Geldart group of powder. The results of these evaluations were:

- Mass median diameter  $d_{50} = 34\mu m$
- Density  $\rho_p = 7000 \text{ kg}/m^3$

Obviously it was impossible to fulfill the similarity for all the dimensionless scaling numbers, and it was necessary to come to compromises to calculate the most effective particle characteristics.

The alternative doesn't imply any scaling calculations: the same values as the hot rig of the two parameters above mentioned have to be chosen. That means:

- Mass median diameter  $d_{50} = 100\mu m$
- Density  $\rho_p = 2000 \text{ kg}/m^3$

The velocity will be selected in a way to obtain the same fluidization regime. So far, tests were made just using the first option; the second one still needs experimentation.

Thus, after using the cold rig to establish the operating guidelines and the process control methodologies, it will be possible to build the hot rig. This will allow the analysis of start-up and shutdown procedures, of equipment reliability during long period operations and of particle attrition, issues that will be fundamental for the design of the industrial application. For information about hydrodynamics, such as residence time evaluation, pressure and particle concentration profile, solids exchange and gas bypassing, we can rely on the cold rig [20].

## 4. Experimental Part

### 4.1. Overall view of the CFM

The CFM built by SINTEF and NTNU is located inside the laboratory of the Energy and Process Department of NTNU (Varme Teknisk Laboratorie). To avoid vibrations during operation, or at least reduce them, a steel bearing structure was added to contain the rig. To further protect people working on it from unexpected explosions, a plastic-glass plate (Lexan shield) was also installed.

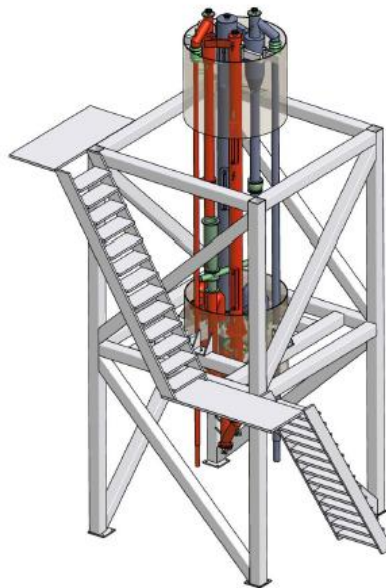


Figure 4-1: 3D CAD General assembly of reactor system

14 are the air injection points, each of them having a mass flow controller (Brooks® Mass Flow Meter Model 5863). Two are located in the lifter (primary and secondary). Then each reactor has six: three in the bottom of the different sections of the loop seal (central, external, internal section) and the other three in the riser (primary, secondary 1 and secondary 2, placed respectively at 0 m, 0.4 m, 0.8 m from the bottom).

Two flap valves are installed in the downcomers to measure the fluxes in the system.

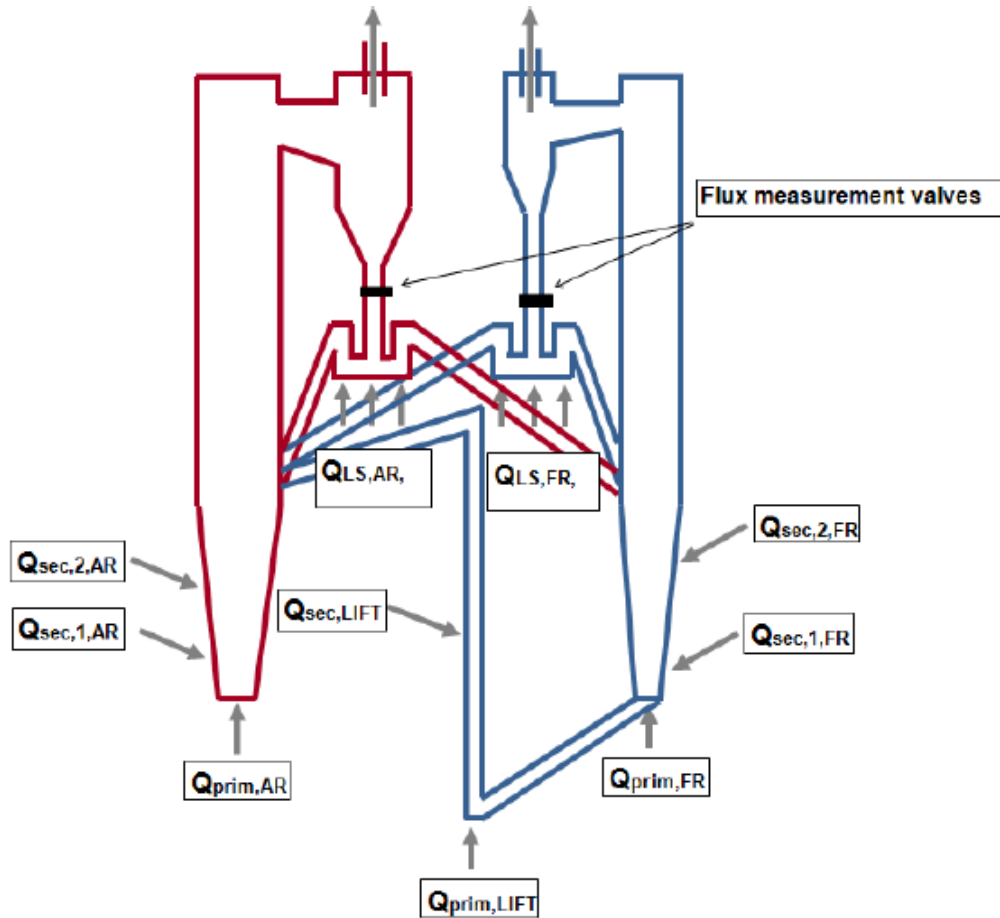


Figure 4-2: CFM scheme in which are shown all the positions for the air injections and the two flap valves.

Essential is the presence of a filter box, downstream the cyclone separators, in order to prevent the particles coming from the cyclones to escape. Extracting the particles from the filter box and weighting them allow the calculations for the cyclone efficiency, for all the different operating conditions. The particles are extracted during the experiments, after a certain amount of time that the rig has been running; this varies every time, depending on the test.



Figure 4-3: On site picture of filter box

For the particles circulating in the system, it was chosen to use Fe-Si powder, which does not react with the air injections. Other characteristics of the particles:

- Particle size  $d_{50} = 34 \mu\text{m}$
- Density  $\rho_p = 7000 \text{ kg/m}^3$
- System inventory 120 kg
- Shape: irregular

Figure 4-4, shows the PSD, both the cumulative volume and the volume frequency, measured by means of a Coulter Counter LS230. The sample was taken according to ASTM standards B 215[23].

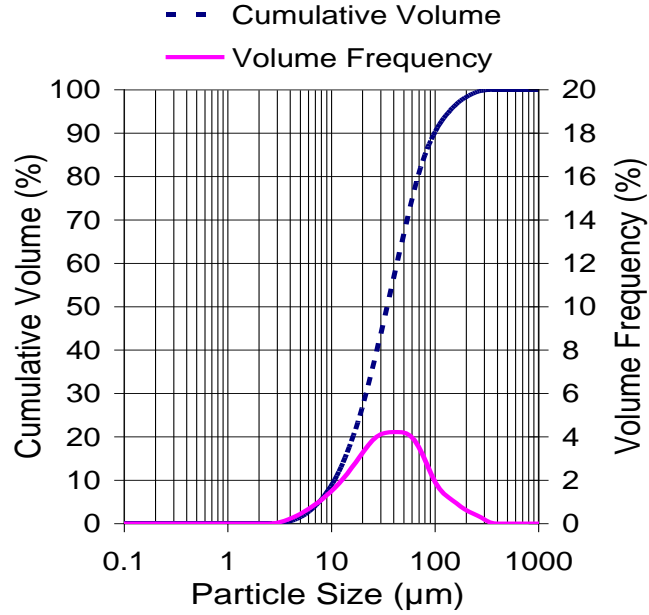


Figure 4-4: Particle Size Distribution (PSD) of the Fe-Si Powder used in the Cold Flow Model (CFM) experiments

Several pressure transmitters are installed in different points of the Cold Flow Model, selected in a way to have the measurements required to plot the pressure profiles for the reactors. Details will be added in the following section.

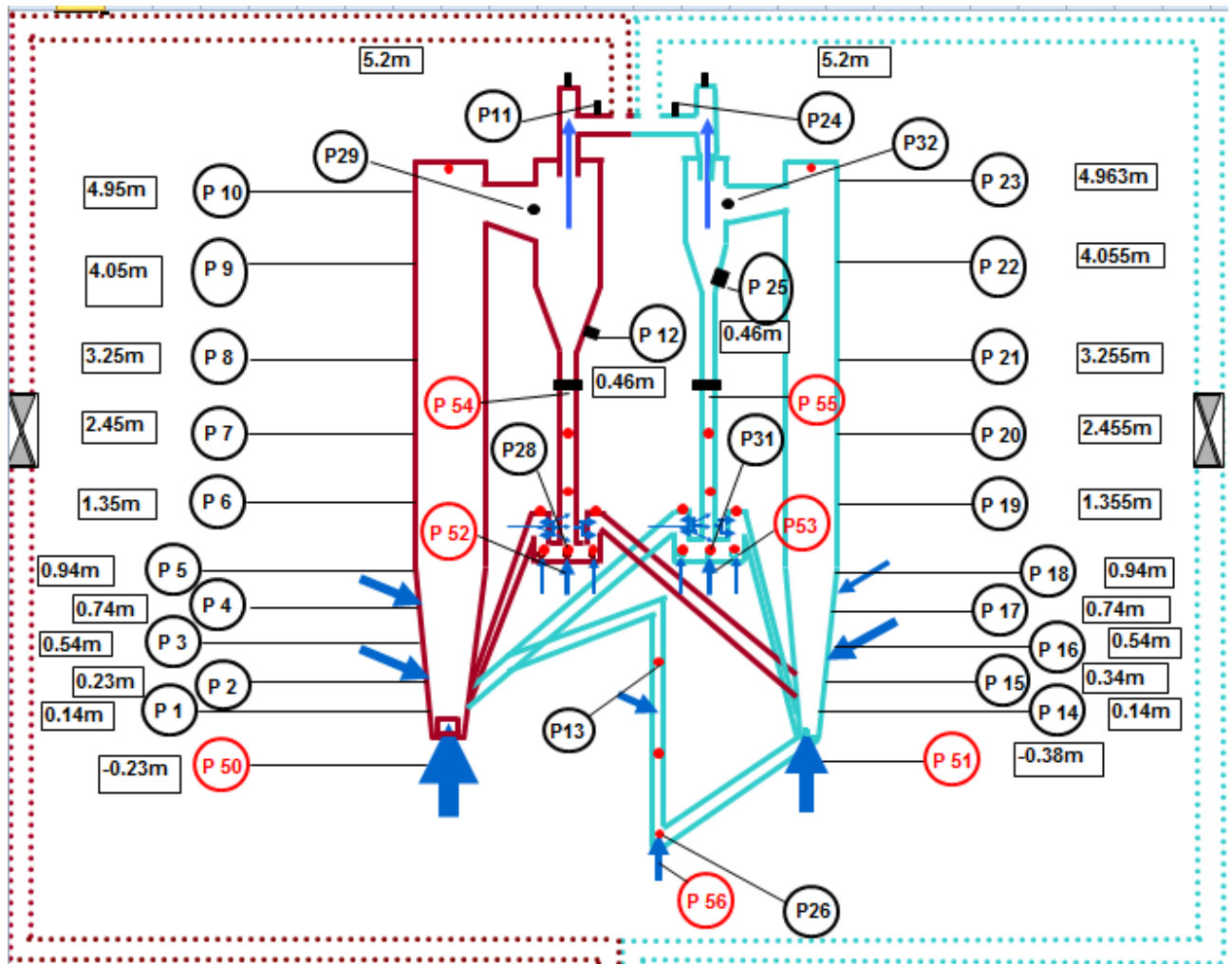


Figure 4-5: CFM scheme in which the positions of the pressure transmitters are shown.

## 4.2. Measurement equipment

### 4.2.1. Mass flow controllers (Brooks® Mass Flow Meter Model 5863)

These elements were installed in the rig so that it would have been possible to control the solids circulation and fluidization, regulating the air entering the system. They accurately measure and control the gas flow allowing the operator to perform quick changes when necessary, having a fast response to command changes. Their design was made to control the actual flow dynamics, in such a way that the transition to steady state flow would be shorter and smoother [24].



Figure 4-6: ® Mass Flow Meter Model 5863

### 4.2.2. Pressure Transducers

As shown in Fig. 23, many pressure transmitters are connected the rig by plastic tubes.

32 of them (the ones with the numbers from 1 to 26, plus 28-29, 31-32 and 74-75) are of the type Fuji FCX-AII. After setting a reference pressure, they measure the relative pressure difference.

In the SINTEF – NTNU CFM, the reference pressures are P10 for the AR and P23 for the FR, located at the top of the reactors. Their measurements are referenced to atmospheric pressure.



About P74 and P75, they were changed during the experimental campaign: at first they were, like the others, referenced to P10 and P23, respectively (and their numbers were 27 and 30; then they were modified and now they are referenced to the atmosphere, so they can be moved in different positions, according to where needed.

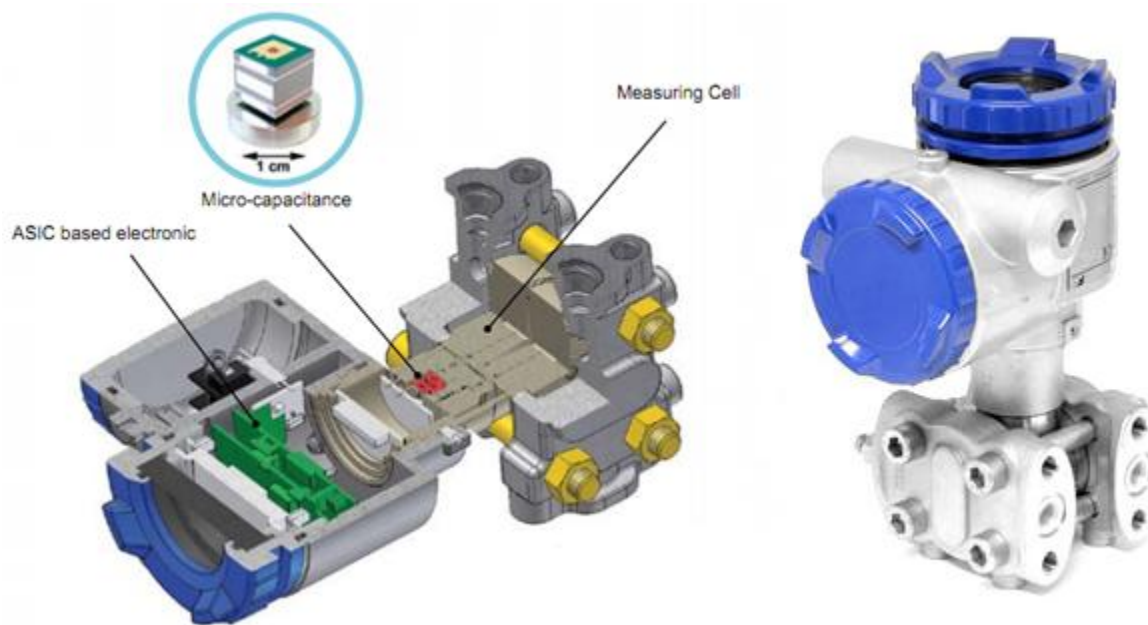


Figure 4-7: Electric FCX-AII V5 Differential Pressure Transmitters [25]



Figure 4-8: Picture of the pressure transmitter which are in used in the Clod Flow Model rig

Other 11 PTs are installed in the system. They all are referenced to the atmosphere. 7 have the numbers from 50 to 56, and they are plugged in the reactors in established places. They are of the type LAB TP14, with 2.5 mbar accuracy. The other 4 (70 – 73) are meant to be moved where required, depending on which part of the system the tests are focusing on. The type is the same of the previous 1-32.

All the PTs were calibrated individually at two different points: high and low pressure, in order to have a linear conversion curve, used then to have a pressure reading proportional to the digital current signal.

Moreover, all of them (apart from 50-56) are equipped with a flushing device, i.e. the tubes that connect the PTs with the rig are coupled by a magnet valve that allows the so-called flushing: a countercurrent air flow applied to the tubes, to avoid possible errors in the measurements caused by presence of solids inside the tubes.

### 4.2.3. Scales

Two are the scales used in the CFM. One is used for online scaling of the particles collected in the filter box; the other one is used to weight the new particles that have to be added to the system during the experiments to compensate the losses, in order to have always the same inventory.

The weights are of the type Mettler Toledo XS 32000L, characterized by a high accuracy.



Figure 4-9: Mettler Toledo XS 32000L

Table 4-1: Technical data for the weight Mettler Toledo XS 32000L

| Technical data  | XS32000L   |
|---|--|
| Stand alone weighing platform   | X32000L  |
| Maximum capacity  | 32100 g  |
| Readability   | 1 g  |
| Repeatability (sd)  | 600 mg   |
| Linearity   | 600 mg   |
| Eccentric load deviation (test load)                                    | 1 g (10 kg)  |
| Sensitivity offset  | $6 \times 10^{-5} \cdot R_{nt}$                    |
| Sensitivity temperature drift   | $1.5 \times 10^{-5} / ^\circ\text{C} \cdot R_{nt}$ |
| Sensitivity stability   | $5 \times 10^{-5} / a \cdot R_{nt}$                |
| Settling time   | 1.2 s  |
| Interface update rate   | 23 /s  |
| <b>a= year, <math>R_{nt}</math>= net weight, sd= standard deviation</b> |  |

### 4.3. Software (LabVIEW)

To operate the model and for the data acquisition, LabVIEW was used to design a control system. Meaning Laboratory Virtual Instrumentation Engineering Workbench, LabVIEW is the development environment for a visual programming language from National Instruments, producer of measurement equipment.

The peculiarity of this language is that of being graphic; in fact it is called G-language, short for Graphic Language.

In the CFM it is extremely important, because it is the feature that allows operating the system, controlling and monitoring the air flow through the injection nozzles other than monitoring the pressures in all the different positions on the reactors. It is also used to perform the flushing for the pressure transmitters, to give the signal to take the measurement, and to adjust the filter frequency.

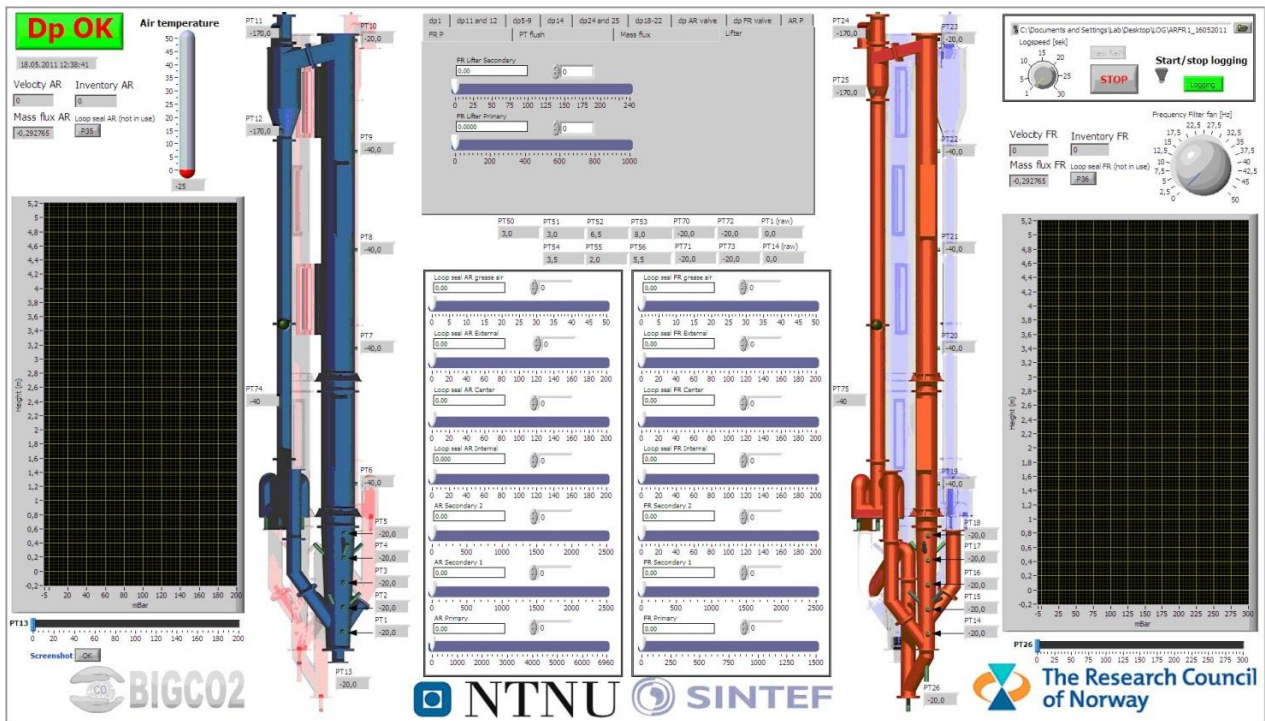


Figure 4-10: The control system layout for the CFM.

Another essential characteristic of the LabVIEW program is that to provide the desired signal, both the incoming and the outgoing signals are processed. This signal processing is for instance the responsible of the fact that even if the pressure transducers operate based on a digital current signal (mA), the pressure is displayed in mbar.

Last but not least, fundamental is the capacity of this program to log and store all the parameters required to analyze the system. In a file are saved all the data regarding pressure measurements, volume flows and temperature. The logging frequency can be modified according to the number of samplings needed. In our case, data are saved every second.

#### 4.4. Mass flux Measurement

As already mentioned, two flap valves installed in the downcomers give the possibility to take measurements.



Figure 4-11: Picture of the flap valve which is used in Cold Flow Model rig

The measurement consists in closing automatically the valve (the one located in the AR downcomer to measure the flux in the AR; similarly for the FR) for an established period of time, checking then, visually, the height of the particles accumulated above the valve.

Using the following equations, then, the mass flux can be estimated.

$$\text{Mass flow rate} = \frac{\pi r^2 \cdot \rho \cdot \Delta h}{\Delta t} \quad \left[ \frac{\text{kg}}{\text{s}} \right] \quad (4-1)$$

$$\text{Mass flux} = \frac{\rho \cdot \Delta h}{\Delta t} \quad \left[ \frac{\text{kg}}{\text{m}^2 \text{s}} \right] \quad (4-2)$$

Where:

$r$  = radius of the downcomer [m]

$\rho$  = particle density, measured on a sample of particles collected in the lab [ $\text{kg}/\text{m}^3$ ]

$\Delta h$  = measured height of particles in the downcomer [m]

$\Delta t$  = amount of time in which the valve was closed [s]

## 4.5. Health and safety

Many issues have to be considered regarding health and safety.

- Dust explosion risk

The explosion conditions can be reached for different causes.

If the air flow rate in the rig is too high, it can happen the formation of high pressure gradients between top and bottom of the riser, other than in the lifter and in the downcomer. This situation may cause an explosion.

If, on the other hand, the amount of particles in the rig is too large (overloading), the air flow injected by the nozzles is not able to fluidize the particles and to let them circulate in the system. Thus, the pressure in the bottom of the riser will suddenly increase, leading to an explosion.

Moreover, incorrect set of the closing time for the flap valves can cause accumulation of particles over the valves in the downcomers. This will bring to an explosion too. To avoid bad consequences, the first thing to do for the operators is a visual control, just after the measurement, of the downcomer, checking that the particles are not accumulating; also, the pressure profiles in the LabVIEW program should be controlled in order to see if something unexpected is happening. In case the conditions seem to get too risky, an emergency switch is installed on the steel structure that protects the rig. If the operators are not able to control the situation, a mechanical device will intervene. A U-tube pressure manometer is installed in the rig; after that there is a water seal. If the pressure goes too high and reaches a critical level, the water will blow out. The advantage of having this device is that the overpressure in the reactor can be always monitored by the operators, while running the rig. Other than that, being mechanical means no malfunction in case of an electrical failure.

- Ambient air quality

The particles used in the CFM are not intrinsically harmful, but their inhalation is not healthy. To assess the risks for the operators connected to inhalation, measurements of the concentration of particles in the air during the experiments were performed. During the

ordinary operation of the rig, the level was proved to be not dangerous. On the other hand, while emptying the filter box and refilling the particles in the rig, the concentration was too high. Therefore, operators have to wear additional protective equipment during these phases, as it will be discussed in the next paragraph.

- Personal protective equipment

The operators are obliged to wear special clothes for their own safety. During the tests, they have to wear helmets with goggles and protective footwear. During the refilling operations is also necessary to wear a protective mask, to avoid inhalation, and it is highly recommended to wear gloves.



Figure 4-12: Picture of protective mask

#### **4.6. Accuracy and Errors**

All measurements have errors and uncertainties, no matter how hard we might try to minimize them. Understanding possible errors is an important issue in any experiments. Uncertainty in a measurement can arise from three possible origins: the measuring device, the procedure of how you measure, and the observed quantity itself.

Equipment has certain measuring range, was defined in the LabVIEW. For accurate result, the potential error source should be considered. Getting the correct data and result needs to calibrate of all equipments as an important features before starting the experimental campaign.

As mentioned above, the procedure of measuring is a great source for possible uncertainties in data. For example for measuring the flux, a flap valve was installed in the downcomers. After closing the flap valve and measure the height of the column of particles accumulating during a certain time interval, the mass flux can be calculated. The process of measuring the height of the particles above the flap valve is done visually.

The operator was tried to minimize all the source of uncertainties for these project. Most of the measurements were taken two or three times after consuming some times for stabilization of the reactors<sup>5</sup> . With increasing the numbers of measurements, the deviation of results decreases in reasonable way and they are close to standard deviation in engineering experiments (less than 10%).

---

<sup>5</sup> 5- 10 min for each measurement depend on the experiments



## **5. Experiments and Results**

### **5.1. Procedure for Starting the Experiments**

The experimental campaign, the main goal of which is finding a stable condition for the system, is started to verify the achievement of the targeted fluidization regime and solids exchange between the AR and FR. The pressure across the reactor system was constantly measured by means of 32 differential pressure transducers. Performing an analysis of the pressure profiles the solids concentration and the amount of solids inventory present in the reactor bodies can be calculated, i.e. the active inventory. These calculations were done equating the measured static pressure drop to the mass weight, neglecting friction and acceleration. The solids flow/flux entrained by the reactors was determined by the visual measurement of the particles accumulation in the loop-seals' downcomers after a sharp loop-seal fluidization interruption. The solids flow measurement of each operating condition was done two times for each reactor and the average value was taken into consideration. If the two measurements were different more than 10% of the average value, a third measurement was taken. The stable Operating conditions were selected between the cases when the pressures in the bottom of the loop-seals and in the bottom and top of each of the two reactors oscillate around a constant average value, over a 5 minutes period [20]. The time span between each of these measurements was 3 to 10 minutes depending on how easy the stable conditions were achieved in the system. It means that the duration of each operating condition was at least around fifteen minutes, up to above forty minutes. The outlet pipes at the cyclones exit are merging into a common filter box equipped with a frequency controlled fan that allows setting the overall backpressure. Each pipe is equipped with a manual valve that allows differentiating the AR and FR backpressures if required. The filter box is positioned over an accurate scale that allows weighting the mass losses on line and allows estimation of the overall reactor system cyclones efficiency. Inventory losses were refilled regularly to preserve a rather constant total solids inventory (TSI) [20].

Table 5-1: Procedure for start up and turn off the rig

| Step | Start-up   | Turn off  |
|------|--|---|
| 1    | Check all the pipes and connections and mass flow controllers              | Set all mass controller and filter frequency to zero          |
| 2    | Check the rig for leakages   | Run PT flush for removing all the particles stick to the wall |
| 3    | Turn the main fan button on  | Close the main air flow valve gradually (V-2)                 |
| 4    | Open the filter box valves (AR&FR)   | Close the mass flow controller valves (V-23 and V-24)         |
| 5    | Check the main air flow valve (V-21)→Close                                 | Turn off the power  |
| 6    | Check the safety of the rig (water level in U tube, nets, Lexan sheets...) | Close the filter box valves                                   |
| 7    | Turn the electricity button on   | Turn off the fan button                                       |
| 8    | Check the main screen of the software (LabVIEW) for error messages         | Check the filter box for leakages                             |
| 9    | Set the value for all mass flow controller in the LabVIEW to zero          | Run the filter box and extract the particles                  |
| 10   | Open the mass flow controller valves (V-23 and V-24)                       | Add new particles to the rig                                  |
| 11   | Open the main air flow valve gradually (V-21)                              | -   |
|      | Set the filter frequency   | -   |
| 12   | Running the PT flush in both reactors                                      | -   |

## 5.2. Overview of experiments

The experimental campaign started on 16/02/2011 until 14/06/2011. During this period, 4 main case studies were tested and analyzed which consist of validating the data and reaching the design conditions, component sensitivity, different operational mode as a consequence of design parameters for hot rig, and the effect of the amount of the inventory on operational modes.

162 experiments were done with CFM to achieve the best state of the stability and proper flow regimes. Two measurements were done for the majority of experiments to validate the data. In some of the experiments, one measurement is taken to explore the condition of reactors and inspecting the fluidization regime. All the experiments were done in the coupled reactors with around 5min duration time for each measurement to stabilize the circulation of particles.

Estimation of the pure time for 162 experiments and 101 times of using filter box and refilling the new particles to the reactors is:

$$T = (162 \times 25 \text{ [min]}) + (101 \times 20 \text{ [min]}) = 6070 \text{ [min]} = 101.2 \text{ [hr]}$$

Average Time for each experiment: 25 [min]

Average time for refilling: 20 [min]

Determination of test matrix was done in weekly meeting with SINTEF and NTNU senior researchers, but some of the test matrixes were determined during the operation.

### 5.3. Validating the data and design condition

Here, one case of steady state conditions achieved for an operating condition approaching the design target is shown in Figure 5-1. The TSI inside the system was approximately 120 kg, while the superficial gas velocity in the AR was  $2.4 \text{ m s}^{-1}$  and  $2.6 \text{ m s}^{-1}$  in the FR. The lift was operated in turbulent mode with a superficial gas velocity of  $1.5 \text{ m s}^{-1}$  and in the AR loop-seal was injected a total amount of air of  $165 \text{ NI min}^{-1}$  while in the FR  $95 \text{ NI min}^{-1}$ . Solids exchange in line with reactor system was here operated without internal recirculation (i.e. with 100% of exchange between AR and FR);  $1.9 \text{ kg s}^{-1}$  ( $\sim 46 \text{ kg m}^{-2} \text{ s}^{-1}$ ) coming from the AR to the FR and  $0.75 \text{ kg s}^{-1}$  ( $\sim 46 \text{ kg m}^{-2} \text{ s}^{-1}$ ) from the FR to the AR through the cyclones and the loop-seals. The missing  $1.15 \text{ kg s}^{-1}$  from FR to AR was exchanged through the bottom lift/extraction. In order to have stable particles column heights in the downcomers and smooth flow of solids, the loop-seals were fluidized. Around 60 cm of moving packed bed (with some bubbles) were reached in the AR downcomer versus 45 cm of bubbling bed in the FR downcomer. The AR downcomer and loop-seal have to process a much higher solids flux than the FR ones due to the fact that the solids flow is higher but they have the same dimensions [20].

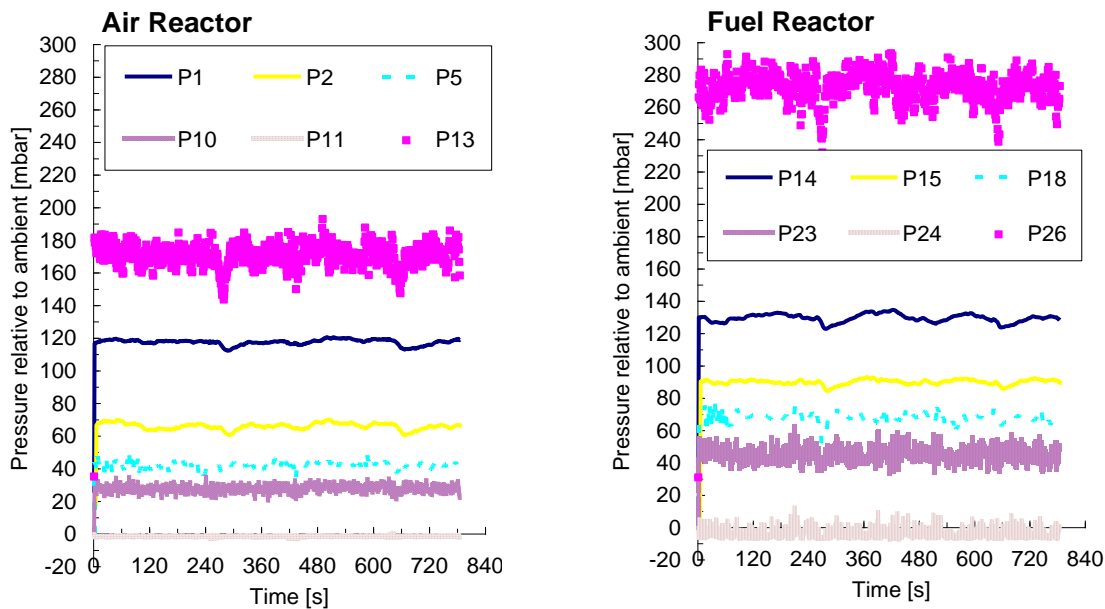


Figure 5-1: Pressure measurements in some key points along the AR (left) and FR (right) reactor bodies

It is possible to observe how several pressures measured across the reactor system, both AR (left) and FR (right) in Figure 5-1, are keeping a constant value along the almost 15 minutes of test. Moreover, the same operational condition was tested several times, always with acceptable results and good repeatability. The pressures before the primary bottom nozzle are presented by P13 and P26, the FR one was originally dimensioned for less air flow, and this explains such high pressure. P1 and P14 are located 14cm above the reactors bottom while P2 and P15 are just about 20 cm above them. Due to its high particles concentration, the bottom bed section can easily gain tens of mbar of pressure in such a short distance. P10 and P23 are at the reactors exits while P5 and P18 are located at the end of the conical bottom part. P23 is higher than P10, due to the higher gas velocities reached in the FR cyclone inlet duct, whose dimensions should be reconsidered; in comparison to the AR one, it gives a higher pressure drop. P11 and P24 are located at the exit of the cyclones, and the filter fan is used to retain the exit pressures at around zero. Figure 5-2, depicts the pressures measured at the bottom of the AR (left) and FR (right) loop-seals, respectively P28 and P31. The reactor system loop-seals are divided into several loop-seals, hence each of them has two return legs. This is a quite common solution in conventional CFB boilers [21] where the two return legs are directed back to two different points located at the same height of the same boiler/reactor, in that case facing roughly the same pressure. In the present set-up, one return leg is directed to the FR and the other one to the AR reactor. Having stable operation requires each of the loop-seals bottom pressures to be higher than the ones experienced in both the return points, and it must also have a safety margin. In other respects, there will be back flow of gas and it will flood the cyclones with a huge loss of inventory in few minutes. The AR is fulfilling this task easily, but not the FR where the internal return leg seems to merge the FR reactor body too low facing a high pressure equal to P14. As a matter of fact, there is a very small margin between the FR loop-seal bottom pressure (P31) and P14, as shown in Figure 5-2 (right). In Figure 5-2, it is also possible to notice when the solids flow measurements were taken in the AR (e.g. around 260 s) and in the FR (e.g. around 430 s) which shows a clear reduction of the pressure measured at the loop-seals bottom due to the abrupt fluidization shut down. In Figure 5-1, it is shown how these pressure disturbances caused by the measurements were affecting the reactor system, especially the measurements taken in the AR; however the stable operating conditions were quickly recovered after each measurement [20].

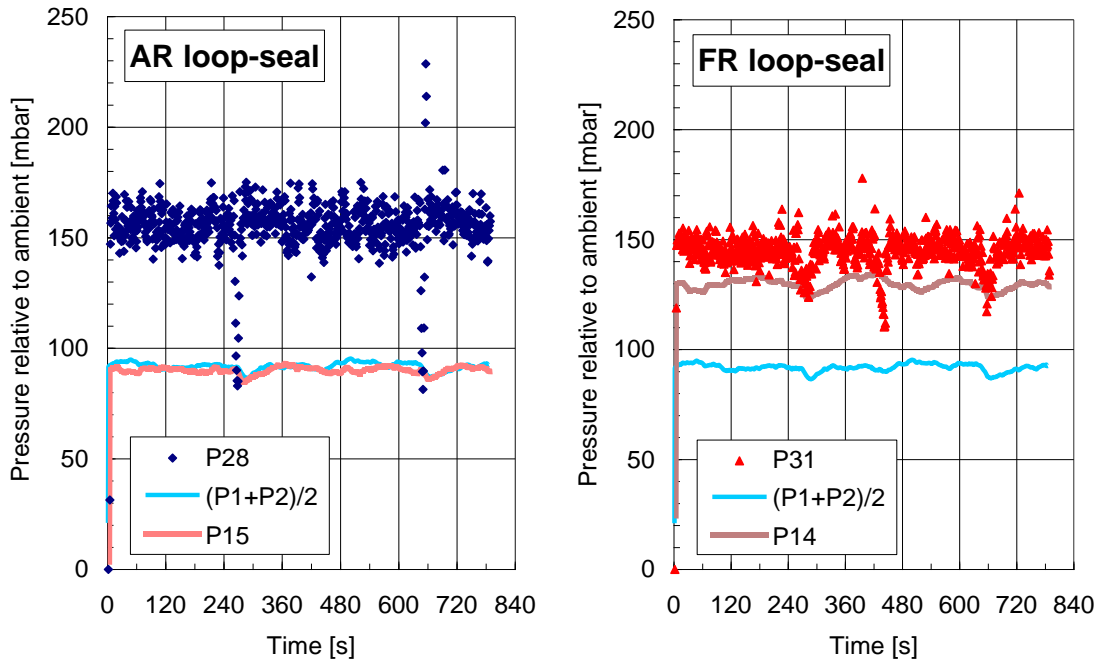


Figure 5-2: Pressure measurements at the bottom AR (left) and FR (right) loop-seals, plotted as function of the time. Example of reactor system operation in steady state conditions. Each of them is plotted together with the AR and FR pressures measured at the points where the two loop-seals return legs are merging

The pressure profile of the DLCFB reactor system and the corresponding solids concentration along the reactors height, are plotted in Figure 5-3, respectively which are based on average values of the above mentioned pressure measurements. The active solids inventory calculated inside the AR body is around 25 kg while the FR is almost 16 kg. These two items represent together slightly more than thirty percent of the TSI in the system. It can be identified from these graphs that both the reactors operate in the border between fast fluidization and turbulent regime. In fact, it is possible to recognize the lower particles concentration, below 1%, in the upper part and the high solids density at the reactors bottom section. Cyclones losses were also monitored and their total efficiency is above 99.9%. It is still not possible to have precise conclusions since the two cyclones losses merge into the same filter box and the AR cyclone is processing much more solids than the FR one and is also having a lower pressure drop [20].

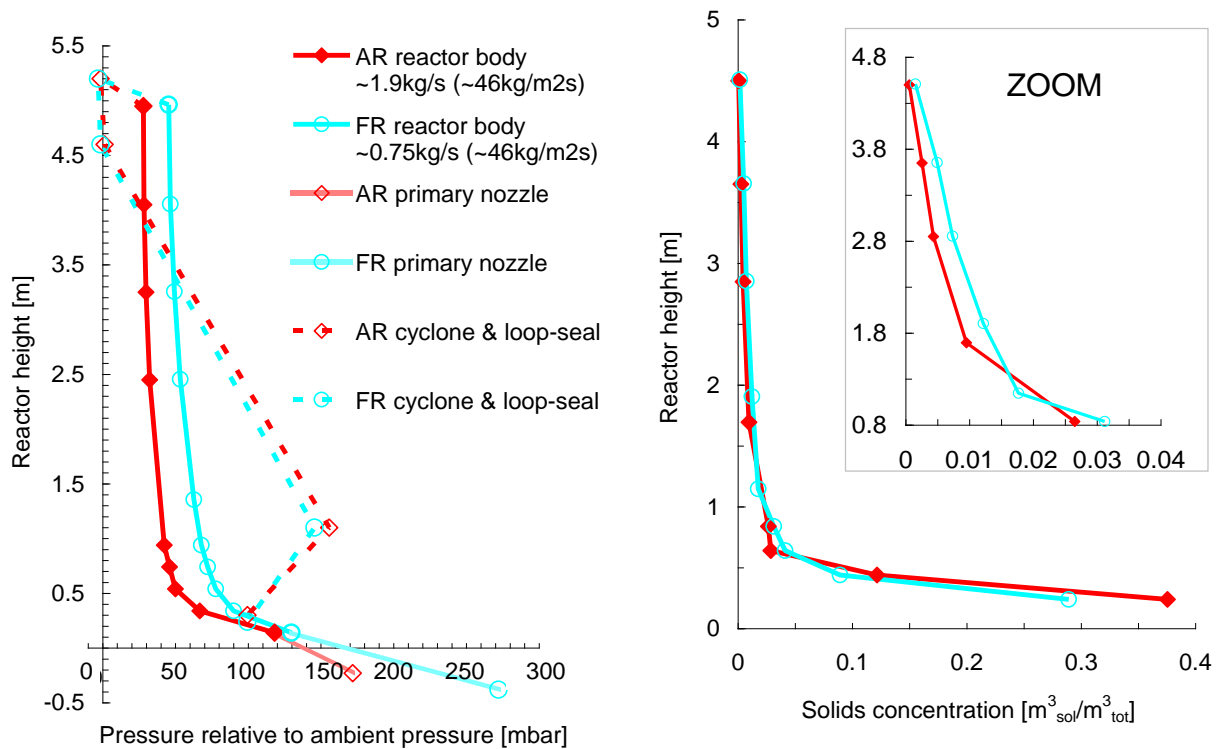


Figure 5-3: left) Pressure profile measured across the DLCFB reactor system in stable operation, which gave high solids exchange, approaching 2kg/s. right) corresponding estimation of the particles concentration along the reactor bodies.

The high pressure experienced in the bottom section of the FR together with the consequent different pressures between AR and FR are the main challenges faced to attain stable operation of the DLCFB reactor system. In this way the divided loop-seals expose to a very high pressure in their FR return leg and an overall pressure unbalance. This may cause problems like solids circulation limitations and gas leakages between reactors. In the worst case, it prevents the formation of the required pressure seal in the downcomers, to “close” the overall pressure loop, resulting in large powder losses through the cyclone; cyclone flooding. Design reasons and operational reasons are among the potential ones. When it comes to the design, the FR cyclone inlet duct is causing a high pressure drop, which affects to somehow the bottom pressure. However, there is not an overall FR pressure curve translation towards higher values. One of the reasons of this pressure unbalance is the return leg location, as highlighted during the description of Figure 5-2(right), and a higher location of the FR internal return leg of just 20cm

will intrinsically increase the operational window, consequently increasing the flexibility of the reactor system. Nevertheless, there is a possibility to find a way to operate the reactor system with the actual design. In fact, the bottom extraction/lift fluidization is the key operational parameter. It is clearly illustrated in Figure 5-4 (right) how an increase of the total amount of fluidizing air in the lift reduces the FR bottom pressure, thus the amount of mass in the FR bottom section which helps in equalizing the AR and FR bottom pressures, allowing the actual design to work in a stable way. As a result both fluidizing air and solid entrainment increase inside the AR. Figure 5-4 (left) shows the AR response to the fluidizing air increase and as can be seen, AR cyclone pressure drop increases with the pressure curve shifting towards higher pressures, mainly in the upper part. Finally, the way the loop-seals are fluidized may play a role in overcoming the reactors pressure difference. Before drawing clear conclusions, more tests in this respect need to be performed. Anyhow the actual loop-seal fluidization system has shown that it cannot overcome such big pressure difference on its own; without the pressure balancing due to increasing the lift fluidization [20].

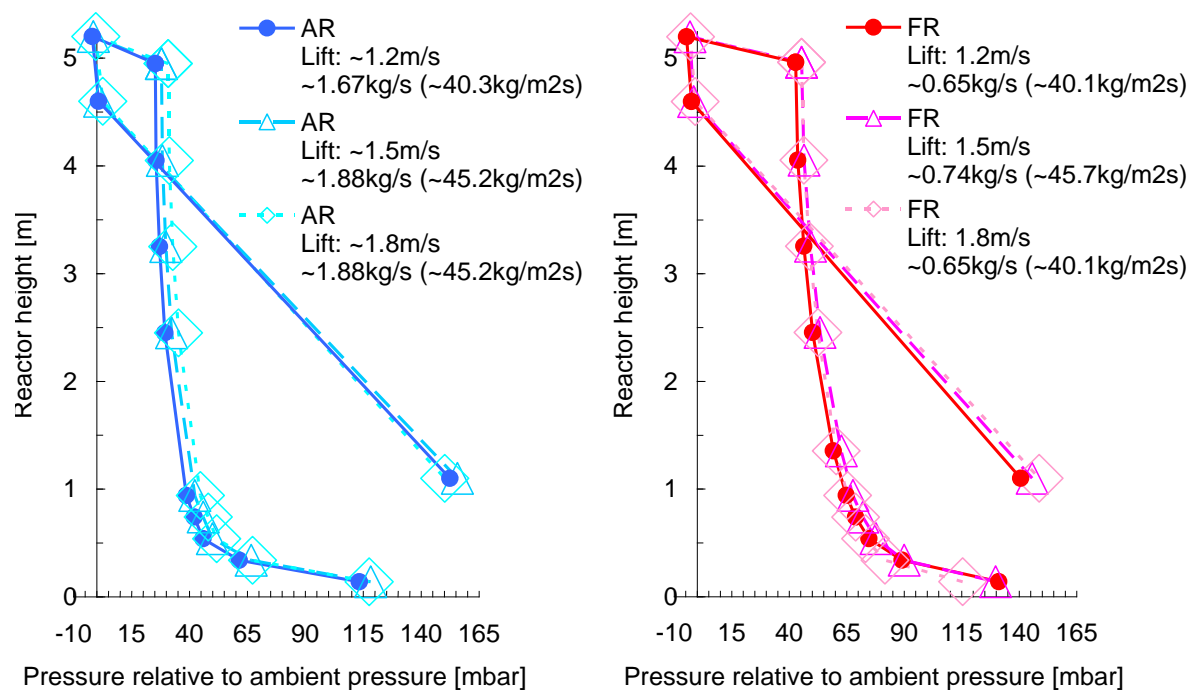


Figure 5-4: Pressure profiles of the DLCFB reactor system at the variation of the bottom extraction/lift superficial gas velocity. Pressures of AR (left) and FR (right) are presented separately for sake of simplicity



After that the targeted operation of the DLCFB reactor system was accomplished, some sensitivity tests were done to understand the FR fluidization better. In Figure 5-5 (left), it is shown that how the FR pressure curves shift towards higher values in the upper part with increased gas flow, but not so much in the lower part. It means that there is a strong reduction of the particles concentration in the lower section of the FR (Figure 5-5, right) as well as a slight increase of concentration in the upper part of the reactor body, which is accountable for the increase of FR solids entrainment (Figure 5-5, right). For sake of simplicity and brevity, the analogous AR pressure and concentration profiles are not shown since they almost did not change [20].

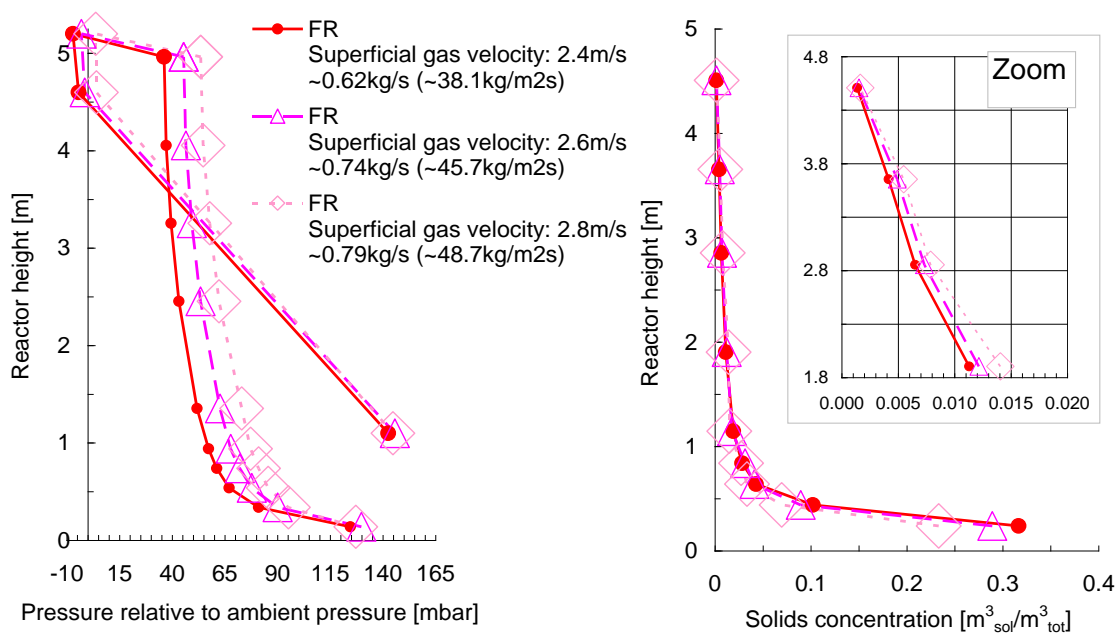


Figure 5-5: Pressure (left) and concentration (right) profiles of the fuel reactor (FR) of the DLCFB reactor system at the variation of the FR superficial gas velocity. Pressure of AR is not presented for sake of simplicity, because it was almost not influenced

The above case study is one the best state of DLCFB to reach steady state condition approaching the design target with the TSI inside the system was approximately 120 kg; this is referred as design case (standard condition). It can be identified from the mentioned graphs that

both the reactors operate in the border between fast fluidization and turbulent regime. This set of experiment is used as reference case, i.e. a starting point for the other cases which are analyzed the different possibilities to reach other, previously established, targets. All other experiments start to run for 10 min as the operating time with these given conditions in order to reach the stability, right before changing any other variables (For each experiment we set these values and we waited 10 minutes before changing any variable, in order to allow the system to reach stability).

The shown values in the following table are corresponding to the operating conditions for the “standard” experiment.

Table 5-2: Amount of air injections in STANDARD test

| Air Injections         | Position of Injection | Air flow[Nl/min] | Total amount of air [m/s] | Share in percent% |
|------------------------|-----------------------|------------------|---------------------------|-------------------|
| Air Reactor Loop Seal  | <b>External</b>       | <b>120</b>       | <b>0.1</b>                | <b>73</b>         |
|                        | <b>Center</b>         | <b>40</b>        |                           | <b>24</b>         |
|                        | <b>Internal</b>       | <b>0</b>         |                           | <b>0</b>          |
|                        | <b>Grease</b>         | <b>5</b>         |                           | <b>3</b>          |
| Fuel Reactor Loop Seal | <b>External</b>       | <b>80</b>        | <b>0.11</b>               | <b>84</b>         |
|                        | <b>Center</b>         | <b>10</b>        |                           | <b>11</b>         |
|                        | <b>Internal</b>       | <b>0</b>         |                           | <b>0</b>          |
|                        | <b>Grease</b>         | <b>5</b>         |                           | <b>5</b>          |
| Air Reactor            | <b>Primary</b>        | <b>3000</b>      | <b>2.4</b>                | <b>55</b>         |
|                        | <b>Secondary 1</b>    | <b>1250</b>      |                           | <b>22.5</b>       |
|                        | <b>Secondary 2</b>    | <b>1250</b>      |                           | <b>22.5</b>       |
| Fuel Reactor           | <b>Primary</b>        | <b>1200</b>      | <b>2.6</b>                | <b>50</b>         |
|                        | <b>Secondary 1</b>    | <b>1000</b>      |                           | <b>42</b>         |
|                        | <b>Secondary 2</b>    | <b>200</b>       |                           | <b>8</b>          |
| Lifter                 | <b>Primary</b>        | <b>500</b>       | <b>1.5</b>                | <b>70</b>         |
|                        | <b>Secondary</b>      | <b>200</b>       |                           | <b>30</b>         |

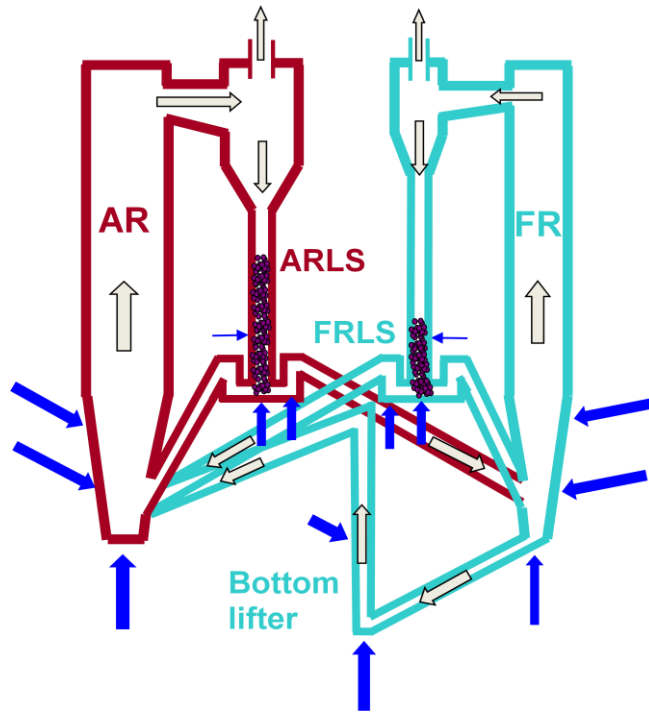


Figure 5-6: The place of air injections (Blue Arrows), and the path of flow in coupled experiment along the body of reactors(White Arrows) in “Standard experiment”

The velocity profiles for “standard test” are calculated as a function of height and are shown in figure 5-6. The friction factor and pressure drop is supposed to be zero along the body of riser after secondary air injection. As result of velocity profiles, the main reduction of occurs after the primary air injection in the bottom of the AR while this point for FR has higher position, after secondary air injection. The maximum velocity is reached at the inlet duct of the cyclones due to the special geometry of the cyclone.

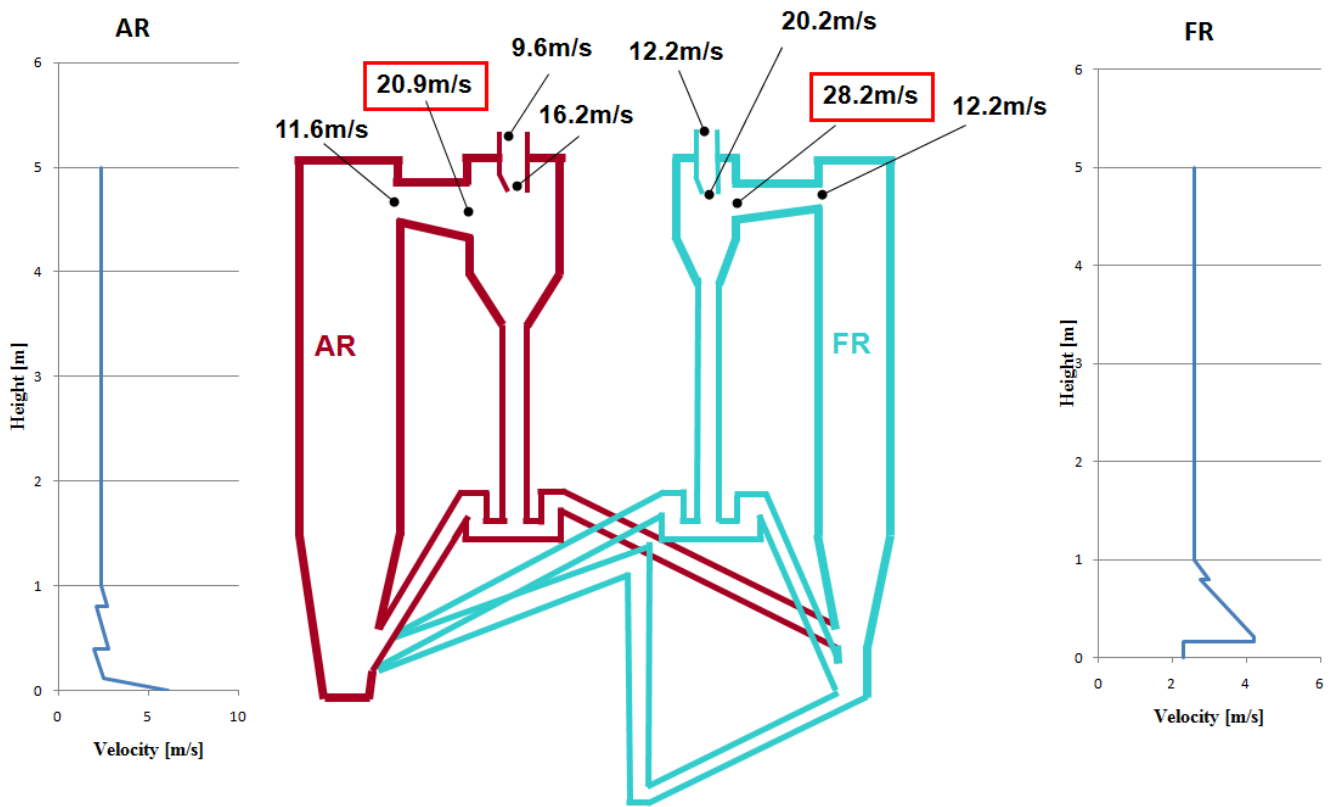


Figure 5-7: Velocity profile along the risers and duct of cyclones in "standard" experiment

## **5.4. Operational Modes**

During the experimental campaign, different conditions for the rig were tested. In each case the goal of the tests was to reach stability, to prove that the system can operate in those conditions. Following experiments were done as a consequence of design parameters for hot rig.

The most important test for operating the CLC in a safe way is the so called part-load, which consists in injecting a lower amount of fuel to the system, having in this way a lower power.

Another interesting condition to test was the maximum power, increasing the amount of oxygen carriers and the fuel to analyze the performance of the rig with more than 150 kw. Increasing the total power of the rig with higher values of the injections for both AR and FR. When the Hot rig will be built, this test will be performed by increasing both the amount of the fuel and air.

Moreover, several tests were done in order to get a better concentration of the particles in the FR, obtained by increasing both the residence time and the entrainment inside the body of the FR. This goal was reached thanks to the loop-seals and the possibility of internal recirculation.

Last, but not least, reforming experiments with different rate of exchange between the reactors were done, to see if the system can be used in Chemical Looping Reforming other than Combustion. More about the reforming will be explained in 4.4.4.

### **5.4.1. Part Load**

It is important to test the behavior of the rig under part load conditions. These conditions are obtained reducing the amount of fuel introduced in the fuel reactor while the air/fuel ratio is kept constant, as well as the temperature and the total mass inventory [28].

This option also can be reached either injecting more oxygen carrier than the constant ratio to combust all the fuel inside the FR body or lowering the amount of oxygen in the FR. Both options were tested to analyze the performance of the cold flow model. But the most stable conditions in terms of stability inside the downcomers and cyclone efficiencies were reached under the previous condition which is called design operation mode for air reactor.

One of the important aspects that we were able to observe and analyze during the part load experiments on cold flow model is the effect of the air injections in the loop seals on the total stability of the system. In order to reach the part load, the total amount of air in both AR and FR was decreased to reach less entrainment. As a consequence, the simulated power, which is an output variable, is decreased. We noticed that the only way to stabilize the whole system was decreasing the total amount of air injections in the LSs. The amount of reduction ratio of the air injections in the ARLS and FRLS is calculated as function of reduction of air flow in AR and FR, respectively.

The shown values in the following table are corresponding to the operating conditions for the “part-load” experiment.

Table 5-3: Amount of air injections in PART-LOAD test

| Air Injections         | Position of Injection | Air flow[Nl/min] | Total amount of air [m/s] | Share in percent% |
|------------------------|-----------------------|------------------|---------------------------|-------------------|
| Air Reactor Loop Seal  | <b>External</b>       | <b>80</b>        | <b>0.06</b>               | <b>84</b>         |
|                        | <b>Center</b>         | <b>10</b>        |                           | <b>11</b>         |
|                        | <b>Internal</b>       | <b>0</b>         |                           | <b>0</b>          |
|                        | <b>Grease</b>         | <b>5</b>         |                           | <b>5</b>          |
| Fuel Reactor Loop Seal | <b>External</b>       | <b>40</b>        | <b>0.05</b>               | <b>80</b>         |
|                        | <b>Center</b>         | <b>5</b>         |                           | <b>10</b>         |
|                        | <b>Internal</b>       | <b>0</b>         |                           | <b>0</b>          |
|                        | <b>Grease</b>         | <b>5</b>         |                           | <b>10</b>         |
| Air Reactor            | <b>Primary</b>        | <b>2700</b>      | <b>2</b>                  | <b>60</b>         |
|                        | <b>Secondary 1</b>    | <b>950</b>       |                           | <b>20</b>         |
|                        | <b>Secondary 2</b>    | <b>950</b>       |                           | <b>20</b>         |
| Fuel Reactor           | <b>Primary</b>        | <b>600</b>       | <b>1.3</b>                | <b>50</b>         |
|                        | <b>Secondary 1</b>    | <b>400</b>       |                           | <b>33</b>         |
|                        | <b>Secondary 2</b>    | <b>200</b>       |                           | <b>17</b>         |
| Lifter                 | <b>Primary</b>        | <b>500</b>       | <b>1.5</b>                | <b>70</b>         |
|                        | <b>Secondary</b>      | <b>200</b>       |                           | <b>30</b>         |

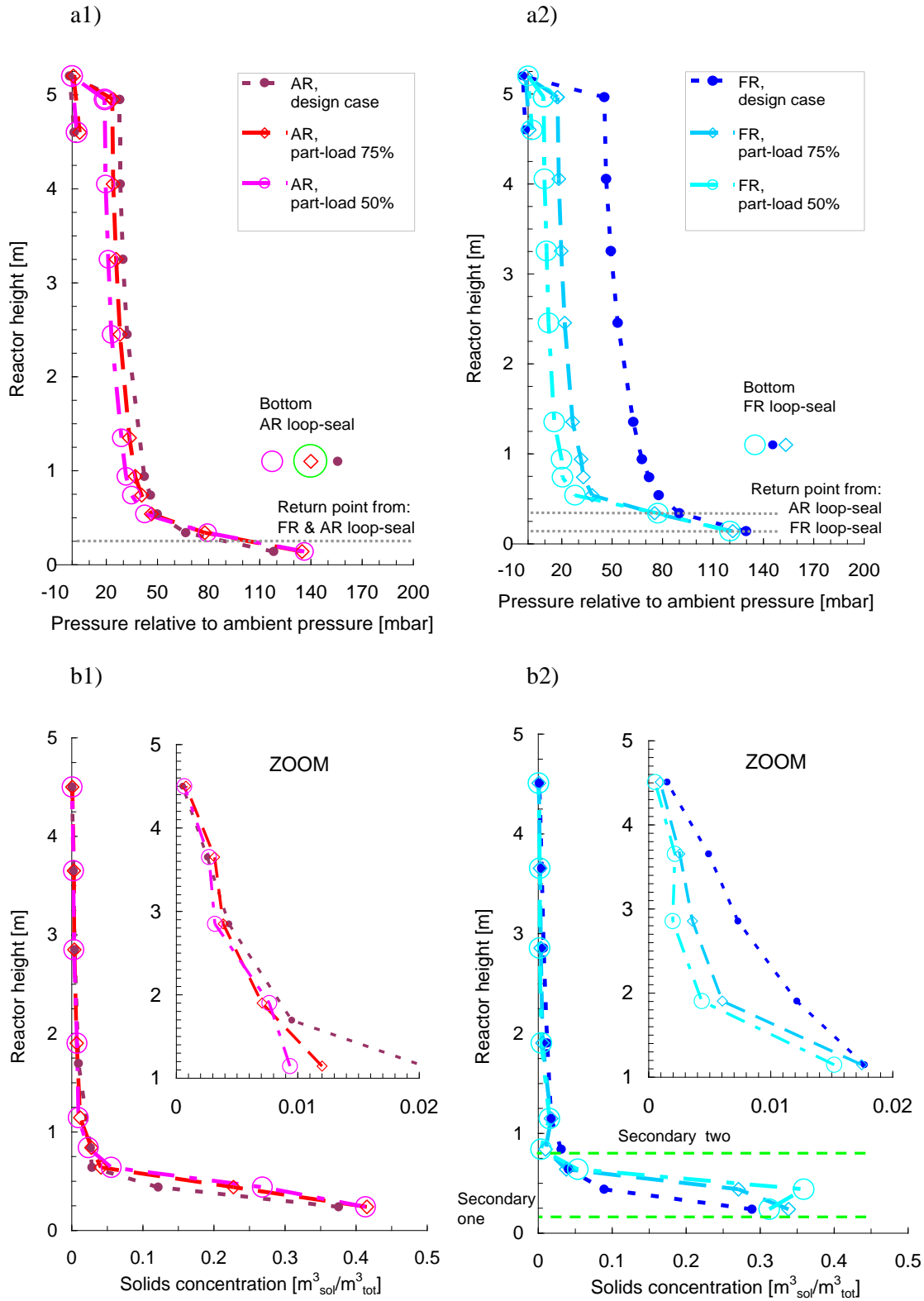


Figure 5-8: Pressure and solids concentration profiles of AR (a1 and b1) and FR (a2 and b2) at part load conditions of 75% and 50% fuel load

The capability of varying the thermal power is another important issue for the chemical looping reactor system and its hydrodynamic viability was verified by means of the CFM. During the part-load experiments, several tests were done reducing the amount of fluidizing air injected in the FR to resemble a reduction of injected fuel. At the same time other control parameters were varied in order to compensate the FR and look for an overall stable configuration. In Figure 5-8 are shown two power reductions from the design case to 75% and down to 50% of the fuel load. In the first case the system was capable to find a balance intrinsically and no other control parameters were varied, in addition the solids exchange reduced as well down to a value of approximately 75% of the design one. The second case affected much more the overall system and it required taking some actions finalized to maintain the equilibrium: first the FR loop-seal fluidization was reduced to fit to the smaller entrainment and avoid that the FR down-comer bubbling bed became a slugging bed with too much air from the loop-seal and damaging the cyclone efficiency. In addition also the AR fluidization was reduced, together with the AR loop-seal, in order to have a smaller solids exchange going down to approximately the 50% consistently with the fuel load. (heating issues). Looking at Figure 5-8 a1), it is possible to notice how the AR bottom pressure increases, due to higher amount of mass, and the upper one reduces, mainly because of the smaller cyclone pressure drop which is the consequence of the smaller solids flow and air flow. While in the second case, those are the clear consequences of the smaller fluidizing air injected, in the first case the AR solids entrainment may be a consequence of the big AR inventory increase which is kind of choking the solids entrainment because of constant superficial gas velocity. In Figure 5-8 b1), the respective concentration profile is showing how it increases in the bottom part of the reactors contributing to the increase of active mass inventory in the reactor body, but it decreases in the upper part reducing the solids entrainment. In Figure 5-8 b1), the FR pressure profile is shown; while the bottom pressure is rather constant the upper one is reducing dramatically because of the big reduction in air and solids flow, and it happen proportionally to the load reduction (cyclone efficiency). This implies also an inventory increase because of a big increase of the overall reactor  $\Delta P$  mainly accumulated in the lower part.

Looking at the concentration profile in Figure 5-8 b2), there is a clear reduction proportional to the load reduction in the upper part of the reactor body (zoom). In the bottom part an unusual



behavior was registered, in fact there is a reduction in the pressure gradient, thus calculated concentration, which at the beginning was interpreted as a measurement problem, but it seems to happen just above the secondary air injection, both secondary one and secondary two, and is proportional to the increase on secondary air injection. In fact the overall fluidizing air reduction in the FR is mainly done by primary air reduction, thus increasing the relative importance of the secondary air injections. This seems to create a kind of concentration increase just above the injection point.

#### 5.4.2. Maximum Power

Opposite to the part load condition is the maximum power. In this series of tests the total amount of the air injection is increased, both in the AR and in the FR, trying to find the values that guarantee the achievement of stable conditions. The purpose of these experiments was to test if it was possible for the system to work with a higher power, with a higher exchange flux.

After many attempts, the best conditions are achieved, always basing our decisions on the visual stability of the downcomers, the mass losses from the cyclones and the flux measurements. The chosen values are shown in the following table.

Table 5-4: Amount of air injections in Maximum Power test

| Air Injections         | Position of Injection | Air flow[Nl/min] | Total amount of air [m/s] | Share in percent% |
|------------------------|-----------------------|------------------|---------------------------|-------------------|
| Air Reactor Loop Seal  | <b>External</b>       | <b>120</b>       | <b>0.1</b>                | <b>73</b>         |
|                        | <b>Center</b>         | <b>40</b>        |                           | <b>24</b>         |
|                        | <b>Internal</b>       | <b>0</b>         |                           | <b>0</b>          |
|                        | <b>Grease</b>         | <b>5</b>         |                           | <b>3</b>          |
| Fuel Reactor Loop Seal | <b>External</b>       | <b>80</b>        | <b>0.1</b>                | <b>84</b>         |
|                        | <b>Center</b>         | <b>10</b>        |                           | <b>11</b>         |
|                        | <b>Internal</b>       | <b>0</b>         |                           | <b>0</b>          |
|                        | <b>Grease</b>         | <b>5</b>         |                           | <b>5</b>          |
| Air Reactor            | <b>Primary</b>        | <b>3300</b>      | <b>2.6</b>                | <b>55</b>         |
|                        | <b>Secondary 1</b>    | <b>1350</b>      |                           | <b>22.5</b>       |
|                        | <b>Secondary 2</b>    | <b>1350</b>      |                           | <b>22.5</b>       |
| Fuel Reactor           | <b>Primary</b>        | <b>1200</b>      | <b>3.2</b>                | <b>41</b>         |
|                        | <b>Secondary 1</b>    | <b>1500</b>      |                           | <b>52</b>         |
|                        | <b>Secondary 2</b>    | <b>200</b>       |                           | <b>7</b>          |
| Lifter                 | <b>Primary</b>        | <b>500</b>       | <b>1.5</b>                | <b>70</b>         |
|                        | <b>Secondary</b>      | <b>200</b>       |                           | <b>30</b>         |

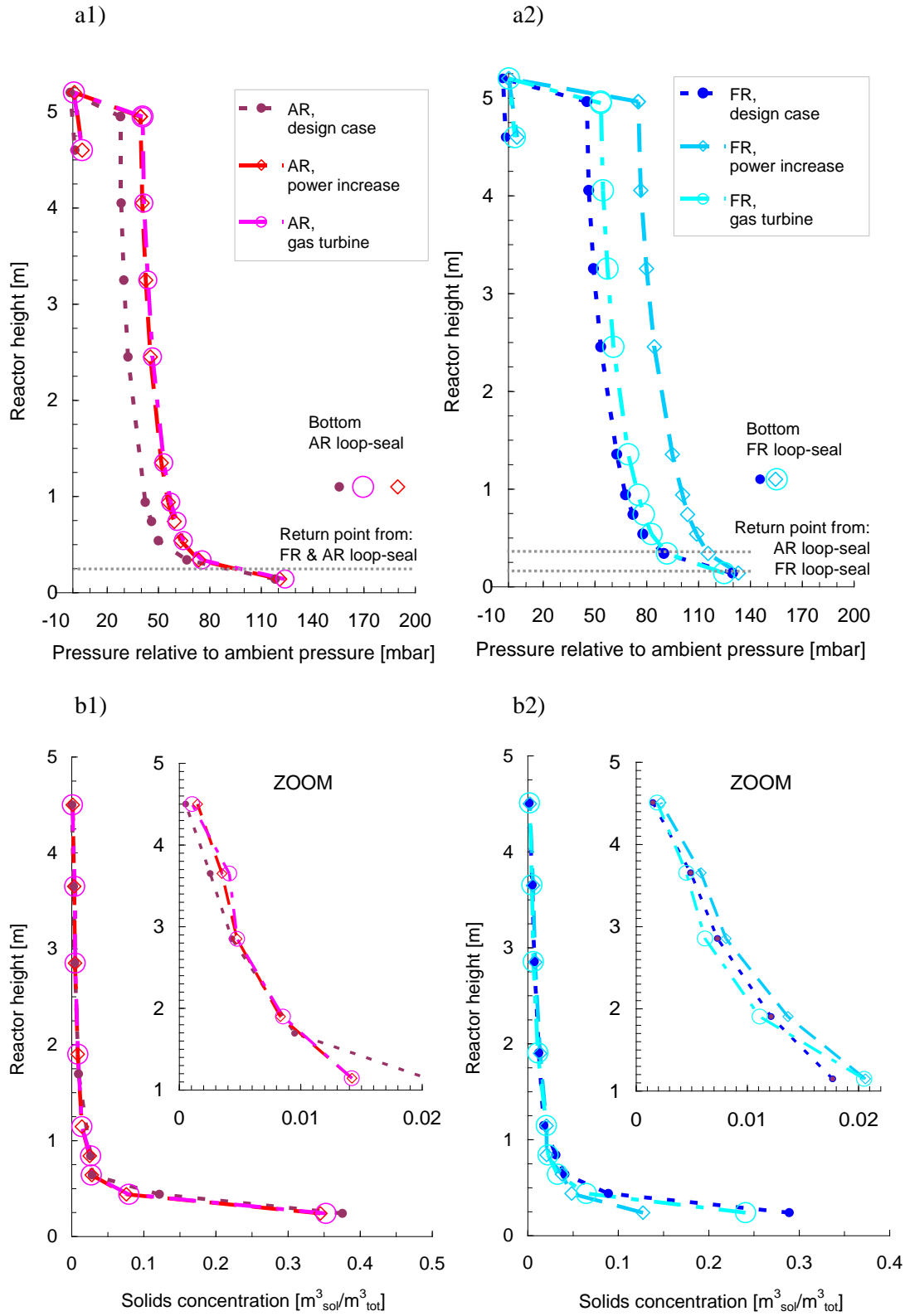


Figure 5-9: Pressure and solids concentration profiles of AR (a1 and b1) and FR (a2 and b2) resembling a power increase and a gas turbine application

The air injection in the FR was increased resembling an increase of fuel injected, while at the same time also the AR fluidizing gas was increased to provide more OC exchange which is required to oxidize the higher amount of fuel. The circulation rate increased of the 15%, while the FR air injection was increased of slightly higher value. This means that the load increase to consider corresponds to the 15% of solids exchange, because the further increase of gas will not have enough oxygen to be fully oxidized. For this reason the other parameter to consider independent for the power increase is the AR fluidization which controls the solids exchange. The loop-seals accomplished to their task without the need of modifying the fluidizing gas injected and the down-comers didn't have major level changes. The pressure profile of the AR has a bigger cyclone pressure drop while the derived concentration profile is rather constant as well as the active mass inventory, with an increase in the last three meters which explains the higher entrainment. The FR has as well a big cyclone  $\Delta P$  increase together with a concentration reduction in the lower part and increase in the upper part, as it happened in the case of FR flux maximization. Another configuration tested was the gas turbine one. In fact the FR fuel load was kept constant and at the same time the AR air flow was increased. In pressurized hot conditions this means that the amount of gas in the exothermic reactor is increased providing a higher amount of flow expanding in the gas turbine and reducing, ideally down to zero, the usage of the cooling devices for the AR. In fact whether the CLC reactor system is used as a steam boiler heat needs to be extracted by the exothermic reactor, but in the case it is pressurized and used as a gas turbine combustion chamber the amount of air to fuel ratio ( $\lambda$  in the design case was 1.2) has to be increased to higher values. Here it is shown just an attempt to get closer to such kind of reactor usage coping with the intrinsic limitations of the design which is actually meant to work as a steam boiler; for this reason the Lift fluidizing air was increased in order to avoid the FR getting full and having a too high pressure in the bottom. Looking at the pressure profiles, the AR is behaving very similar to the previous case of load increase, while the FR is just slightly increasing the pressure drop most likely because of the higher amount of air due to the increase of primary lift fluidization. The FR concentration is smaller compare to the design case both in the lower and upper part because of the big solids exchange happening through the bottom extraction.

### 5.4.3. Maximum Fuel Reactor Concentration

This condition is reached increasing the fuel reactor air injection, other than playing with the loop seals air injections. In fact, in this case an important role is related to the internal section of the fuel reactor loop seal, here used to have an internal recirculation in the FR.

This is done in order to simulate the increase of fuel and steam injection in the FR, assisted by the internal recirculation, which will allow the hot rig to achieve a higher concentration. Higher concentration means better entrainment, i.e. better solids-gas contact, for a more uniform reaction, that leads to a better combustion.

Thus, the total amount of air injected in the FR was increased, together with the external section of the air reactor loop seal and the internal one of the fuel reactor loop seal, while the injections in the lifter were decreased. All these changes were made, as explained before, in such a way to have a higher exchange flux in the FR. The air reactor air injections stay the same as the standard case. The values selected as the ones that can lead to the best (more stable) conditions are shown in the following table.

Table 5-5: Amount of air injections in Maximum Fuel Reactor Concentration test

| Air Injections         | Position of Injection | Air flow[Nl/min] | Total amount of air [m/s] | Share in percent% |
|------------------------|-----------------------|------------------|---------------------------|-------------------|
| Air Reactor Loop Seal  | <b>External</b>       | <b>180</b>       | <b>0.14</b>               | <b>80</b>         |
|                        | <b>Center</b>         | <b>40</b>        |                           | <b>18</b>         |
|                        | <b>Internal</b>       | <b>0</b>         |                           | <b>0</b>          |
|                        | <b>Grease</b>         | <b>5</b>         |                           | <b>2</b>          |
| Fuel Reactor Loop Seal | <b>External</b>       | <b>30</b>        | <b>0.25</b>               | <b>13</b>         |
|                        | <b>Center</b>         | <b>10</b>        |                           | <b>4</b>          |
|                        | <b>Internal</b>       | <b>198</b>       |                           | <b>83</b>         |
|                        | <b>Grease</b>         | <b>0</b>         |                           | <b>0</b>          |
| Air Reactor            | <b>Primary</b>        | <b>3000</b>      | <b>2.4</b>                | <b>55</b>         |
|                        | <b>Secondary 1</b>    | <b>1250</b>      |                           | <b>22.5</b>       |
|                        | <b>Secondary 2</b>    | <b>1250</b>      |                           | <b>22.5</b>       |
| Fuel Reactor           | <b>Primary</b>        | <b>1350</b>      | <b>3.5</b>                | <b>43</b>         |
|                        | <b>Secondary 1</b>    | <b>1600</b>      |                           | <b>51</b>         |
|                        | <b>Secondary 2</b>    | <b>200</b>       |                           | <b>6</b>          |
| Lifter                 | <b>Primary</b>        | <b>400</b>       | <b>1.2</b>                | <b>73</b>         |
|                        | <b>Secondary</b>      | <b>150</b>       |                           | <b>27</b>         |

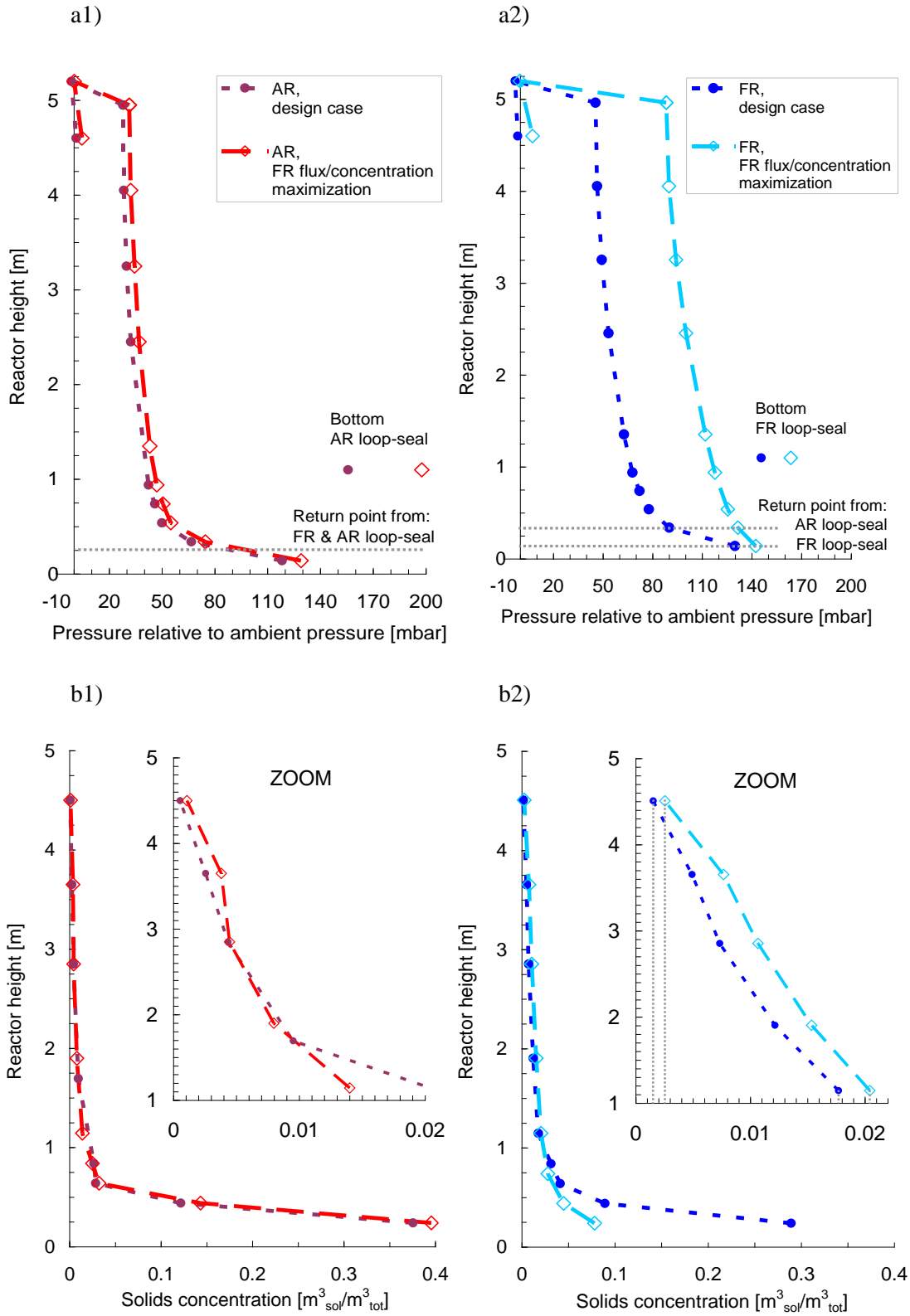


Figure 5-10: Pressure and solids concentration profiles of AR (a1 and b1) and FR (a2 and b2) at FR maximum solids flux/concentration achieved

Among the chemical looping configurations investigated several attempts were done to increase the concentration in the upper part of the FR and consequently the solids entrainment together with a reduction of the bottom inventory. The aim is to provide an overall better contact between gas and particles in the upper region (risers) avoiding a very dense bottom zone, typical of turbulent beds. This is expected to improve the fuel conversion of the 150kW<sub>th</sub> set up despite the smaller particles residence time, especially for highly reactive OC. This task was not straightforward; because of design limitations which made the reactor system less flexible, therefore a significant increase of solids concentration in the FR upper part was the consequence of several simultaneous actions, which separately haven't been so effective. First of all, the FR superficial gas velocity was increased and assumed to resemble in the hot set-up a CO<sub>2</sub> recirculation, while a fuel increase would have required a corresponding increase of OC exchange to oxidize the increased amount of fuel. This should help entraining more solids from the dense bottom zone to the lean one, shifting the fluidization regime more toward fast fluidization. The external air injection in the FR loop-seal was brought down to a smaller value and at the same time the internal one was increased up to the maximum allowed. The high internal fluidization is meant to increase as much as possible the internal recirculation, thus the OC residence time increasing the probability of having several FR loops; in addition it will eventually lead to a steady state characterized by a higher amount of mass in the fuel reactor body, especially above the return point. The external leg of the FR loop-seal was kept fluidized because it will increase the area available to the solids flow, leading towards higher FR entrainment. The lateral air injection was switched off because of the high increase of the overall bottom injections considering that a share of it goes anyhow through the down-comer; in fact the down-comer was clearly fluidized as bubbling bed. At the same time a third operation was done: the bottom extraction lift superficial gas velocity was reduced, to keep more mass in the FR body. A reduction of lift fluidization will increase the FR bottom pressure because of the increase of mass, anyhow it is compensated by the increase of fluidizing air which combined with the mass increase should shift more of it in the upper part of the reactor. The FR solids entrainment was increased of almost the 20%, which is the consequence of a high concentration increase in the FR upper body (highlighted in figure 5-10 b2) from around 15% of the design case value at 1m height up to almost 40% of the design case at the reactor exit. At the same time the bottom pressure drop, thus concentration, decreased pretty much;

this means a big reduction of mass in the bottom zone of the reactor leading to an overall mass active mass reduction of almost 50%. This fact reduces the residence time to half, without considering the recirculation but just determining it as inventory divided by the solids flow. The superficial gas velocity and solids entrainment increases (figure 5-10 a2) had the consequence to increase very much the FR cyclone pressure drop. The AR behaviour is not changing so much except an slight increase of concentration both in the lower and upper part leading to a slight solids entrainment increase and to an overall active mass increase of around 25%.

#### 5.4.4. Chemical Looping Reforming

Other than CO<sub>2</sub> capture, the concept of Chemical Looping Combustion can be developed in order to obtain the production of synthesis gas by means of reforming processes.

Synthesis gas or syngas is mainly composed by H<sub>2</sub> and CO<sub>2</sub> and it is mostly used as a fuel or as a source of H<sub>2</sub> in the production of ammonia. This gas can be produced following various reactions. A first classification can be made considering the different type of fuel used.

For heavy fuels' reforming is mainly used a partial oxidation, slightly exothermic:



For light fuels we have another reaction, the steam reforming reaction, highly endothermic:



If is required synthesis gas with a high CO content, the reaction to choose is called CO<sub>2</sub> reforming and is highly endothermic as well:



Nowadays, the most used between the three is the steam reforming.

However, a further step is required if the goal of the reforming is the production of pure H<sub>2</sub>: the water-gas shift reaction, slightly exothermic, in which CO and H<sub>2</sub>O are transformed in CO<sub>2</sub> and H<sub>2</sub>, as it follows:



Thus, the result is a gas mixture consisting in almost just CO<sub>2</sub> and H<sub>2</sub>. The latter has to be separated from the former, and there are different ways to perform this, but in any case a purity of over 99.99% is obtained [28].

Using the separation of carbon dioxide to produce hydrogen, two are the processes that have been studied:

#### **5.4.4.1. Chemical looping Auto-Thermal Reforming [CLR(a)]**

In this option, the reaction in the air reactor is the same as in a normal chemical looping combustion cycle. The only difference is in the air/fuel ratio, which in this case is reduced. So, there will be a smaller amount of oxygen that is transported from the air to the fuel reactor, due to a lower circulation rate of the oxygen carrier that besides has been subjected to a smaller oxidation. In the fuel reactor the situation is more complicated because various reactions take place, such as the full oxidation, the partial oxidation, the steam reforming and the CO<sub>2</sub> reforming.

The main advantage of this technique lies in the fact that is not required an Air Separation Unit (ASU), component that usually is one of the most energy demanding [28].



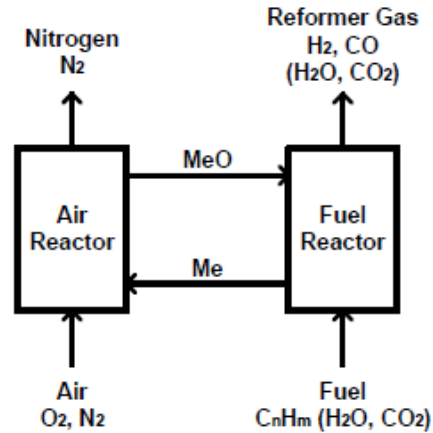


Figure 5-11: basic process of CLR(a)

#### 5.4.4.2. Chemical Looping Steam reforming [CLR(s)]

Here, an H<sub>2</sub>/CO<sub>2</sub> stream is used as a fuel for a chemical looping combustion cycle that in this way generates the heat required by a conventional steam reformer. The reaction takes place in reformer tubes that can be located inside the fuel reactor or in a separated fluidized bed heat exchanger fed by the air reactor. Thus, all the technologies needed are conventional, and this is the main advantage of using this second option.

Table 5-6: Amount of air injections in reforming test

| Air Injections         | Position of Injection | Air flow[Nl/min] | Total amount of air [m/s] | Share in percent% |
|------------------------|-----------------------|------------------|---------------------------|-------------------|
| Air Reactor Loop Seal  | <b>External</b>       | <b>80</b>        | <b>0.07</b>               | <b>76</b>         |
|                        | <b>Center</b>         | <b>20</b>        |                           | <b>19</b>         |
|                        | <b>Internal</b>       | <b>0</b>         |                           | <b>0</b>          |
|                        | <b>Grease</b>         | <b>5</b>         |                           | <b>5</b>          |
| Fuel Reactor Loop Seal | <b>External</b>       | <b>80</b>        | <b>0.1</b>                | <b>84</b>         |
|                        | <b>Center</b>         | <b>10</b>        |                           | <b>11</b>         |
|                        | <b>Internal</b>       | <b>0</b>         |                           | <b>0</b>          |
|                        | <b>Grease</b>         | <b>5</b>         |                           | <b>5</b>          |
| Air Reactor            | <b>Primary</b>        | <b>2500</b>      | <b>1.9</b>                | <b>56</b>         |
|                        | <b>Secondary 1</b>    | <b>1000</b>      |                           | <b>22</b>         |
|                        | <b>Secondary 2</b>    | <b>1000</b>      |                           | <b>22</b>         |
| Fuel Reactor           | <b>Primary</b>        | <b>1200</b>      | <b>2.6</b>                | <b>50</b>         |
|                        | <b>Secondary 1</b>    | <b>1000</b>      |                           | <b>42</b>         |

|        |                    |            |            |           |
|--------|--------------------|------------|------------|-----------|
|        | <b>Secondary 2</b> | <b>200</b> |            | <b>8</b>  |
| Lifter | <b>Primary</b>     | <b>500</b> | <b>1.5</b> | <b>70</b> |
|        | <b>Secondary</b>   | <b>200</b> |            | <b>30</b> |

The last chemical looping process presented in the paper is the chemical looping reforming. The feasibility of auto-thermal chemical looping reforming has already been proven by Vienna University of technology, by a reduction of AR fluidization which reduces the OC entrainment and consequently the amount of oxygen provide to the FR reduction reaction where an incomplete combustion will take place producing CO and H<sub>2</sub>. Two CLR were tested, the first one is based on the same principle of Vienna and the AR fluidizing air was reduced together with the AR loop-seal fluidization.

The pressure profiles behave as expected: the AR has a smaller cyclone delta P and higher bottom pressure drop with consequent higher concentration in the bottom and lower in the upper part and a total active inventory increased of the 35%. The FR pressure profile changes slightly in the upper part giving a smaller concentration, in addition because of the smaller solids flow arriving from the AR the FR total almost halves mainly due to a dramatic reduction in concentration in the lower part. In this case it was possible to see how the reactor system reacts to an almost 40% of solids exchange reduction. In the second case the AR fluidization was kept constant and the OC exchange was reduced making use of the divided loop-seal, the internal leg of the loop-seal was fluidized in order to re-circulate part of the entrained solids. Ideally 50% in this case, but it has been proven that with the actual loop-seal design the split between the two legs is determined both by the air injected and the pressure difference between the reactors (out of paper scope). In this case the AR inventory increases due to the internal recirculation while the FR loses mass because of the less amount of solids coming from the FR, with a big reduction in concentration in the bottom part, partly balanced by the lift fluidization reduction.

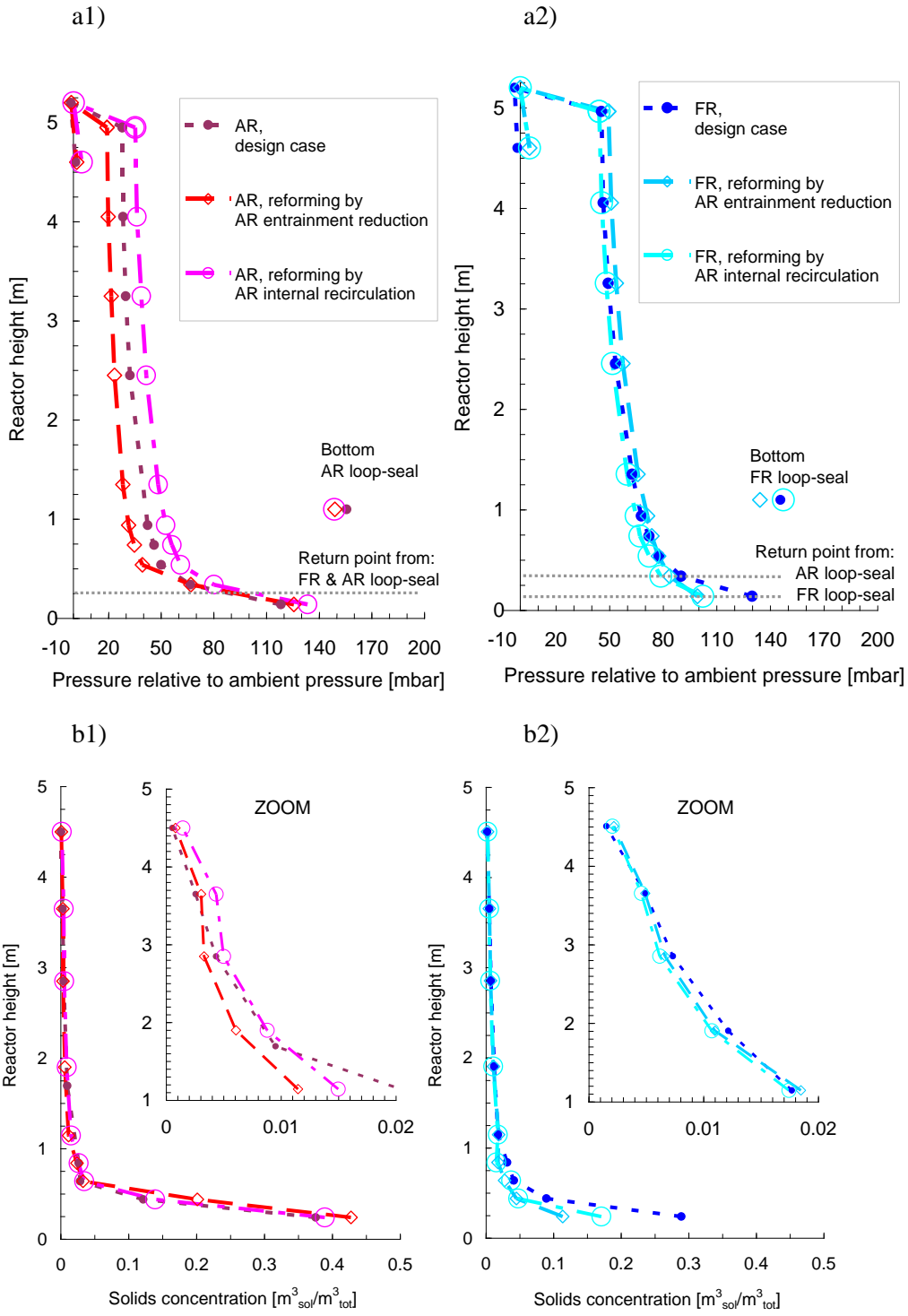


Figure 5-12: Pressure and solids concentration profiles of AR (a1 and b1) and FR (a2 and b2) resembling two reforming applications

## 5.5. Inventory

After having tested several times the five different operational modes, the best condition for each experiment which is evaluated as stable, is chosen as a reference case. The effect of the total mass inventory circulating in the system and especially for operational modes was investigated for the next step.

This was done in order to test the flexibility of the rig, and to discover if the behavior was, or not, influenced by the amount of solids.

It was decided to try two different options: reducing the inventory of 20 kg, and increasing it of 20 kg, from the original quantity. This means that the total entrainment would have been:

- 100 kg in the first case
- 140 kg in the second

In both cases, the rig should have been run repeating all the five operational modes and checking the behavior of the components and the fluxes.

At first, it was decided to start with lowering the inventory. The most effective way to do it was selected to be the loss of the quantity requested from the cyclones. To obtain this, the system was run in very unstable conditions for a few minutes. The main parameters that made the behavior unstable were:

- The lifter was set with very low values of the air injections;
- The heights of the mass in the various chambers of the loop seals were not equal.

The first thing made the exchange between the two reactors lower: more mass was accumulating in the FR. The second caused instabilities and fluctuations in both the downcomers of the reactors. These two reasons led to very big fluctuations in the FR downcomer, which caused high quantities of solids going through the back pipe which are connected the cyclones to the filter.

The filter, and the second scale present in the lab as a double-check, were used to measure the amount of mass which had been extracted from the cold flow model, so that to be sure that the

numbers were coherent with the ones established. Thus, 20 kg were removed, and the final inventory was reduced to 100 kg.

The five operational modes were then tested, in this order: standard conditions (design), part load, maximum power, maximum FR concentration and reforming.

For the first two sets, standard and part load, the stability was reached in a few minutes: visually, the system was behaving like it did with 120 kg of mass. The only difference was that bubbles were seen in the FR downcomer, as a consequence of the smaller quantity of solids circulating in the system. The grease air in the loop seals is used to help the fluidization in the downcomer, but when the amount of mass is lower, there is no need to use it because the fast fluidization regime is already fully achieved.

Besides, problems were founded in testing the maximum fuel reactor concentration conditions. Fluctuations were visible in the FR downcomer, with a lot of particles going to the filter. More tests were done to find a solution for the instability problem. Again, the solution was playing with the loop seals air injections; another evidence of the fact that the role of these components is fundamental for a correct behavior of the system. So, the internal recirculation was maintained, but some values were changed: the grease air injection was working again, the one in the internal section was a bit decreased while the external one increased, in order to gain more balance. The lifter was set on higher values, to avoid the unwanted accumulation of too much mass in the FR, but still trying to achieve the goal of the set, i.e. having a better gas/solids contact in the reactor.

Curious results were shown when the system was set on the reforming case. Visually, the behavior was perfectly stable: no fluctuations in the downcomers, and also during the measurements. However, from the analysis of the pressure profiles, it was noticed that the pressure in the bottom of the AR had a slightly increasing trend during the whole experiment. This is normally a sign of the fact that the reactor is getting full. So, the test was repeated again with the same values, but the behavior was exactly the opposite: while having still stable visual conditions, the pressure profile of the bottom pressure in the AR had a decreasing trend; the reactor was getting empty. This set is a proof of the influence of the mass inventory on the

global behavior of the system, and of the fact that in some cases precautions have to be taken to avoid stability problems.

After these sets of experiments, the total inventory is increased up to 140 kg. The additional quantity was simply added to the reactors such as normal refilling, trying to add equal amounts in the two reactors, to avoid unbalances in the system.

Due to accumulations of particles in both down comers, it was impossible to run the rig. In many cases the down comers height is became really high, with the mass almost reaching the cyclones. Also, a lot of static electricity was recorded to be present in the downcomers.

The inventory was then reduced again to 120 kg, and the standard conditions were tested again. The system was working normally.

Therefore, just 10 kg of particles added to the system, and total amount of inventory become 130 kg. With this value, the five operational cases were tested, and the model did not show any malfunctioning.

In conclusion, these tests are evidences of the fact that the inventory cannot be modified without thinking of the consequences. Like every other parameter, it affects the whole behavior of the system and it can create problems, in some cases serious problems that can even lead to the impossibility of running the rig. In this respect, the experiments made show that; in general, bigger problems are caused by bigger additions of solids.

The comparison of the pressure profiles and solid concentration for operational modes with different solid inventory in the system are shown in the appendix I.

## 5.6. Loop seal sensitivity

A specific set of tests was dedicated to the understanding of the maximum pressure difference a divided loop-seal can handle during operation when just one of its return legs is on use. In fact it was noticed that when just one of the two return legs is used to circulate solids, there is the bigger risk of gas leakages through the one not in use which provides an easy path to the gas coming from the reactor body high pressure which affects the loop-seal sealing capability and cyclone efficiency.

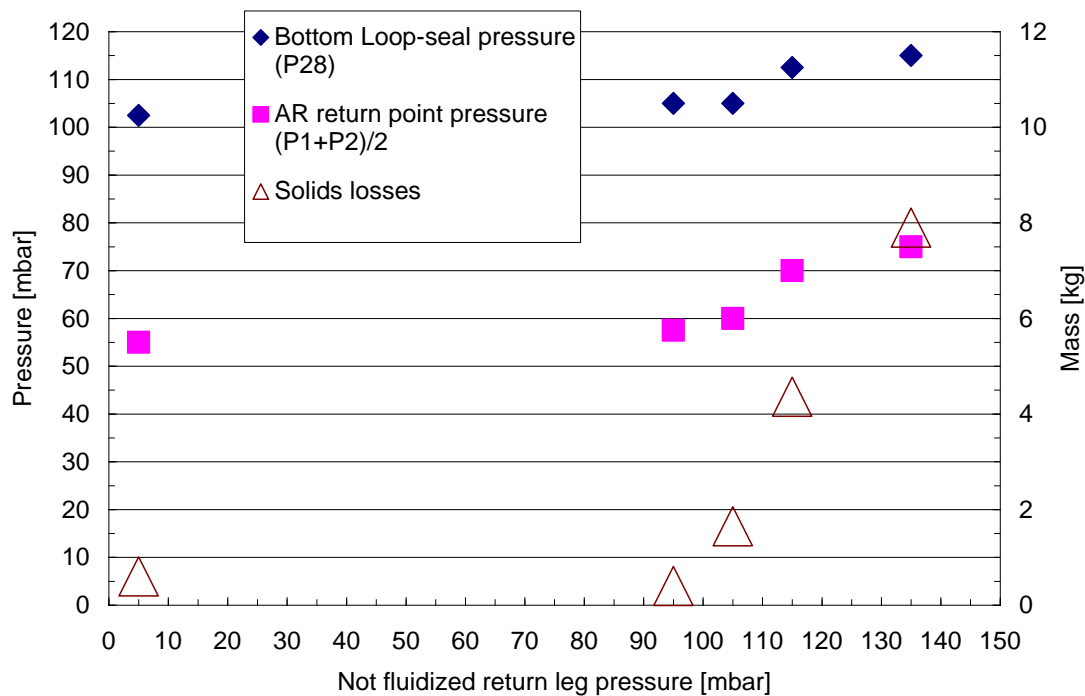
The selected loop-seal was the AR one which was re-circulating internally the entrained flux while the FR was used as a pressure chamber. The valve located on the back-pipe was partially closed and at the same time the FR superficial gas velocity was varied in order to set the desired pressure in correspondence of the AR loop-seal return leg merging into the FR (P15). The AR was operated at constant conditions with superficial gas velocity of 2.4m/s and a rather conventional LS fluidization injecting 40NI/min in the central nozzle and 120 NI/min in the internal one, inverted with what usually is the external that in this case is not fluidized.

The solids entrainment was constantly monitored as well as the downcomer height and the solids losses. Figure 5-13 is summarizing some key parameters measured as function of the pressure measured in the point where the loop-seal return leg merges in the FR reactor.

Looking at the solids losses it can be easy to see that below 100 mbar of pressure the mass losses are constant, while above it they increases dramatically. Anyhow visually it was possible to see strong fluctuations just above 115mbars, for the last two points. Those two were not operable in a stable way and also the pressure fluctuations, looking at the raw data were much bigger. This means that the visual observation is enough to understand if it is possible to achieve a steady state condition, but may not be enough to understand which should be the optimal condition and it may have affected to some extent the whole test campaign. In an infinite time interval, none of those are stable, but the “visual” one will clearly last much less because of the mass losses.

Other interesting information that can be derived is the fact that such big pressure will affect both the bottom loop-seal pressure and the reactor one in the return point of the loop-seal leg in

use. The loop-seal bottom has proven in many other tests that fits to the reactor one and can keep intrinsically the equilibrium. These results mean that the divided loop-seal not in use propagates the effects not just to the loop-seal, but also to the hydrodynamics of the reactor.



5-13: pressure measurement in the point where the loop-seal return leg merges in the FR reactor



## 6. Conclusion

A complete overview of the most common scaling criteria for designing cold flow models (CFM) was finalized to study. A new scale-up fluidized bed system has been provided for this experimental study. The most common approach in academia consists of building a small scale CFM resembling the hydrodynamics of a larger hot rig by keeping constant set of dimensionless numbers. On the other hand, the approach of the industry is mainly consists of building full scale CFMs which can be used to better understand the influence of design solutions and operation on the system performance, to test process control and measurement methodologies.

The CFM built by SINTEF Energy Research and the Norwegian University of Science and Technology (NTNU) was designed as full scale, i.e. with the same dimensions as a 150kWth hot unit which is at the final stage of construction. The aim is to fulfill both the above mentioned approaches to estimate the hydrodynamics of a larger industrial prototype plant of size ~15MWth, and to troubleshoot the 150kWth hot unit to be built. The combined use of the 150kWth hot pilot rig and the 1:1 scale CFM represents an important tool in further scale-up of chemical looping processes under investigation [20].

The cold flow model was commissioned and is using Geldart A particles since it has quick mixing properties during the operation, and also has the flexibility to choose wide range of operating modes. The CFM performance is described, in terms of solid flux, rate of circulation and solid exchange between reactors by considering pressure and concentration behavior.

The system has been validated against the design target of 2kg/s (solid exchange) between the air reactor and fuel reactor. This targeted solid exchange was obtained when the TSI inside the system is 120kg. This is referred as the design case (standard condition). Also, it can be identified from the mentioned graphs<sup>6</sup> that both the reactors operate in the border between fast fluidization and turbulent regime. This set of experiments is used as reference case, i.e. a starting point for the other cases which are analyzed with different possibilities of operational modes in chemical looping combustion resembling cold flow model.

---

<sup>6</sup> Section 4.3

The cyclone efficiency as well as velocity profile along the reactors was calculated. During the study the cyclone showed collective efficiency at approximately 99%.

The solids flux entrainment and the pressure profiles along the air reactor and the fuel reactor were examined. The sensitivity of solid flux and pressure profiles was analyzed in relation to superficial gas velocity, secondary air injection, solid inventory and loop-seal fluidization. Especially the way loop-seal affects the reactors performance was systematically analyzed in order to find the best combination of air flow to the central, internal and lateral air injections.

At the same time the system hydrodynamic and sensitivity to the fluidization of components such as the bottom extraction/lift and the fuel reactor was studied. Some of the specific design issues were addressed, especially when it comes to the location of the divided loop-seals return legs, which is discussed in detail at section 4.3.

Series of experiments were done in order to validate the operational modes of CLC by means of CFM. The most important test for operating the CLC in a safe way is operating in part-load condition, which consists of injecting a lower amount of air to the system. Compared to the design case this causes lower power output from the system. Another interesting condition was to study the maximum power mode. The air injection in FR was increased to resemble an increase in fuel injection, while AR fluidizing gas was increased to provide more OC exchange which is required to oxidize the higher amount of fuel.

Moreover, several tests were done in order to get a better concentration of the particles in the FR, obtained by increasing both the residence time and also by entrainment inside the body of the FR. The aim is to provide an overall better contact between gas and particles in the upper region (risers) avoiding a very dense bottom zone.

Reforming experiments were done by reduction of AR fluidization which reduces the OC entrainment and consequently the amount of oxygen provide to the FR reduction reaction. So that an incomplete combustion will take place producing CO and H<sub>2</sub>. Another way to conduct reforming was by reducing fluidized air in the AR together with the AR loop-seal fluidization.

It was possible to operate the reactor system in a stable way and according to design targets. At the same time the hydrodynamic viability was addressed qualitatively, of several other

chemical looping configurations which in principle can be managed by the double loop circulating fluidized bed architecture: FR fast fluidization regime, load flexibility with variation from 50% to 120%, gas turbine combustor and chemical looping reforming (CLR). It was possible to find one or more configurations resembling each of them. On one hand the hydrodynamics were balanced to get the CFM running stably in steady state [20].

The overview of results (operational modes) is depicted in the appendix II.

Still further research is needed in order to establish a complete mapping of the reactor system operability. The cyclones separation efficiency needs to be evaluated more precisely.

Another area of further study is the impact of Total Solid Inventory (With different size and type of particles) at the above mentioned operational modes.

## 7. Reference

- [1] B. Metz, O.R. Davidson, P.R. Bosch, R. Dave, L.A. Meyer (eds), 2007, contribution of working group III to the fourth assessment report of the intergovernmental panel on climate change, Cambridge University Press, Cambridge, United Kingdom and New York, NY, USA.
- [2] A. Bischi, Ø. Langørgen, J-X Mornic, J. Bakken, M. Ghorbaniyan, M. Bysveen, O. Bolland, 2010, Performance analysis of the cold flow model of a second generation chemical looping combustion reactor system, doi:10.1016/j.egypro.2011.01.074
- [3] A. Bischi, Ø. Langørgen, I. Saanum, J. Bakken, M. Seljeskog, M. Bysveen, J-X. Morin, O. Bolland, 2010. Design study of a 150kWth Double Loop Circulating Fluidized Bed reactor system for Chemical Looping Combustion with focus on industrial applicability and pressurization. *Int. J. Greenhouse Gas Control*, doi:10.1016/j.ijggc.2010.09.005.
- [4] H. Chalmers and J. Gibbins, 2009, Carbon capture and storage: the ten year challenge, doi: 10.1243/09544062JMES1516.
- [5] The International Institute for Sustainable Development, Earth negotiations bulletin, 2001, Vol. 12 No. 165
- [6] Bert Metz, Ogunlade Davidson, Heleen de Coninck, Manuela Loos, Leo Meyer (eds), 2007, IPCC Special Report on Carbon Dioxide Capture and Storage, ISBN 92-9169-119-4
- [7] Mohamed Kanniche, René Gros-Bonnivard, Philippe Jaud, Jose Valle-Marcos, Jean-Marc Amann, Chakib Bouallou, 2009, Pre-combustion, post-combustion and oxy-combustion in thermal power plant for CO<sub>2</sub> capture, doi:10.1016/j.applthermaleng.2009.05.005
- [8] O. Bolland, 2008, CO<sub>2</sub> capture in power plants compendium TEP03, Norwegian University of Science and Technology, Department of Energy and Process 2011
- [9] BAILEY, D. W. & FERON, P. H. M. , 2005, Post-combustion decarburization processes. *Oil and Gas Science and Technology, Rev. IFP*, 60, 461-474.
- [10] The Bellona Foundation- Fact sheet: CO<sub>2</sub> Capture, 2007, [www.bellona.org](http://www.bellona.org)

[11] International Panel on Climate Change (IPCC), “Carbon Dioxide Capture and Storage”, <http://www.ipcc.ch/activity/ccssp.pdf>

[12] Ø. Brandvoll, O. Bolland, 2004, Inherent CO<sub>2</sub> Capture Using Chemical Looping Combustion in a Natural Gas Fired Power Cycle. J. Eng. Gas Turbines Power, Volume 126, Issue 2, 316 (6 pages), doi:10.1115/1.1615251

[13] Ivar M. Dahl, Egil Bakken, Yngve Larring, Aud I. Spjelkavik, Silje Fosse Håkonsen, Richard Blom, 2009, On the development of novel reactor concepts for chemical looping combustion, doi:10.1016/j.egypro.2009.01.198

[14] Niall R. McGlashan, Peter R. N. Childs, Andrew L. Heyes, 2010, Chemical Looping Combustion

Using the Direct Combustion of Liquid Metal in a Gas Turbine Based Cycle, DOI: 10.1115/1.4001984

[15] P. Basu, 2005, Combustion and Gasification in Fluidized Beds. Taylor & Francis Group, LLC CRC Press, ISBN: 0-8493-3396-2

[16] J.R. GRACE, 1990, High-velocity fluidized bed reactors, Chemical Engineering Science, Vol. 45, No. 8, pp. 1953-196

[17] John R Grace, A A Avidan, T M Knowlton, 1997, Circulating fluidized beds, Blackie Academic & Professional, ISBN: 0751402710 9780751402711

[18] Xu, Min, 2010, Chemical looping combustion: cold model hydrodynamics and modeling of methane combustion, the University of British Columbia, Chemical and Biological Engineering

[19] D. Geldart, 1972, Types of Gas Fluidization, Elsevier Sequoia SA, Lausanne

[20] Aldo Bischi, Øyvind Langørgen, Jean-Xavier Morin, Jørn Bakken, Masoud Ghorbaniyan, Marie Bysveen, Olav Bolland, 2011, Hydrodynamic viability of chemical looping processes by means of cold flow model investigation, Third International Conference on Applied Energy, May 2011, Perugia, Italy

- [21] Khairy Elsayed, Chris Lacor, 2010, The effect of cyclone inlet dimensions on the flow pattern and performance, *Applied Mathematical Modelling*, Elsevier Inc., doi:10.1016/j.apm.2010.11.007
- [22] Erich Hugi, Lothar Reh, 2000, Focus on solids strand formation improves separation performance of highly loaded circulating fluidized bed recycle cyclones, *Chemical Engineering and Processing*, Volume 39, Issue 3, doi:10.1016/S0255-2701(99)00072-0
- [23] ASTM, 2008. "Standard Practices for Sampling Metal Powders", B 215-08. ASTM International, West Conshohocken, PA, USA.
- [24] Brooks Instruments User Manual, 2008, Installation and Operation Manual - Brooks® Mass Flow Meter Model 5863, [www.brooksinstrument.com](http://www.brooksinstrument.com), 22/12/2010
- [25] Fuji Electric Instrumentation & Control, FCX-AII Series User Manual, Differential Pressure Transducer, [www.coulton.com](http://www.coulton.com), 23/12/2010
- [26] Issangya A.S., Bai D., Bi H.T., Lim K.S., Zhu J., Grace J.R., 1999. "Suspension densities in a high-density circulating fluidized bed riser", *Chemical Engineering Science*, Vol 54, No 22, pp. 5451-5460.
- [27] Monazam E.R., Shadle L.J., 2004. "A transient method for characterizing flow regimes in a circulating fluid bed". *Powder Technology*, Vol 139, No 1, pp.89-97.
- [28] Bischi Aldo, 2008, Experimental results of a chemical looping auto-thermal reforming of natural gas in a dual circulating fluidized bed reactor system using a NiO-based oxygen carrier

## 8. Appendix

### 8.1. Appendix I

#### Standard

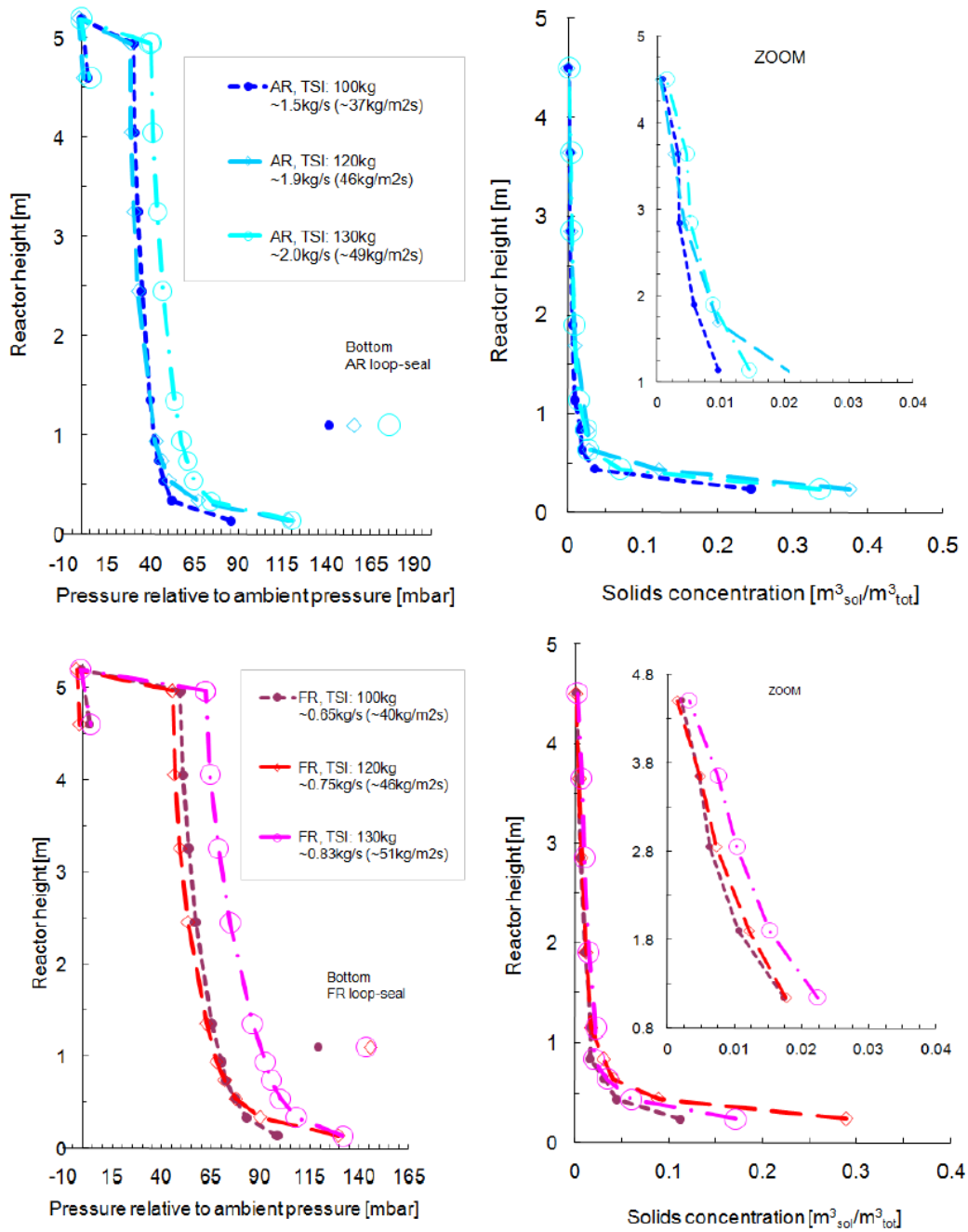


Figure 8-1: Pressure and solids concentration profiles of AR and FR in standard condition with different inventories

**Part load**

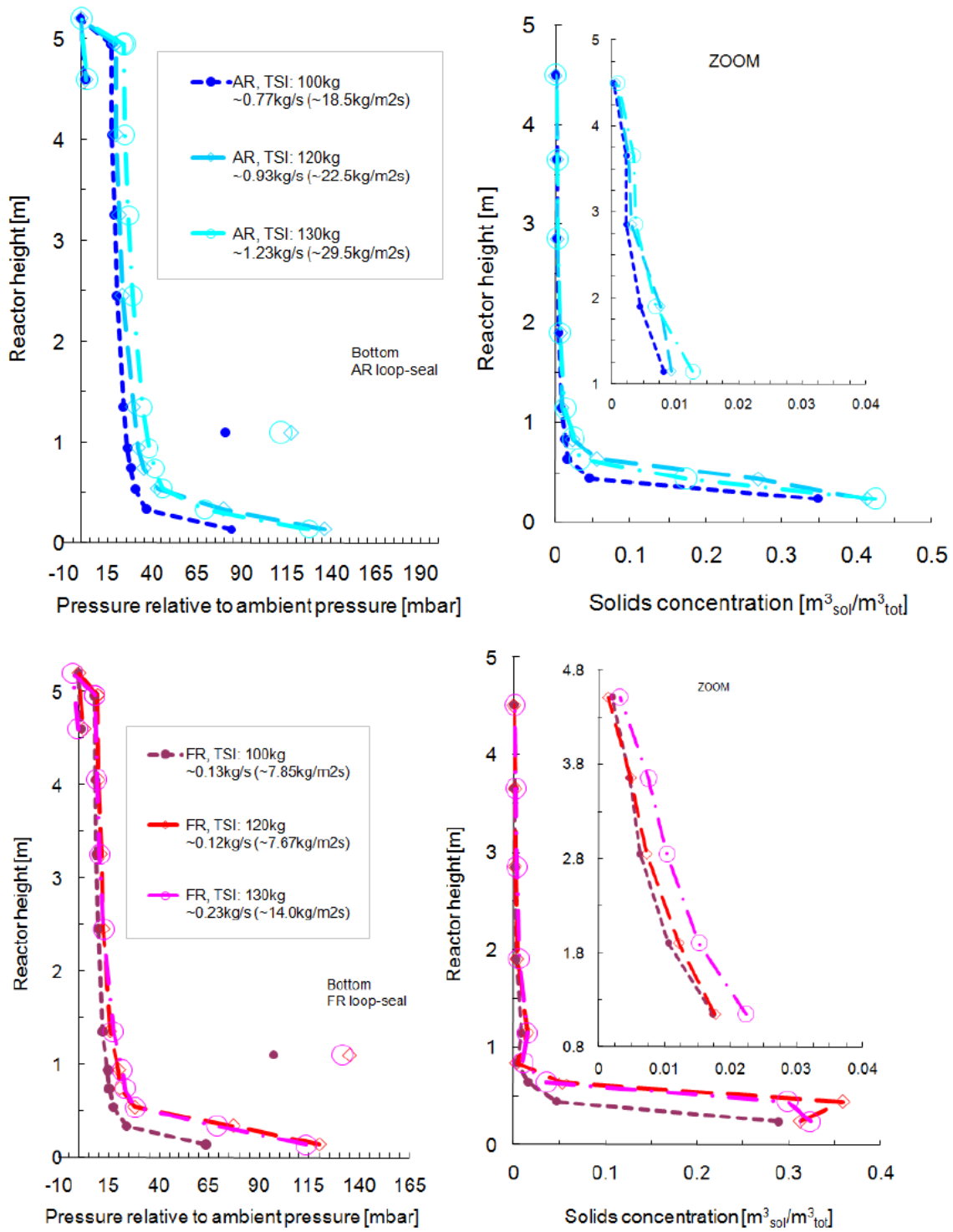


Figure 8-2: Pressure and solids concentration profiles of AR and FR in part load operation with different inventories



**Maximum power**

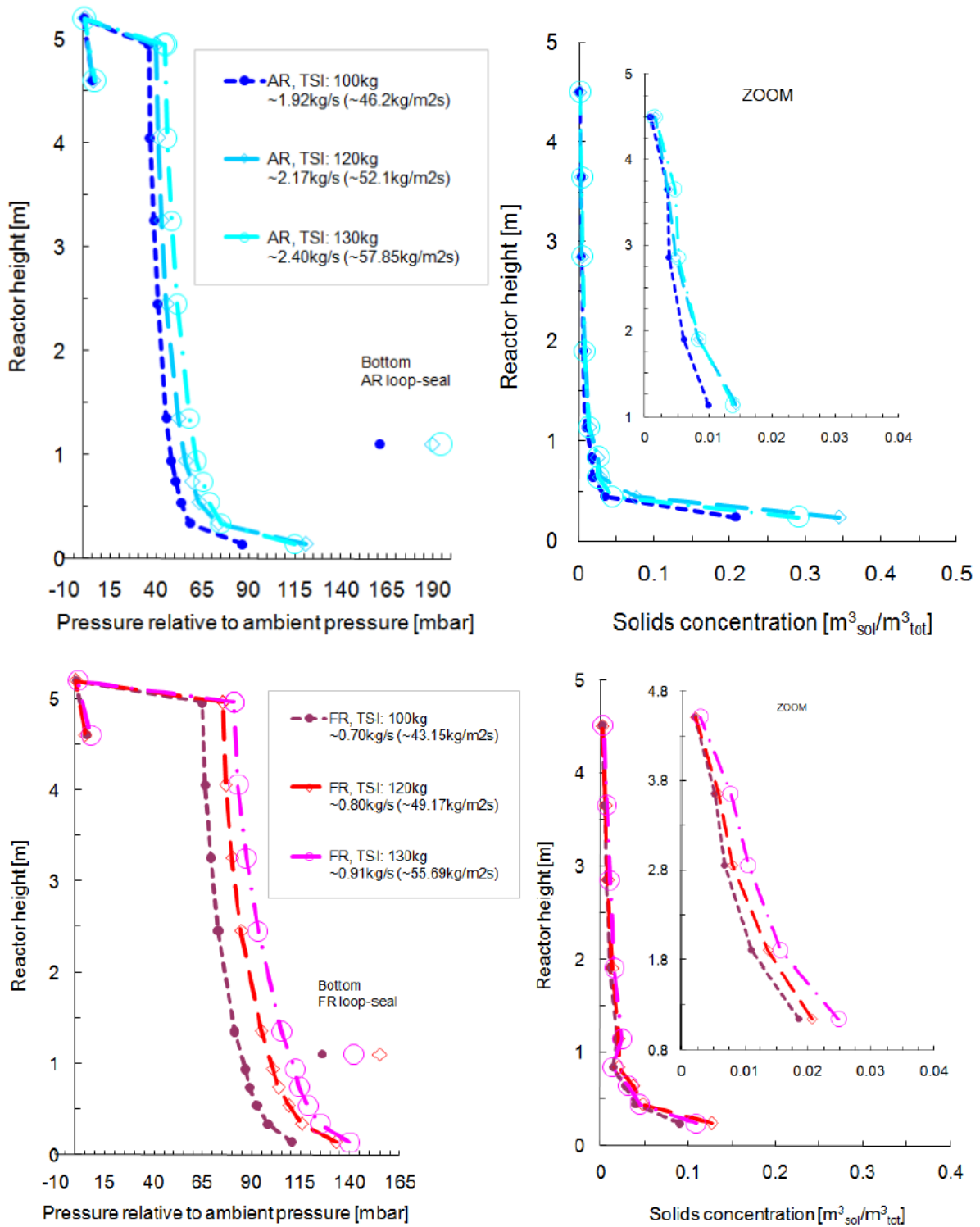


Figure 8-3: Pressure and solids concentration profiles of AR and FR in maximum power condition with different inventories

**Maximum fuel reactor concentration**

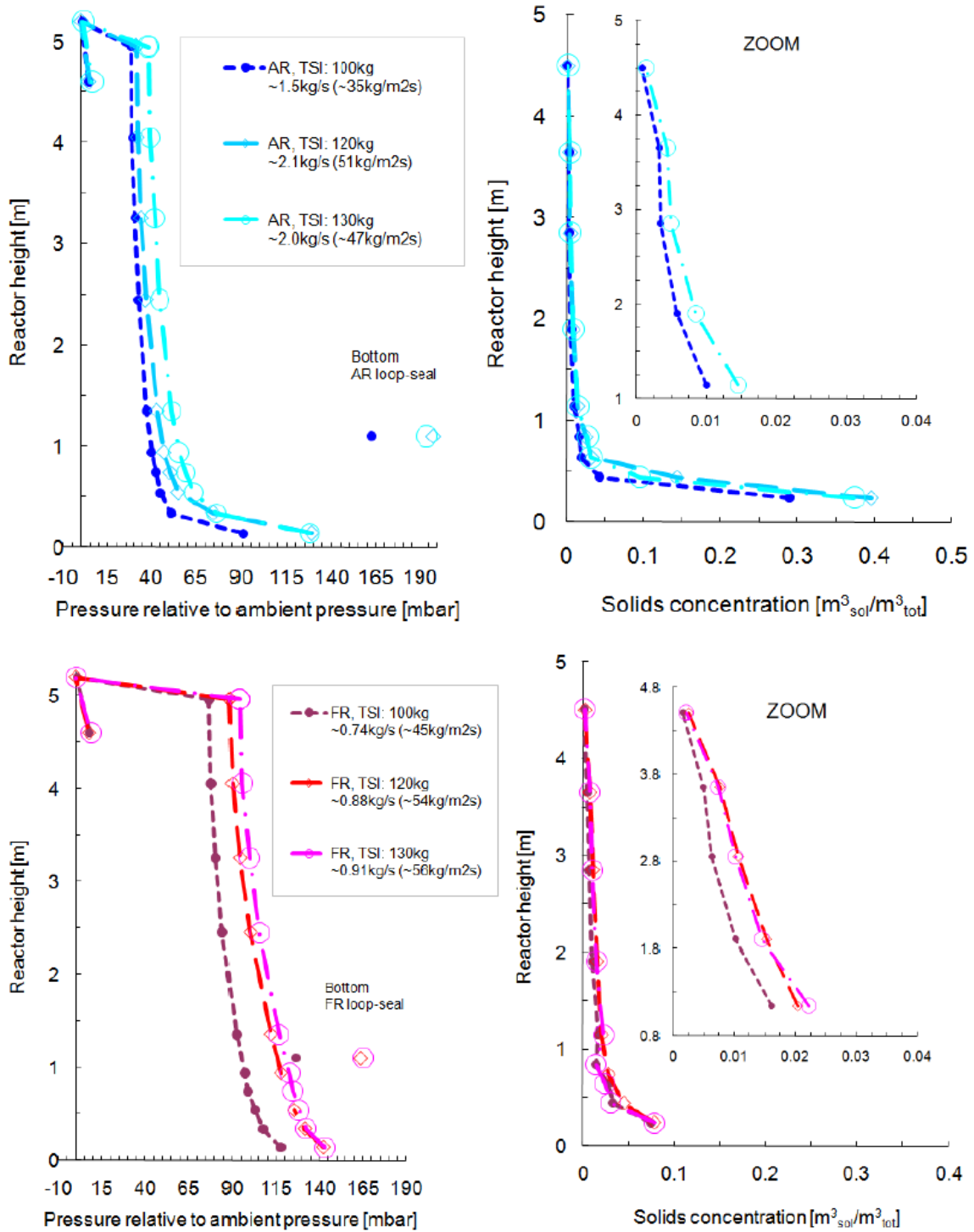


Figure 8-4: Pressure and solids concentration profiles of AR and FR in maximum fuel reactor concentration condition with different inventories

## Reforming

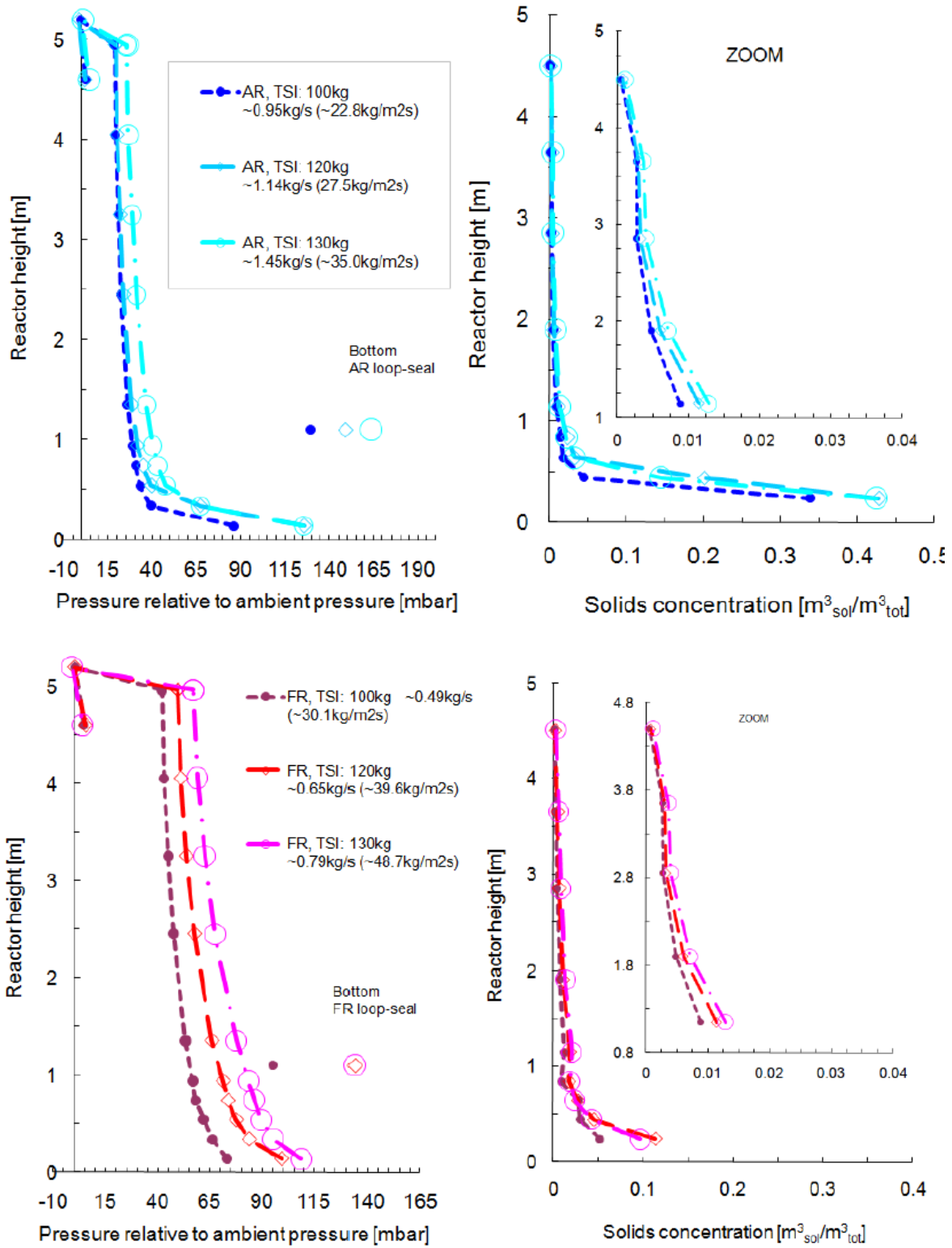


Figure 8-5: Pressure and solids concentration profiles of AR and FR in reforming condition with different inventories

## 8.2. Appendix II

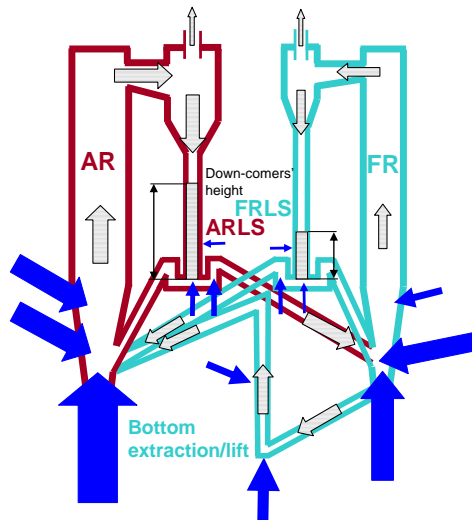
### Design case

#### Control parameters

Reactors' superficial gas velocity:  
 AR: **2.4**, FR: **2.6**, Lift: **1.5** [m/s]  
 Loop Seal air injection:  
 External/Central/Internal/Lateral  
 AR: **120/40/0/5**[NI/min]  
 FR: **80/10/0/5**[NI/min]

#### Measured results

Reactors' solids entrainment,  
 Flow: AR **~1.88**, FR **~0.74** [kg/s].  
 Flux: AR **~45.2**, FR **~45.7** [kg/m<sup>2</sup>s].  
 Reactors' active mass:  
 AR **~26**, FR **~15** [kg].  
 Down-comers' and lift flux:  
 AR **~230**, FR **~91**, Lift **~139** [kg/m<sup>2</sup>s].  
 Down-comers' height:  
 AR **~0.60**, FR **~0.43** [m].



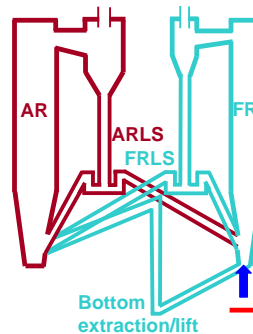
### Part load 75% fuel

#### Control parameters

Reactors' superficial gas velocity:  
 AR: **2.4**, FR: **1.8 (-31%)**, Lift: **1.5** [m/s]  
 Loop Seal air injection:  
 External/Central/Internal/Lateral  
 AR: **120/40/0/5**[NI/min]  
 FR: **80/10/0/5**[NI/min]

#### Measured results

Reactors' solids entrainment,  
 Flow: AR **~1.50 (-20%)**, FR **~0.33 (-55%)** [kg/s].  
 Flux: AR **~36.2**, FR **~20.1** [kg/m<sup>2</sup>s].  
 Reactors' active mass:  
 AR **~36 (+48%)**, FR **~15**[kg].  
 Down-comers' and lift flux:  
 AR **~184**, FR **~40**, Lift **~147 (+6%)** [kg/m<sup>2</sup>s].  
 Down-comers' height:  
 AR **~0.30÷0.35**, FR **~0.40÷0.45**[m].



## Part load 50% fuel

### Control parameters

Reactors' superficial gas velocity:  
AR: **2.0 (-17%)**, FR: **1.3 (-50%)**, Lift: **1.5** [m/s]

Loop Seal air injection:

External/Central/Internal/Lateral

AR: **80 (-33%)**/**10 (-75%)**/**0**/**5**[NI/min]

FR: **40 (-50%)**/**5 (-50%)**/**0**/**5**[NI/min]

### Measured results

Reactors' solids entrainment,  
Flow: AR **~0.93 (-51%)**, FR **~0.12 (-84%)** [kg/s].

Flux: AR **~22.5**, FR **~7.7** [kg/m<sup>2</sup>s].

Reactors' active mass:

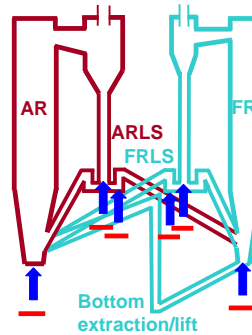
AR **~38 (+46%)**, FR **~15**[kg].

Down-comers' and lift flux:

AR **~114**, FR **~15**, Lift **~99 (-29%)** [kg/m<sup>2</sup>s].

Down-comers' height:

AR **~0.37**, FR **~0.4**[m].



## FR flux/concentration maximization

### Control parameters

Reactors' superficial gas velocity:  
AR: **2.4**, FR: **3.5 (+35%)**, Lift: **1.2 (-20%)** [m/s]

Loop Seal air injection:

External/Central/Internal/Lateral

AR: **180 (+50%)**/**40**/**0**/**5**[NI/min]

FR: **30 (-62.5%)**/**10**/**198 (+undef.)**/**0 (-100%)**[NI/min]

### Measured results

Reactors' solids entrainment,  
Flow: AR **~2.08 (+11%)**, FR **~0.88 (+19%)** [kg/s].

Flux: AR **~50.2**, FR **~54.2** [kg/m<sup>2</sup>s].

Reactors' active mass:

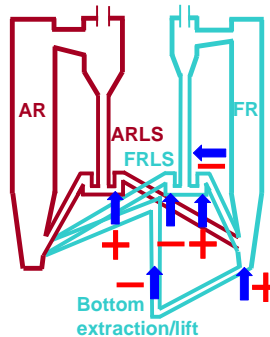
AR **~33 (+27%)**, FR **~8 (-47%)**[kg].

Down-comers' and lift flux:

AR **~255**, FR **~108**, Lift: und. [kg/m<sup>2</sup>s].

Down-comers' height:

AR **~0.70**, FR **~0.40** [m].



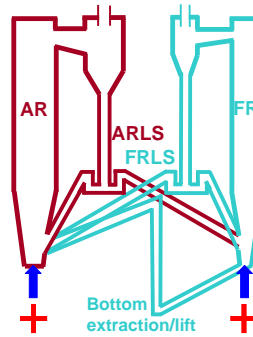
## Power increase

### Control parameters

Reactors' superficial gas velocity:  
AR: **2.6 (+8%)**, FR: **3.2 (+23%)**, Lift: **1.5** [m/s]  
Loop Seal air injection:  
External/Central/Internal/Lateral  
AR: **120/40/0/5**[NI/min]  
FR: **80/10/0/5**[NI/min]

### Measured results

Reactors' solids entrainment,  
Flow: AR **~2.16 (+15%)**, FR **~0.80 (+8%)** [kg/s].  
Flux: AR **~52.1**, FR **~49.2** [kg/m<sup>2</sup>s].  
Reactors' active mass:  
AR **~28 (+8%)**, FR **~11 (-27%)**[kg].  
Down-comers' and lift flux:  
AR **~270**, FR **~98**, Lift **~167 (+20%)** [kg/m<sup>2</sup>s].  
Down-comers' height:  
AR **~0.70**, FR **~0.45÷0.47**[m].



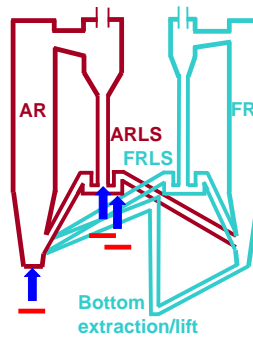
## Chemical Looping Reforming (AR entrainment reduction)

### Control parameters

Reactors' superficial gas velocity:  
Flow: AR: **1.9 (-21%)**, FR: **2.6**, Lift: **1.5** [m/s]  
Loop Seal air injection:  
External/Central/Internal/Lateral  
AR: **80 (-33%)/20 (-50%)/0/5**[NI/min]  
FR: **80/10/0/5**[NI/min]

### Measured results

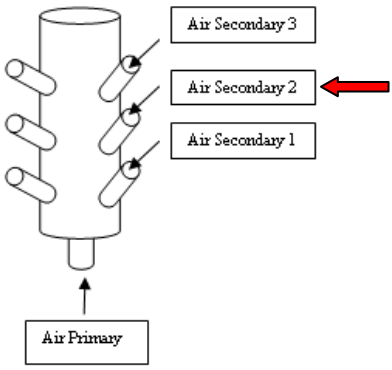
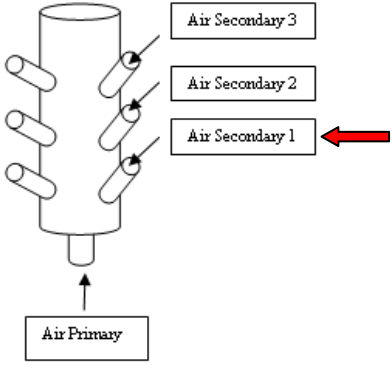
Reactors' solids entrainment,  
Flow: AR **~1.14 (-39%)**, FR **~0.65 (-12%)** [kg/s].  
Flux: AR **~27.5**, FR **~39.6** [kg/m<sup>2</sup>s].  
Reactors' active mass:  
AR **~35 (+35%)**, FR **~8 (-47%)**[kg].  
Down-comers' and lift flux:  
AR **~140**, FR **~79**, Lift **~61 (-56%)** [kg/m<sup>2</sup>s].  
Down-comers' height:  
AR **~0.72**, FR **~0.40** [m].



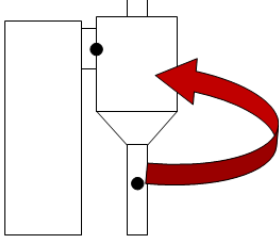


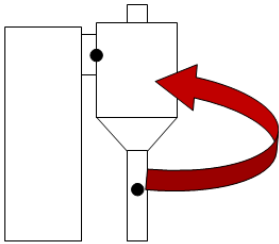
### 8.3. Appendix III

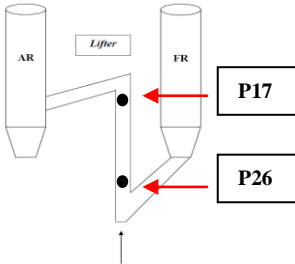
#### Problems during experiments

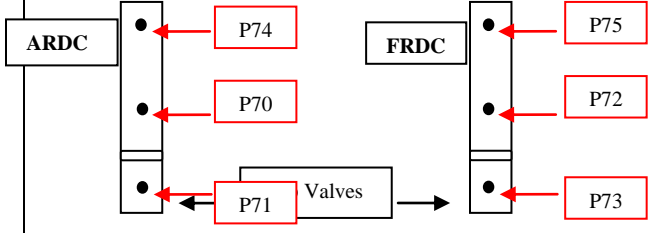
| Date       | Task   | Specification  | Problem  |
|------------|--|--|--|
| 16/02/2011 | <p>-Remove the seals between the AR &amp; FR body (located in the lifter) for starting the coupled operation</p> <p>-Start point: Reach the pervious conditions(last stable operation 16/11/2010)</p> <p>-Compare the results of the secondary air injection place with the same total amount of air in FR (specially pressure profiles) and analyze the effect of the air injection place on concentration of the FR</p>  | Total amount of air in the FR: 2400 lit/min  | <p>-Due to the leakage in the cyclone of the fuel reactor the operation has stopped.</p> <p>-Duration between this experiment and the next one, the calibration for PTs is changed by lab technicians.</p> |
| 28/02/2011 | <p>-The place of the secondary air injection in FR is changed to lower part of riser</p>  <p>-The position of P29 changed in AR as you see below due to see the effect of position changed in the cyclone and also analyze the pressure drop between these two point in the cyclone when the new PTs will be installed</p>  | The same specification with pervious test matrix except the place of the secondary air injection in FR | Leakage in FR(the connection part between cyclone and riser)   |



|            |  |                              |  |
|------------|--|------------------------------|--|
|            |                   |                              |  |
| 03/03/2011 | -Repeating the pervious test matrix  | The same with pervious test  | Leakage in FR in the same place  |
| 07/03/2011 | -Repeating the pervious test matrix  | The same with pervious test  | Leakage in the AR loop-seal P28 (operator glued the leakage place to remove the problem )  |
| 08/03/2011 | - Repeating the pervious test matrix   | The same with pervious test  | The flow of main air injection to the system decrease suddenly, due to the problem in the other section of the lab.  |
| 10/03/2011 | - Repeating the pervious test matrix   | The same with pervious test  | The flow of main air injection decrease again during the experiment. Operators tried to use the pervious Ver. Of LabVEIW to solve the problem  |
| 14/03/2011 | - Repeating the pervious test matrix   | The same with pervious test  | Sudden increase in back pressure pipes to the filter. Operators found out that the problem was the misplacement of the filter fan located at downstairs. Also the online scaling system didn't work but with defining the new range for zero in the setting, this problem was abolished. |
| 15/03/2011 | - Repeating the pervious test matrix<br>-Increase the internal recirculation of the FR with adding | -The same with pervious test | Without any problem  |

|            |  |   |   |
|------------|--|---|---|
|            | the air flow in the internal section of FR loop-seal   | -Total amount of air to FRLS is the same with pervious test(the share of air to internal and external part is 50% for each) |   |
| 16/03/2011 | -The effect of the total air injection in AR on FR concentration and mass exchange between the reactors<br>-The place of the PTs at the top of the cyclones(FR&AR) is changed due to gain better result without any disturbance of flowing air   | -The total amount of air in the AR increased 500 lit/min in each step   | Losing large amount of particles because of unstable condition and high air flow in AR  |
| 17/03/2011 | -With analyzing the pressure profiles, the inventory of FR reduced after a while so tried to increase the inventory with changing the condition for internal and external section of ARLS  | -The share of the air injection to ARLS external and internal are 50%-50%, 75%-25%, 25%-75%                                 | Without any major problem   |
| 18/03/2011 | -Analyze the effect of the total air injection to FR on concentration and amount of mass exchange in reactors<br>-The position of P32 changed in FR as you see below due to see the effect of position changed in the cyclone and also analyze the pressure drop between these two point in the cyclone when the new PTs will be installed<br><br> | -total amount of air of FR increased 500 lit/min in each step   | Without any problem   |
| 21/03/2011 | -  | -   | The main controller of the rig (laptop) didn't work. The operators placed a new laptop in the section which is borrowed from other section SINTEF |
| 24/03/2011 | -The effect of the place of the air flow injection to AR, FR and together with the same total amount of air flow(for FR:2400& for AR:5500)   | -changing 500lit/min for each reactor from primary to secondary   | Without any problem   |
| 25/03/2011 | -Increasing the air injection to external part of ARLS and internal part of FRLS in different arrangements to increase the inventory and concentration in FR   | -the ratio for increasing the air was 0.75  | Without any problem   |
| 28/03/2011 | -An analyze of reaching to stable condition with online refilling for one hour and see the effect of the measurements and calculating the time to reaching the stable condition after each measurement   | -specification is the same with 16/02/2011  | Operators forget to save the logging file   |
| 29/03/2011 | -Repeat the pervious experiment  |   | Without any problem   |

|            |   |   |   |
|------------|---|---|---|
| 04/04/2011 | -Lifter sensitivity in design conditions<br>-The metal cyclone is in placed in the FR   | -total amount of air in lifter is started from 300lit/min up to 104lit/min in 4 steps   | Without any problem   |
| 05/04/2011 | - Analyze the effect of the LPs on circulation rate and try to increase the entrainment in the FR<br>-The position of P26 and p17 is changed to the bottom and top of the lifter, respectively<br> | -the share of the air injections to the LSs is changed as following:<br>External Internal<br>100% 0%<br>70% 30%<br>50% 50%  | The flow of main air injection to the system decrease suddenly, due to the problem in the other section of the lab. |
| 06/04/2011 | -Continue the pervious program  | -Increase the amount of total air injection in the LSs with the same share as previous experiment   | Without any problem   |
| 07/04/2011 | -LSs sensitivity in design conditions   | - different share of the LSs was tested with the same amount of total air injections in the LSs   | Without any problem   |
| 08/04/2011 | -Maximum FR concentration   | - the best condition was reached with 225lit/min and 240lit/min total amount of air in the ARLS and FRLS, respectively  | Without any problem   |
| 11/04/2011 | -P17 moved to the bottom of FR<br>-P28 moved to the upper part of the FRLS<br>-P31 moved to the upper part of the ARLS<br>-P13 moved to the lifter  |   |   |
| 12/04/2011 | -Reduce the amount mass going to FR and less mass exchange based on Reforming operation in the CLC  | -reduce AR air injections<br>-reduce the lateral air injection in ARLS<br>-decrease lifter<br>-increase internal air injection in the FRLS<br>-reduce the FR fluidization | Without any problem   |
| 20/04/2011 | -Reduce the amount of circulation based on Part-Load operation in the CLC   | -reduce the total amount of air injection in AR and FR<br>- reduce the total amount of air injection in ARLS and FRLS   | Packed bed in the ARDC, stop the operation and using the flushing system  |

|            |  |  |   |
|------------|--|--|---|
| 29/04/2011 | -The new version of LabVIEW is installed and the plan for installing the new pressure transmitters was confirmed<br>-Test the components and air injections in the new version of LabVIEW                                | -  | P28 does not work in the new version of software                      |
| 02/05/2011 | -Continue the Part-Load experiments<br>-The new hole for P28 is drilled  | -  | Without any problem   |
| 03/05/2011 | -Continue the Part-Load experiments  | -  | Without any problem   |
| 04/05/2011 | -Continue the Part-Load experiments  | -  | Without any problem   |
| 05/05/2011 | -The new 6 pressure transmitters are installed in the rig<br><br>-The Reforming experiments repeat with these new pressure transmitters | -  | Without any problem   |
| 06/05/2011 | -Continue the previous program for Reforming   | -  | Without any problem   |
| 16/05/2011 | -Reduce the inventory to 100kg and repeat the 5 reference experiments(Standard, Part-Load, Maximum Power, Maximum FR Concentration, Reforming)   | -  | Without any problem   |
| 24/05/2011 | -Change the position of new PTs<br>-repeat the pervious experiments  | -  | System shut down because of a leakage in the FR cyclone               |
| 25/05/2011 | -Increase the inventory to 140kg and repeat the 5 reference experiments(Standard, Part-Load, Maximum Power, Maximum FR Concentration, Reforming)   | -  | The height of the ARDC is very high, operate the system is impossible |
| 26/05/2011 | -Reduce the inventory to 120kg to reach the stability  | -  | Without any problem   |
| 07/06/2011 | -Increase the inventory to 130kg and repeat the 5 reference experiments(Standard, Part-Load, Maximum Power, Maximum FR Concentration, Reforming)   | -  | Without any problem   |
| 10/06/2011 | -Reduce the inventory to 120kg<br>-Reach the normal distribution<br>-Block the external pipe of the FRLS<br>-Seal the connection pipe between the filter box and FR cyclone  |  | Without any problem   |
| 14/06/2011 | -Operational window for LS   | Changing the botoom pressure of the FR and calculate the cyclone efficiency for each set of experiments(bottom pressure is increased | Without any problem   |

|            |   |  |                     |
|------------|---|--|---------------------|
|            |   | from 100mbar to 160mbar in 3 steps and also decreased to 0 mbar in 3 steps ) |                     |
| 27/06/2011 | -Repeat the previous experiments to validate the data | -  | Without any problem |